

NUREG/CR-2482
BNL-NUREG-51494
Vol. 1

Review of DOE Waste Package Program

Subtask 1.1 - National Waste Package Program

Prepared by M. S. Davis, D. G. Schweitzer

Brookhaven National Laboratory

Prepared for
U.S. Nuclear Regulatory
Commission

NOTICE

This report was prepared as an account of work sponsored by an agency of the United States Government. Neither the United States Government nor any agency thereof, or any of their employees, makes any warranty, expressed or implied, or assumes any legal liability or responsibility for any third party's use, or the results of such use, of any information, apparatus, product or process disclosed in this report, or represents that its use by such third party would not infringe privately owned rights.

Available from

GPO Sales Program
Division of Technical Information and Document Control
U. S. Nuclear Regulatory Commission
Washington, D. C. 20555

Printed copy price: \$6.00

and

National Technical Information Service
Springfield, Virginia 22161

Review of DOE Waste Package Program

Subtask 1.1 - National Waste Package Program

Manuscript Completed: November 1981
Date Published: February 1982

Prepared by
M. S. Davis, D. G. Schweitzer

Brookhaven National Laboratory
Upton, NY 11973

Prepared for
Division of Waste Management
Office of Nuclear Material Safety and Safeguards
U.S. Nuclear Regulatory Commission
Washington, D.C. 20555
NRC FIN A3164

Availability of Reference Materials Cited in NRC Publications

Most documents cited in NRC publications will be available from one of the following sources:

1. The NRC Public Document Room, 1717 H Street, N.W.
Washington, DC 20555
2. The NRC/GPO Sales Program, U.S. Nuclear Regulatory Commission,
Washington, DC 20555
3. The National Technical Information Service, Springfield, VA 22161

Although the listing that follows represents the majority of documents cited in NRC publications, it is not intended to be exhaustive.

Referenced documents available for inspection and copying for a fee from the NRC Public Document Room include NRC correspondence and internal NRC memoranda; NRC Office of Inspection and Enforcement bulletins, circulars, information notices, inspection and investigation notices; Licensee Event Reports; vendor reports and correspondence; Commission papers; and applicant and licensee documents and correspondence.

The following documents in the NUREG series are available for purchase from the NRC/GPO Sales Program: formal NRC staff and contractor reports, NRC-sponsored conference proceedings, and NRC booklets and brochures. Also available are Regulatory Guides, NRC regulations in the *Code of Federal Regulations*, and *Nuclear Regulatory Commission Issuances*.

Documents available from the National Technical Information Service include NUREG series reports and technical reports prepared by other federal agencies and reports prepared by the Atomic Energy Commission, forerunner agency to the Nuclear Regulatory Commission.

Documents available from public and special technical libraries include all open literature items, such as books, journal and periodical articles, and transactions. *Federal Register* notices, federal and state legislation, and congressional reports can usually be obtained from these libraries.

Documents such as theses, dissertations, foreign reports and translations, and non-NRC conference proceedings are available for purchase from the organization sponsoring the publication cited.

Single copies of NRC draft reports are available free upon written request to the Division of Technical Information and Document Control, U.S. Nuclear Regulatory Commission, Washington, DC 20555.

Copies of industry codes and standards used in a substantive manner in the NRC regulatory process are maintained at the NRC Library, 7920 Norfolk Avenue, Bethesda, Maryland, and are available there for reference use by the public. Codes and standards are usually copyrighted and may be purchased from the originating organization or, if they are American National Standards, from the American National Standards Institute, 1430 Broadway, New York, NY 10018.

CONTENTS

CONTENTS	iii
EXECUTIVE SUMMARY.	iv
1. INTRODUCTION.	1
2. WASTE FORMS	1
2.1 Probable DOE Program	1
2.2 Summary of Existing Information on Borosilicate Glass.	4
2.3 NRC Information Needs on Borosilicate Glass.	6
2.4 NRC Information Needs on SYNROC.	7
3. CONTAINER MATERIALS	8
3.1 NRC Information Needs on TiCode-12	9
4. BACKFILL.	10
4.1 NRC Information Needs on Backfill.	11
5. WHOLE PACKAGE TESTING	11
5.1 NRC Information Needs on Whole Packages.	12
5.2 NRC Information Needs for Prediction	13
6. ACCELERATED TESTING	14
6.1 Temperature Acceleration	14
6.2 Isothermal Acceleration and Prediction	15
6.2.1 Corrosion	15
6.2.2 Failure Modes	18
6.2.3 Problems with Mechanisms of Waste Form Leaching	18
6.2.4 Conclusions	19
7. REFERENCES.	19
APPENDIX: GLASS CORROSION - A REVIEW	

EXECUTIVE SUMMARY

The purpose of this report is to continue the assessment of the state of the DOE waste package development effort for high level waste. The report updates past reviews on waste forms, container materials, and backfill materials. The new reviews also emphasize evaluation of the materials with respect to their demonstrated or potential abilities to satisfy NRC performance objectives. The report also reviews whole waste package testing where such information exists. A major objective of this report is to begin describing the information that DOE must submit so that NRC can complete its licensing actions and other identified NRC objectives.

Present information indicates that the DOE programs on waste forms will emphasize borosilicate glass and SYNROC.

The information NRC will need to license a waste package in which the high level waste form borosilicate glass is given either partial or full credit for containment or for controlled release rates does not exist at present. After 1000 year containment, radionuclide release from a borosilicate glass waste form will be determined by how leaching of the long lived actinides is affected by variables in the waste form and in the environment surrounding the breached waste package. Almost all the existing information deals with leaching of the short lived fission products. These will have become essentially innocuous after 1000 years. In addition to many of the problems associated with the leaching of alkali and alkaline earth fission products in glass, preliminary experiments on waste glass loaded with actinides indicate new and complex problems that have not yet been studied to any appreciable extent. For example, actinides exist in glass in various oxidation states which may have different leach properties.

The report summarizes the information needed by NRC on TiCode-12 if it is to be used for compliance with 1000 year containment.

Some problems associated with prediction and accelerated testing are noted.

1. INTRODUCTION

The definition of the waste package used here is that given in the Federal Register/Vol. 460, No. 130/July 8, 1981:

"'Waste package' means the airtight, watertight, sealed container which includes the waste form and any auxiliary enclosures, including shielding, discrete backfill, and overpacks".

The definition of the waste form taken from the same publication is:

"'Waste form' means the radioactive waste materials and any encapsulating or stabilizing materials, exclusive of containers".

For reasons to be elaborated upon in the text, this report will emphasize existing information and information NRC will require for (a) borosilicate glass as the candidate waste form, (b) TiCode-12 as the container or overpack choice, and (c) synthetic zeolites as the discrete backfill material. The existing work on total waste packages will be summarized and deficiencies and generic recommendations for additional work are noted.

The report discusses problems of accelerated testing for the specific purpose of developing predictive capabilities for long term performance related to (a) waste form leaching, (b) container corrosion, and (c) container failure mode propagation.

2. WASTE FORMS

2.1 Probable DOE Program

Present information indicates that the DOE research and development programs on waste forms will emphasize borosilicate glass and one alternative. The alternative waste form is to be selected from recommendations of the "Alternative Waste Form Peer Review Panel"¹ and a Savannah River Review Group.

The objective of the Peer Review study was to consider the relative merits and potential of (eight) 8 alternative waste forms being considered for the solidification and disposal of high level radioactive wastes. The eight waste forms were selected from a list of (fifteen) 15 previously evaluated by the Peer Review Panel. Data and reports used for the review were provided to panel members by the DOE project teams.

The ranking of waste forms given by the Peer Review Panel are:

- (1) borosilicate glass,
- (2) SYNROC,
- (3) porous glass matrix (high silica glass),
- (4) tailored ceramics,
- (5) pyrolytic carbon (PyC) and silicon carbide (SiC) coated particles,
- (6) concrete (FUETAP),

- (7) metal matrices,
- (8) plasma spray coatings.

Since disparate values of leach rates for various waste forms were cited in the Program Review meeting by various waste form developers, the Panel compiled a summary table of leach rates to use in its deliberations (Table I.) A range of values is given in Table I because of the wide variability reported for the leaching of the various waste forms.

The Panel recommended that independent laboratory confirmation of leaching behavior of waste forms be obtained using standardized and comparable conditions. The Panel also recommended that a much broader range of leach variables, particularly flow rates, be investigated in order that a comparison table, such as Table I, can be more relevant to repository conditions and more sensitive to the variability and characteristics of specific waste forms.

The Panel considered that a principal advantage of a glass waste form is that it involves basically a one-step processing operation. The glass-waste mix can be melted and cast directly into a metal canister or melted within the canister. Such a simple process was considered attractive for the radioactive and remote hot canyon operations required for high level wastes.

The Panel also claimed that positive factors in favor of glass as a waste form were the experimental evidence that the process is insensitive to possible variations in waste stream variability and that the product is relatively insensitive to radiation damage.

In selecting SYNROC as the best alternative to borosilicate glass the Panel claimed:

"The concept inherent to this polycrystalline ceramic waste form is the partitioning of radionuclides into specific crystal phases as a constituent of the host crystal structure or contained in solid solution within the host lattice. The phases of primary interest in this system are titanate-based, including perovskite (CaTiO_3), Ba-hollandite ($\text{BaAl}_2\text{Ti}_2\text{O}_{16}$), and zirconolite ($\text{CaZrTi}_2\text{O}_7$). Ideally, when appropriate additions of CaO , TiO_2 , BaO , and ZrO_2 are mixed intimately with a specific waste formulation, and densified at elevated temperatures, a phase assemblage develops such that each radionuclide is incorporated into its most stable host lattice. The dense ceramic resulting from such a product should have leaching characteristics limited only by the inherently low solubility of the crystal phases within the ceramics. The titanate phases are selected as the host lattices in this waste form because of the relative radiation insensitivity of natural analogs of these minerals. Therefore it is anticipated that effects of radiation on leaching or structural integrity may be minimal during the geological times of storage.

"The Panel feels that this is now the best characterized and understood of the non-borosilicate glass waste forms. The volume fraction of the

Table I¹

Normalized Leach Rates (g/m² day) of Waste Forms @ 90°C,
D.I.H₂O, 28 Days in MCC-1 Static Leach Test

	Cs	Na	Sr	Ca	Ba	Fe	Al	Si	U or Pu	B	Remarks
Borosilicate Glass, SRL 131, PNL 76-68	1.4	0.9	(<.04) to 2.6	(.07)	1.6	0.007	--	0.55	--	0.8	Variables studied include: pH, radiation, long time (3 years), composition, need more confirmation data, 10X between labs
SYNROC-D	.06 to 0.4	.01 to 1.0	0.3 to 0.5	0.03 to 0.4	--	--	0.02 to 0.2	--	(<.0001) to 0.02	--	Variables: strong dependence on processing pO ₂ which affects densification (comparisons at high)
Porous Glass Matrix	--	0.10 to 0.15	0.08 to 0.33	--	--	0.13	--	0.06	0.005	--	Comparison at critical flow rates improves performance another 10X over borosilicate glass
Tailored Ceramics	(<0.1)	2.3	(<.004)	--	--	(<.0004)	(<.004)	--	0.008	--	() means below the developers lab's detection limit, not confirmed
PyC, SiC 7 day leach test	(<.001)	(<.0006)	(<.00001)	(<.0002)	--	(<.00003)	(<.0001)	--	(<.00001)	--	Coatings are successful using fluidized bed technique, no independent or statistical confirmation of low results
Concrete (FUETAP)	10+10	--	0.45+4	--	--	.009+.007	3+3	--	--	--	Very poor results in brine, at least 4X worse Pu release rate of 0.2 at 25°C
Metal Matrices	.04 to .02	.06 to 0.03	(<.02)	--	--	--	--	.02	--	--	Best data on PNL 76-68 glass in Pb matrix (14 day data)
Thermal Spray Coatings	(<.003) to 0.6	(<.0003) to 0.12	(<.002) to 0.03	--	--	--	--	(<.0004) to 0.05	--	--	Best results by Sn alloy using wire gun, only porous Al done with plasma gun

various phases formed in SYNROC has been identified and the partitioning of the ions in the phases are generally known".

In considering coated sol-gel particles, BNL has in the past noted² that this waste form has the potential of easily satisfying the NRC 1000 year containment criterion when placed in any of several canister and overpack systems. The Panel's comments on this waste form are shown below.

"Pyrolytic C, SiC Coatings of Sol-Gel Particles"

"The approach of this waste form is to produce polycrystalline SYNROC-D ceramic particles by internal gelation and to subsequently coat the particles with impervious PyC and SiC coatings. Chemical vapor deposition of the coatings with fluidized bed coaters result in impressively low leach rates for the coated particles (Table III).^{*} However, these results have not yet been confirmed by independent testing.

"There are advantages of the sol-gel technology for preparation of SYNROC-D powders. The spherical powders are very easily handled by pneumatic or liquid-like piping. Low temperature and low pressure sintering probably results although this is yet to be demonstrated. The process has been demonstrated to be routinely reliable in HTGR fuel production and is potentially one of the best for monitoring for quality assurance.

"However, the Panel concludes that the inherent disadvantages of the process and the final product outweighs the potential advantages. The waste form is intrinsically one of high surface area and high dispersibility. Since the particle sizes are restricted to about 1-mm or smaller, there is concern that after the canister is gone the waste will be in a form much more easily transportable by unforeseen water flows than would be the more monolithic waste forms. In addition, the process as is presently developed requires not only separate handling of Cs in a second stream following washing of the sol-gel particles but also the handling of nine times the volume of liquids than are presently in the waste tanks. The Cs must be incorporated in a non-SYNROC phase for which no present characterization or leaching studies have been conducted. Even though coatings of the Cs-containing phase have been demonstrated, processing will require handling dual products which is a major disadvantage as well. There are no data regarding radiation effects on the coatings, or He buildup within the coated particles. All in all, the combination of these uncertainties coupled with the questions still remaining for SYNROC, the process complexities and intrinsic small particle size of this waste form makes it relatively unattractive in spite of its potential for achieving ultra low leach rates".

2.2 Summary of Existing Information on Borosilicate Glass

BNL in Task 1,² Task 4,⁴ and in "Glass-Corrosion - A Review" by Tae-Moon Ahn and Emil Veakis (Appendix 1) have reviewed processes for degradation of glass. Below are summarized some of the findings from these efforts.

¹
^{*}Not reproduced here.

From experimental results on the leaching of binary systems, diffusion controlled dealcalization is predominant in the beginning with a square root time dependence while the appearance of network dissolution occurs with a linear time dependence following the diffusion process. However, the development of the time laws for this process is still too idealized to permit a valid extrapolation to geological times.

Solution and environmental variables have a direct effect on the durability of glass. As dealcalization proceeds, the nature of the solution will change. The solution composition effects are difficult to discern since these are inter-related to pH changes and passive film formation and destruction at the glass surface. Typical reactions in simple systems involve silica network dissolution in high alkaline solutions and lower leach rates in neutral and acidic environments. Multicomponent glass systems also exhibit better durability in acidic environments. Changes in pH and the effects of erosion resulting from variations in flow rates may result in unpredictable leach rates. For hydrothermal conditions, the alteration product resulting from glass-solution interaction is one of the most important variables determining the leach rate. A thorough understanding of the role played by the altered zone is needed in order to adequately identify the mechanisms involved in the leaching process.

Glass composition is one of the most important factors determining the leach rate. Generally, network formers and divalent modifiers increase durability while monovalent modifiers have the opposite effect. The effects of phase separation on leaching is dependent on the microstructure and can either enhance or retard durability. The ratio of solid surface area to solution volume is another important parameter effecting leach rates. However, the difficulty in the determination of the total surface area makes the exact formulation of this parameter extremely difficult. Other parameters, having secondary effects on the leaching process, include partial devitrification, internal stress, surface roughness, and local inhomogeneity contribute to changes in the leach rate. No quantitative data on the contribution of these parameters are available at the present time.

Radioisotopes may escape from the waste form by solid state diffusion. Tabulations of gas and ionic diffusivity in glass indicate that such events are very unlikely under repository conditions.

In glass, local corrosion is not any more severe than general corrosion. Static fatigue, however, should be recognized as an important mode of disintegration over geological time. From well-defined fracture mechanics, it is known that there is a fatigue limit for borosilicate glass below which no cracking occurs; however, changes at the microstructural level may modify the fatigue limit hypothesis. Modifications may arise due to surface stress, solution pH, humidity, temperature, pressure, compositional and microstructural inhomogeneity.

Radiation would probably not affect the leach rate by more than one order of magnitude as a result of radiolysis. An indirect effect such as microfracturing may be avoided by a proper design of a multibarrier glassy waste form.

Typical values for the dissolution rate of waste borosilicate glass range from 10^{-7} to 10^{-4} g/cm²-d, depending on the component. From the data at hand on the chemical and mechanical aspects of glass durability, and given an adequate design incorporating sacrificial layers, waste form integrity, at least for the first thousand years, is achievable. It is still premature to attempt quantifying material released from glass over geological time since major uncertainties exist in the identification of the various mechanisms involved in glass leaching.

2.3 NRC Information Needs on Borosilicate Glass

If the DOE intends to take credit for the properties of borosilicate glass in contributing to the containment or controlled release rate of the waste package, the BNL staff feels that the NRC will require additional information on:

- the effects of ions on the selective leaching and passive film formation, especially the ions in the groundwater such as bicarbonate ions;
- pH effects on nuclear waste glass--to explain why acidic solutions affect leaching in binary glass differently from leaching in multi-component systems;
- the flow rate effect in multicomponent systems, especially the relative changes of solution pH and passive film formation;
- the surface chemistry of the alteration zone during leaching, especially during hydrothermal reactions;
- the optimization in tailoring the glass composition for best leach resistance along with a formulation of the mechanisms involved, especially in multicomponent systems incorporating nuclear waste;
- the optimum microstructure for high leach resistance based on the principle of phase separation;
- valid means of defining and measuring the surface area of powdered and cracked samples, local pH changes and corrosion cell formation in powdered samples should be thoroughly understood;
- partial devitrification, surface roughness and local inhomogeneity effects on leach rates;
- ionic and gas diffusivity in glass at ambient temperatures; especially the diffusivity of fission products in nuclear waste glass;
- the wet-dry cycle effect on glass and comparison of the results to natural and archaeological analogs;

- a more mechanistic approach in understanding static fatigue--the effects of surface stress on crystallization is one example as opposed to relying on the well defined artificial stress intensity. More quantitative studies of the effects of pH, humidity, temperature, pressure, and glass composition are needed; especially in the area of nuclear waste glass development;
- radiation effects; especially on leaching either by radiolysis or by indirect effects;
- more sophisticated and comprehensive modeling of glass corrosion processes, computerized code generation may be a necessary step in the assessment of the complex process and in the area of long-term prediction of glass durability.

While fission products dominate the first few 100 years, long lived actinides become and remain the hazard after containment fails. The distributions of these species within the waste form are subject to changes induced by thermal decay over long periods of time. There is also some indication that different actinide valence states may be distributed in an inhomogeneous manner from the surface to the bulk. Although the mobility of the actinides in glass may be lower than the fission products, they may also tend to redistribute in a thermal gradient. Each valence state may diffuse differently, and changes of valence states by radiation may occur as ions migrate. Additional valence changes may be caused by redox reactions of the actinides with components and impurities in the matrix as the actinides migrate through the bulk. If borosilicate glass is to be given full or partial credit for controlled release after 1000 years containment, the NRC will need an extensive data base on actinide leaching, almost none of which exists at present.

2.4 NRC Information Needs on SYNROC

If the DOE intends to take credit for the properties of SYNROC in contributing to the containment or controlled release rate criteria, the BNL staff estimates that as a minimum NRC will require information on:

- thermodynamic stability of SYNROC materials with each other and with the titanate host phase;
- thermodynamic stability of SYNROC in repository waters;
- stability of SYNROC to variations in waste composition and concentration;
- properties of large samples of SYNROC produced under oxygen potential variations that may be unavoidable in remote processing;
- explanation of leaching dependence on oxygen potential;
- kinetics of SYNROC dissolution of matrix components, fission products, and actinides for intended waste loadings;

- leach dependence on density changes due to irradiation;
- leach rate information under all pertinent repository conditions for which borosilicate glass has been studied;
- radiation stability.

3. CONTAINER MATERIALS

The present DOE programs on metallic containers for high level waste are centered at Sandia National Laboratories and Pacific Northwest Laboratory.* Both laboratories appear to have finished their screening tests. After the initial screening studies, Sandia selected pure titanium, Ti-Pd and TiCode-12 for additional study. Although titanium shows excellent corrosion resistance to hot brines and seawater, it shows severe crevice corrosion above 120°C. Many titanium alloys show susceptibility to stress corrosion cracking (SCC) in sea water. The presence of halide ions accelerates the susceptibility. Titanium alloys show hot salt cracking in chloride salt and gaseous environment cracking in humid air, halide vapor or HCl gas.

Alloying elements change the susceptibilities significantly: oxygen and aluminum increase the susceptibility, while elements for improving SCC resistance are Sn, Mo, V, and Pd. Microstructural variation alters the susceptibility also. The acicular alpha phase with a continuous beta matrix or martensitic structure improve the resistance.

There are two current opposing views on the mechanism of stress corrosion cracking in titanium alloys. A number of workers consider the role of hydrogen and its embrittlement effect while others support anodic dissolution mechanisms. The hydrogen responsible for embrittlement can be generated in various ways including melting, process production, and electrochemical or chemical reactions during corrosion processes. Anodic dissolution is considered to arise from film formation and its subsequent rupture giving rise to an anodic cell. A monolayer of halide is an example of such film. A generalized reaction model has not yet been developed to explain all of the basic aspects of stress corrosion cracking in titanium and its alloys.

Delayed failure by hydrogen absorption has been observed in CP titanium, alpha titanium alloys, and alpha plus beta alloys such as Ti-6Al-4V at hydrogen contents from 10-ppm to 360-ppm depending on the alloying elements included. These levels of hydrogen are usually in excess of the room temperature solubility limit of CP titanium which is about 20-ppm. Increasing the alloying elements generally increases the solubility limit.

The detailed mechanism for crack nucleation is not known. However, there are several likely processes such as hydrogen-induced changes in the critical strain for fracture, fracture at hydride particles or at the interface between

*For a recent review and evaluation see reference 2.

hydride and matrix, or hydride embrittlement by localized plastic deformation. There is a general consensus that hydride formation at crack tips plays a major role in the delayed failure of titanium. Crack growth kinetics are strong functions of hydrogen concentration, strain rate, temperature, chemistry, and microstructure. Based on these observations and several crack velocity equations derived in assumed rate limiting steps, it is considered that a crack grows at the interface of alpha and beta phases and that hydrogen diffusion in the beta phase is the rate limiting step in the transport of hydrogen to the crack front.

The redistribution of hydrogen due to stress intensification in the vicinity of notches or other structural irregularities has drawn attention to fracture toughness parameters as a basis for characterizing the conditions necessary for the onset of cracking under sustained local conditions. The selection of TiCode-12 by Sandia is based on their studies and literature reviews which show that TiCode-12 is resistant to crevice corrosion below 300°C. It is also resistant to stress corrosion cracking in chloride salts at temperatures below 300°C and no more susceptible to hydrogen pickup than is pure titanium.

PNL has not selected any metals for further studies after the screening tests on corrosion properties described in Task 1.¹ They have an ongoing program on mechanical properties of Ti and TiCode-12 in support of the Sandia work.

3.1 NRC Information Needs on TiCode-12

It is the opinion of the BNL staff that the DOE programs on container materials will concentrate on TiCode-12 as the corrosion resistant overpack that will be placed around an internal canister. Mechanical strength for the waste package would be supplied by the internal canister.

For this choice, the information the NRC will need in evaluating a licensing application in which the DOE takes credit for containment due to TiCode-12 will include:

- an extended and thorough data base on corrosion in repository environments;
- predictive models for long term performance of TiCode-12 based on substantiated corrosion mechanisms;
- data on the presence or absence of interactions between the TiCode-12 overpack and the backfill and interior materials;
- evidence on how hydrogen concentration and its redistribution under applied stress may effect delayed fracture;
- evidence on whether or not hydrogen leads to slow crack growth;
- delayed fracture thresholds when hydrides may be present in flaws or cracks;

- evidence on relationship between internal hydrogen, hydrogen introduced from external sources, stress intensity, and slow crack growth;
- studies by liner-elastic fracture mechanics to assess the potential for predicting the resistance of TiCode-12 to delayed fracture and sustained load cracking;
- systematic studies of all the above applied to welds;
- fabrication and welding studies to determine if any compositional or microstructural changes from the bulk occur;
- corrosion testing and passivating film testing of welds.

4. BACKFILL

The BNL staff believe that both containment and radionuclide specific controlled release rates of one part in 10^5 per year or lower can be justified with reasonable assurance by developing an appropriate data base on synthetic zeolites used as backfill in high level waste repositories.

Although a considerable amount of data has been generated on backfills, few of the reported investigations deal directly with the proposed NRC 1000 year containment and/or 10^{-5} /yr radionuclide controlled release criteria. These performance objectives have to be addressed if the DOE takes credit for backfill as an effective barrier to the migration of released radionuclides in a repository.

The DOE researchers have considered the use of a montmorillonite clay as the primary component of a backfill barrier. The swelling nature of the clay would limit groundwater access to the waste container thereby delaying the onset of corrosion. Reduced water flow near the waste package would also restrict radionuclide migration to diffusional transport. Some preliminary research has been initiated with regard to the parameters which control the swelling nature of these clays. The cation form of the clay and the composition of the groundwater are important factors. If credit is to be taken for backfills of this type the NRC will require information on the reversibility of these properties with wet and dry cycling.

The use of multi-component backfills to achieve the properties necessary to effectively carry out the multiple functions of the backfill is currently envisioned. These accessory components are added in order to aid in the sorption or fixation of highly mobile radionuclide species such as TcO_4^- , I^- , IO_3^- and SeO_4^{2-} . The NRC will require information on the effectiveness of these accessory components in the presence of other intended backfill components.

Research concerning the sorptive properties of mixtures of zeolites and clays has been performed and preliminary results indicate that synergistic effects can cause a more superior sorption than expected. Again, the NRC will require a supporting data base for these properties.

A critical factor in the use of backfills in HLW repositories is that of thermal stability. Thermodynamic stability calculations have not proved conclusive in this area. Research on the thermal stability of clays and zeolites under hydrothermal conditions has indicated that some clays and zeolites may be unsuitable for HLW repositories due to their degradation at high temperatures. Some montmorillonite clays and mordenite zeolites, however, performed well under such conditions. The NRC will require information on the thermodynamic stability, changes due to aging, and radiation stability of the backfills selected by the DOE.

While experimental data are available on properties of candidate backfills, more work must be done to characterize these factors to allow for the quantitative evaluation of backfill performance with respect to proposed NRC criteria.

4.1 NRC Information Needs on Backfill

The NRC will require:

- further research on the swelling nature of montmorillonite clays since this aspect appears to be crucial to backfill performance. The influence of clay cation content and groundwater composition deserve continued attention along with pH, Eh, radiation, and temperature effects. Dehydration, wet-dry cycling, anisotropy, and the presence of accessory minerals also require expanded data bases if the DOE intends to take credit for backfill;
- more adequate data on near field pH and Eh control; this is particularly significant with respect to container corrosion;
- data on the thermal and hydrothermal behavior of backfill components; this is particularly important for the disposal of commercial HLW, the effect of various repository environments and the presence of accessory components need to be considered with respect to backfill stability and behavior;
- research on potential synergistic interactions; very little work exists in this area and on the basis of what research has been conducted, such interactions can have a significant impact on the overall performance of the backfill.

5. WHOLE PACKAGE TESTING

The limited work on simple simulations of whole package testing were reviewed in Task 4.³

While the behavior of individual components of the waste package is pertinent to performance of the whole package, the ability to provide reasonable assurance of long term containment is dependent on a thorough understanding of the behavior of the total package as an entity. Such information on whole package behavior is almost non-existent. The NRC must evaluate a DOE data base

that provides reasonable assurance for predicting long term containment from short term experiments. DOE may take credit for controlled release from the waste package. The NRC must therefore assess a data base the DOE must use to predict waste package behavior in relation to this unique controlled release rate problem.

5.1 NRC Information Needs on Whole Packages

Important technical areas, requiring information the NRC will need on containment and controlled release rate predictive models for both individual package components and whole waste packages include: corrosion, leaching, solubility, oxidation/reduction, gas generation, mechanical stresses, chemical stability, decay heat effects, statistics, etc. Moreover, for the whole waste package NRC will require information on:

- interactive effects that occur at the interface of components; i.e., the compatibility of waste package components;
- geometric effects related to failure modes and subsequent release of radionuclides from the package as an entity.

In order to provide reasonable assurance of long term containment and controlled release, if required, it is also necessary that the uncertainty boundaries and confidence levels associated with the above measurements be identified by DOE for use in modeling the long term performance of the waste package.

A potential problem with long term prediction of waste package behavior results from its kinetic nature. At present, there is no scientific concept or theory that can predict kinetic behavior in any but the simplest of systems.

The NRC will require information for developing a methodology for predicting long term performance of waste packages. As a minimum this plan should include identification of:

- (1) any inadequacies and major sources of uncertainties in existing DOE information for selected packages;
- (2) areas in which further development of data and modeling is required to pass performance objectives of the total package;
- (3) assumptions on which the measurements and the methodology used for license applications will be based.

The primary problem is to understand the degradation of the waste package as an entity. The degradation mechanisms and processes of the waste package may or may not be deducible from knowledge of the degradation processes and mechanism of the individual components. However, it is necessary to understand the behavior of individual waste package components in order:

- (1) to identify those reasons for possible deviations of the waste package behavior from summation of component behavior;
- (2) and, in those cases where the waste package does behave in a manner that is predictable from a summation of component behavior, to provide a data base for comparing components when selecting various waste package designs in which components may be interchanged.

5.2 NRC Information Needs for Prediction

The information NRC will need to evaluate the assumptions that the methods of prediction will be based on includes:

- degradation mechanisms and processes of individual waste package components and a comparison of these with degradation mechanisms and processes that occur in a waste package;
- an evaluation of the applicability and limitations of existing predictive methods and accelerated test procedures;
- an evaluation of the applicability and limitations of new predictive methods developed by DOE;
- an evaluation of the uncertainties and confidence limits of the data and for the models utilizing the data submitted for licensing;
- and an identification of both the scenarios and environmental conditions under which the model(s) are applicable and valid.

Methods of prediction are required by the NRC to assess:

- the length of time after repository closure over which the waste package can, with reasonable assurance, contain the radionuclides;
- the rate at which radionuclides will be released from the engineered system after the period of total containment.

For each assessment, information is needed to address processes which can adversely affect the ability of the package to meet the performance objectives as established in 10CFR60.

Parameters pertinent to the waste package components and package durability should be identified. Relationships between these parameters and waste package material degradation should be established. As a minimum the following parameters should be addressed:

Environmental:

- a) pressure;
- b) temperature;

- c) radiation;
- d) solution chemistry (e.g., pH, Eh, flow rate, chemical composition, and changes in composition);
- e) effects of wet and dry cycling;
- f) host rock characteristics and changes as they affect the waste package.

The most important models for degradation of the waste package may in fact come from a complex coupling of two or more of the above variables. For example, the groundwater chemistry will be a sensitive function of pressure, temperature, radiation, etc. Changes in one or more of these variables will alter the properties of the groundwater. It is therefore important for the DOE to develop information in which individual variables are changed under controlled conditions, as well as combinations of these variables. As a minimum these should include:

Waste package Parameters:

- a) waste package components and structure;
- b) leachability and corrosion properties of the components;
- c) ion exchange and sorptive properties of the components;
- d) component compatibility;
- e) waste loading;
- f) thermal history;
- g) effect of fabrication (e.g., welding).

Information on the following degradation processes will be required to the extent that they are pertinent to the durability of materials and will be necessary to evaluate a license applications.

- a) selective leaching and matrix dissolution by the groundwater;
- b) corrosion--general (bulk), stress corrosion, pitting corrosion, crevice corrosion, etc.;
- c) geochemical interactions;
- d) mechanical failure;
- e) embrittlement.

6. ACCELERATED TESTING

6.1 Temperature Acceleration

The effects of changing temperatures in chemical kinetics are covered by Arrhenius' concepts and theories. These concepts are valid only if it is confirmed that the same mechanism occurs over the temperature range studied. If this is the case, then the ratio of the rates at different temperatures can be used to obtain the numerical value of a constant called the activation energy. This numerical value can then be used to speculate on what processes are involved in delaying the reactants from forming the thermodynamically more stable products instantaneously.

If several rate measurements are made at several temperatures and if they are precise enough to demonstrate a single numerical value for the activation energy, this type of result can be used to claim that the data are consistent with the assumption that the mechanism did not change over the temperature range studied.

Rigorously, however, these measurements do not prove the existence of a single mechanism. Thermal barriers (activation energies) for different mechanisms can have similar values. An additional necessary test to verify a constant mechanism is to demonstrate that the individual rate constants at all temperatures are identical in functional form with respect to all the variables involved in the corrosion process. This requirement implies that temperature acceleration is subject to all the problems and uncertainties of isothermal prediction techniques in addition to many complications that can be introduced by the temperature variation itself. It should be clear that a temperature change that causes a phase change in any reactant (i.e., water going to steam) has the potential to drastically alter the mechanism.

6.2 Isothermal Acceleration and Prediction

6.2.1 Corrosion

Corrosion is a kinetic, non-equilibrium process. The rates and mechanisms of corrosion are dependent upon, among other parameters, the reactants and products of the various corrosion processes.

In order to predict the corrosion rate for times appreciably longer than those studied, the mechanisms of corrosion must be accurately known and it must be assumed that they remain the same over the time required. One of the major obstacles in determining corrosion mechanisms results from observations that rates of corrosion can be seriously altered by the corrosion products and how they are distributed or removed from the corroding interfaces. (Corrosion products can cause either catalysis or inhibition.)

In general, there are more requirements for heterogeneous systems than for homogeneous systems on the use of isothermal rates to predict for times much longer than the time over which the rates were measured. Homogeneous kinetic systems tend toward equilibrium states that are usually well defined. If the isothermal rate expression is rigorously correct and truly represents the mechanisms of the reaction, it will include all the chemical, physical, and geometric factors that are known to alter the rate. For homogeneous systems this can be tested by using the known equilibrium values and showing that the rate goes to zero.

This test is generally not feasible for complicated heterogeneous reactions such as solids corroding in liquids. Here too, it is mandatory in determining the mechanism to show that the isothermal rate expression includes the correct functional dependence of the corrosion rate on all the chemical and physical variables known to affect the rate of corrosion. For heterogeneous reactions, however, it is also necessary to prove that neither the metal nor the metal-

solution interface undergoes any structural, physical, or chemical change that can alter the corrosion rate over the total time for which the prediction is intended.

For metals such changes might include:

- isothermal bulk annealing;
- formation and subsequent breakaway of a surface film;
- stresses developed or removed by formation or cracking of a corrosion product or film;
- diffusion of corrosion products into or out of the metal surface;
- initial selective attack at a site that eventually is depleted;
- grain size changes;
- grain boundary precipitation, etc.

Any or all of these might lead to a change in the corrosion rate with time. In general, the overall corrosion rate of most metals represents contributions from several different mechanisms with different temperature dependencies. These can interact with each other sequentially. For example, consider a corrosion process where an oxide layer is formed by one component in an alloy, eventually builds up, spalls, and continues to form depleting the zone beneath the surface. Over periods of time that are long compared to the time necessary to form the film, the component will diffuse from the bulk to the surface depleted zone. If this component is in equilibrium with its own carbide for example, depletion of the bulk concentration by formation of a surface oxide will eventually cause the carbide to decompose increasing the carbon activity of the alloy. This, in turn, could lead to formation of a new carbide with a different component of the alloy so that short term corrosion rates will not represent the corrosion rates that would occur over longer times. Even in the case of uniform corrosion, Uhlig has noted⁴ "it is often not safe to extrapolate a reported rate to times of exposure far exceeding the test period".

Altering concentrations of reactants and products to test if a single rate expression accounts for the observed corrosion behavior may be more significant for uniform corrosion than for pitting corrosion. Nevertheless, it is, even for uniform corrosion, a necessary but not sufficient condition for justifying time predictions.

In the cases of pitting corrosion, the basic properties of the pitting phenomena indicate that several mechanisms operate simultaneously. For a single mechanism, pits should occur uniformly on the metal surface, proceed with the same depth dependence on time, and develop the same shapes. In real systems, pitting generally occurs at structural irregularities or chemical inhomogeneities that vary from sample to sample. Measurements within the pits, of solution compositions and corrosion product concentrations, show that each pit can be a different chemical system with different mechanisms operating at different times. This is also supported by the wide variability in induction periods, the variability in rates of penetration, and the variabilities in shape development and pit morphology.

For corrosion data in such systems to be meaningful, some type of statistical description of the pitting behavior has to be given. The quality of the statistical description with respect to its ability to predict long term corrosion behavior will be dependent on the quantity and precision of the experimental data. We note as an illustration of some of the problems associated with describing specific pitting corrosion, a discussion from a recent report on a Westinghouse conceptual design for a waste package (AESD-TME-3087 Draft, March 1981):

"Pitting can have its inception in a microscopic surface chemical inhomogeneity, in a physical irregularity, or even in a statistical fluctuation in local corrosion rate. If incipient conditions stabilize sufficiently, pit formation occurs; rapid dissolution occurs within the pit while the cathodic reaction occurs outside it, on adjacent surfaces. The process is autocatalytic, tending to produce an excess of positive charge within the pit, which attracts negatively charged chloride ions (the less mobile OH^- ions remain outside the pit and participate in the cathodic reaction); these further stimulate metal dissolution and create more positive charge. The hydrolysis of excess FeCl_2 accumulating within the pit produces excess hydrogen ions, and the pH decreases (pH values as low as two have been measured in pits occurring in basic bulk solution environments); this further stimulates dissolution. At the pit/solution interface, insoluble corrosion products tend to form due to a reaction between the OH^- ions outside the pit and the ferrous ions within it.

"Pit growth can be impeded by the resistance thus interposed to the migration of ions, or it can be impeded by the pit's own depth and low aspect ratio, which also reduces the rate of ionic migration. Thus, a pit can stop growing if choked with its own debris. However, in a solution which is sufficiently aggressive, so many pits may form that they tend to coalesce. When this occurs, the effect is that of general corrosion, advancing, however, at the higher rate associated with pit formation.

"The solution within a pit tends to be concentrated, and therefore more dense than the bulk solution. Accordingly, gravity has an effect, so that lateral and especially inverted pits tend to cease growth quickly, as the denser solution drains out. On the other hand, lateral pits can turn downward from gravitational influence and can form long channels underneath and parallel to a vertical surface. Further general corrosion will then expose such undercut grooves, and the groove surfaces can be sites for further pits. Top surfaces, of course, represent the worst pitting sites, because the gravity effect tends to stabilize pit growth and pit progress is exactly in the direction for maximum depth of penetration".

Stressing that the most valid justification for predicting long term corrosion rates is the existence of an explicit, highly precise isothermal reaction rate which includes the correct functional description of the corrosion rate on all possible parameters involved in corrosion, we believe that there is as yet no such evidence for any metal being considered for use in a high level waste package.

We believe the NRC will require an isothermal rate expression for the corrosion of TiCode-12 in appropriate repository environments.

6.2.2 Failure Modes

If the failure mode is determined by a single activated process, accelerated temperature testing may be valid. In this case the NRC will require information justifying the failure mode and demonstrating the temperature range over which the process shows a single mechanism.

6.2.3 Problems with Mechanisms of Waste Form Leaching

In support of our concern that the observation of a singly activated process is a necessary but not sufficient condition for justifying a single mechanism, we wish to note a problem associated with the leaching of borosilicate glass.

There is general consensus that in a static condition stage 1, dealcalization reactions occur with a square root time dependence at low to intermediate pH values while the appearance of stage 2, network dissolution reaction occurs with a linear time dependence at high pH. The fractional power relation between the amount of alkali removed Q and the time t , therefore, may be expressed in the form of

$$Q = a t^{1/2} + bt \quad (1)$$

where a and b are appropriate constants. No comprehensive mechanistic studies are available at the present time to explain this relation except that the square root is derived from a diffusion controlled reaction and the linear relation is an interface controlled reaction. The relation is more or less empirical in nature. Most of the experiments are reconcilable with an overall rate process which varies as the ' $t^{1/2}$ ' at short times and low temperatures, and ' t ' at long times and high temperatures.

Although there has been considerable controversy over the transition between the square root to linear regimes, as well as in the extent of the transition and the origin of it, it is generally acknowledged that the change from diffusion controlled stage 1 to interface controlled stage 2 primarily depends on the time required for the pH to reach a value of 9-10. It has been observed that the long transition period occurs only when glass powders are corroded. In powdered glass, concentration cell effects locally increase the surface to volume ratios causing a rapid increase in the pH surrounding many of the glass particles.

At least three different stages are involved in the reaction of water with a silicate glass containing alkali ions: the first is ion exchange of hydronium (H_3O^+) or hydrogen ions from the water with alkali ions in the glass; the second is the partial hydration of the silicon-oxygen network of the glass; and the third is the dissolution of the glass into the contacting solution. Either

or both of the first two steps can be absent, depending upon glass composition or solution pH, and the third is absent when the glass reacts with water vapor instead of liquid water or a solution.

In view of the complexity of the leaching of glass with respect to several different mechanisms which occur or do not occur depending on varied conditions, it would be expected that temperature acceleration is not a valid means of predicting long term performance. In spite of this, some workers have attempted to express the temperature dependence of alkali extraction in terms of the Arrhenius equation. It is not easy to assign a single activation energy, since alkali extraction is always associated with pH changes and these depend not only on the quantity of alkali released but also on that of silica. In addition, below approximately 80°C, a siliceous layer forms on glass which acts to retard further leaching. Metasomatic reactions, in which new crystalline compounds form from some of the glass constituents, can also occur at the glass surface, particularly at elevated temperatures. Such complications make it difficult to theoretically define a single rate-determining step in a given temperature range. Nevertheless, for a large number of nuclear waste glasses, the apparent leach rate appears to follow the Arrhenius equation. (A detailed description of these results are given in the BNL report, "Glass Corrosion - A Review" by Tae-Moon Ahn and Emil Veakis, Appendix A.)

6.2.4 Conclusions

In summary, we believe (1) that existing isothermal corrosion data are inadequate for demonstrating long term integrity for any metallic component being considered for a high level waste package (2) that the use of temperature accelerated corrosion rates to estimate long term corrosion at lower temperatures is, by itself, unacceptable for assuring long term integrity for metallic components of the waste package, and (3) that the use of temperature accelerated leach rates of borosilicate glass, is without additional information on the mechanisms, unacceptable for predicting long term leach behavior of this waste form.

7. REFERENCES

1. "The Evaluation and Review of Alternative Waste Forms for Immobilization of High Level Radioactive Wastes", DOE/TIC-11472, July, 1981.
2. "Nuclear Waste Management Technical Support in the Development of Nuclear Waste Form Criteria for the NRC, Task 1: Waste Package Overview," R. Dayal, et al., NUREG/CR-2333, Vol. 1, BNL-NUREG-51458, February 1982.
3. "Nuclear Waste Management Technical Support in the Development of Nuclear Waste Form Criteria for the NRC, Task 4: Test Development Review," T.M. Ahn, et al., NUREG/CR-2333, Vol. 4, BNL-NUREG-51458, February 1982.
4. H. H. Uhlig, Corrosion and Corrosion Control, p. 13, John Wiley and Sons, New York, NY, 1963.

APPENDIX

GLASS CORROSION - A REVIEW

T. M. Ahn and E. Veakis

EXECUTIVE SUMMARY

This report constitutes a review of various chemical and mechanical processes involved in the degradation of commercial and nuclear waste borosilicate glasses in aqueous environments. An evaluation of the performance of glass in contact with water is warranted given that the material is currently a primary candidate for nuclear waste encapsulation whose behavior in a "worst case" flooded repository condition is in need of assessment. The idealized corrosion kinetics of binary glass systems follow a square root time dependence followed by a linear time law. With multicomponent glass compositions, complications arise as a result of unpredictable behavior of the numerous direct and indirect variables such as temperature, pressure, solution pH, flow rate, glass composition, phase separation and some secondary parameters such as partial devitrification, internal stress, surface roughness and local inhomogeneity. Further, static fatigue is recognized as an important mode of disintegration in the presence of water, and tabulations of gas and ionic diffusivity in glass indicate that toxic radioisotopes may not escape from the waste form by solid state diffusion under repository conditions. Although a quantitative performance assessment cannot be made, given the complications, a qualitative evaluation may be possible. From the data of typical values for the dissolution rate of waste borosilicate glass and from the existence of a static fatigue limit, waste form integrity, at least for the first thousand years, is achievable by an adequate design of waste glass incorporating sacrificial layers avoiding the potential damage arising from radiation damage. For a more quantitative and solid assessment several research topics are also presented for consideration.

CONTENTS

ABSTRACT.	iii
CONTENTS.	v
FIGURES.	vii
TABLES.	x
ACKNOWLEDGMENTS	xiii
1. INTRODUCTION.	1
2. GENERAL CORROSION	2
2.1 Kinetic Law.	2
2.2 Reaction Mechanisms and Kinetic Models	3
2.3 Solution Effects	6
2.3.1 Solution Composition.	6
2.3.2 Solution pH	7
2.3.3 Flow Rate	12
2.3.4 Temperature and Hydrothermal Effects.	16
2.3.5 Reprecipitation	19
2.4 Effects of Various Glass Characteristics	20
2.4.1 Glass Composition	20
2.4.2 Phase Separation.	25
2.4.3 Devitrification	28
2.4.4 Glass Surface Area (SA) to Solution Volume (V) Ratio	28
2.4.5 Surface Stress.	31
2.4.6 Cracking.	31
2.4.7 Other Pretreatments	31
2.5 Cation Selectivity and the Diffusion of Ions and Gases	33
2.6 Weathering	36
3. LOCAL CORROSION AND STATIC FATIGUE.	44
3.1 Static Fatigue Mechanisms.	44
3.2 Slow Crack Growth.	45
3.3 The Law of Time to Failure	45
3.4 Effects of Environmental Interaction	48
3.4.1 Solution pH	48
3.4.2 Humidity.	49
3.4.3 Temperature and Pressure.	49
3.4.4 Glass Composition	49
3.4.5 Flaws	50
3.4.6 Microstructure and Plastic Deformation.	50

CONTENTS, Continued

4. RADIATION EFFECT.	51
5. LONG-TERM PREDICTION MODELS	52
6. CONCLUSIONS AND RECOMMENDATIONS	53
7. REFERENCES.	56
APPENDIX A - SOLUBILITY AND LEACH DATA FOR COMMERCIAL AND WASTE BOROSILICATE GLASS	62
APPENDIX B - APPROXIMATE COMPOSITIONS OF GLASSES MENTIONED IN TEXT (WEIGHT PERCENT)	102

FIGURES

2.1	Five types of surfaces developed during the leaching of silicate glasses	4
2.2	Durability of low-expansion borosilicate glass versus pH of the reagent at a temperature of 95°C.	8
2.3	Rate of attack on Corning 7740 in 5% NaOH at 95°C	8
2.4	Dependence upon pH of the rate of extraction of sodium oxide [mg g-glass ⁻¹ (√min) ⁻¹] from S15 glass at 35°C.	9
2.5	Dependence upon pH of the removal of silica from P15 glass at 35°C	9
2.6	The effect of pH on the leach rate of glasses 189 and 209 at different temperatures	11
2.7	Silica dissolution vs pH curve of SRP glass	11
2.8	Cumulative leaching based on ⁹⁰ Sr analysis of SRP glass	12
2.9	Soxhlet and static water leach rates for glass 189	14
2.10	Soxhlet and static water leach rates for glass 209	15
2.11	Leach rate of waste glass as a function of temperature	17
2.12	Commercial glass composition areas	20
2.13	Effects of components of PNL four components glass on Soxhlet leach rate	24
2.14	Soxhlet leach rate vs change in component from centroid of PNL 11 components glass	25
2.15	Immiscibility boundary of Na ₂ O-B ₂ O ₃ -SiO ₂ glass system	27
2.16	Solution pH vs exposure time for various surface area-to-solution volume ratios (SA/V)	29
2.17	Changeover time in kinetics (t _c) as a function of (SA/V) for various materials	30
2.18	Leach rate (g-glass/m ² -d) based on silicon vs time for 1.90-cm-diameter pellets (solid cylinder is an uncracked sample and the rest are simulated cracked samples).	32
2.19	Diffusion coefficients of sodium in sodium silicate glasses at 386°C as a function of sodium concentration	34

2.20	Self-diffusion coefficients of Ca^{2+} , Sr^{2+} , Ba^{2+} , Pb^{2+} , and Si^{4+} ions in various silicate and borate glasses	34
2.21	Weight change of soda-lime and moderately resistant borosilicate glass after weathering at 98% RH and 50°C.	36
2.22	Na_2O on surface after weathering of moderately resistant borosilicate glass tubing at 98% RH and 50°C	37
2.23	Visual appearance, Na_2O and H_2O generated on moderately resistant borosilicate glass tubing and powder weathered at different RH	37
2.24	H_2O adsorbed on several glasses as a function of RH after 7 days	38
2.25	The effect of cyclic and static RH on visual appearance of various glasses.	38
2.26	Cross section of the weathering crust on a 17th-century wine bottle	42
2.27	Enlarged section of a piece of window glass buried for 288 years	43
3.1	Effect of glass composition on crack propagation rate.	46
3.2	Proof test diagram for borosilicate crown glass II	47
A.1	Material removed at high temperatures from sealed glass tubes exposed to distilled water	63
A.2	Rates of attack by distilled water versus temperature on several glass compositions	64
A.3	Alkali extracted from glass powders of Table A.2 at 25°C and 90°C	65
A.4	Comparative resistance of NBS glasses to acid reagents and water	66
A.5	Comparative resistance of NBS glasses to alkaline reagents	67
A.6	Comparative resistance of NBS glasses to nearly neutral reagents	67
A.7	Corrosion tests on borosilicate glasses in water	69
A.8	Dissolution rates based on individual glass components for borosilicate glass at 70°C	71

A.9	Dissolution rates based on individual glass components for high-silica PGM glass at 70°C	71
A.10	Leach result of Italian glass at 30°C	74
A.11	Leach result of Italian glass at 80°C	75
A.12	Leach result of Italian glass at 100°C.	76
A.13	Leach result of Italian glass at 100°C, water-vapor cycled.	77
A.14	Weight loss of Italian glass as a function of time (T = 50°C)	78
A.15	Weight loss of Italian glass as a function of time (T = 80°C)	79
A.16	Evolution of the total amount of the analyzed elements as a function of time in Italian glass 50°C and 80°C	80
A.17	Leach depth vs time at 90°C when there is Lim RPB in water from Corning test.	85
A.18	Relevance of sodium data of Corning test to the Arrhenius expression	87
A.19	Soxhlet leaching of Mo from glasses (SLA,BNW) and ceramic (STW) loaded with 25 w/o waste oxide simulant from Sandia Test.	90
A.20	Comparison of Soxhlet leaching of mobile (Cs) and immobile (Mo) elements from glass (SLA) loaded with 25 w/o waste oxide simulant from Sandia Test	90
A.21	Estimated corrosion rates (ranges and "probables") as a function of pH of Corning test	99

TABLES

2.1	Results of Soxhlet Tests of U.K. Glass for Yearly Intervals . .	13
2.2	Percent Element in Solution After Hydrothermal Treatment of 76-68 Glass	18
2.3	Leachability Results of 76-68 Glass and Super-Calcine SPC-4 at 350°C	18
2.4	Results of Scouting Autoclave Leach Tests of Various Glasses, Ceramics and Minerals at 250°C	19
2.5	Summary of Defense Waste Glass Durability	23
2.6	Molecular Diffusion in Sodium Borosilicate Glass	35
2.7	Eisenman's Selectivity Orders Among the Alkali Ions	35
2.8	Summary of Visible Damage and Generated Alkali on Various Glasses Weathered 14 Days at 98% RH and 50°C	39
2.9	Profiles of Medieval and Roman Glasses	40
3.1	Parameters for Various Glasses With Different Surface Treatments	46
3.2	Critical Stress Intensity Factor $K_{IC}(MN/m^{3/2})$ of Borosilicate Glasses.	48
A.1	Water Resistance of Glasses (After Nordberg)	62
A.2	Composition of Glasses Studied by Taylor and Smith	63
A.3	Approximate Compositions of Glasses A, B, C, and D of Figure A.2	65
A.4	Compositions of NBS Glasses	66
A.5	Comparative Loss of Material With Varying Surface Areas	68
A.6	Composition of Glass Used in German Leach Tests	72
A.7	Parameters in Italian Waste Glass Research	73
A.8	Leaching Data of Italian Glass	73
A.9	Additional Glass Compositions Examined by Lanza and Parnisari	78
A.10	Variations in Composition of the Surface Layer of Italian Glass	81

A.11	Estimated Thickness of Leached Layer of 72-68 glass	82
A.12	Corrosion Rates of Elements From Nuclear Waste Glass 72-68. .	82
A.13	Composition of Materials Studied at Corning	84
A.14	Relative Values of Results for Standard Tests of Corning. . .	85
A.15	Sodium Reaction Rates at 1 Week and 20 Weeks From Corning Test	86
A.16	Reaction Rate Ranges Based on SiO ₂ Dissolution Results of Corning Test	86
A.17	Predicted Reaction Rates of Corning Test.	87
A.18	Comparison of Chemical Resistance From Corning Test	88
A.19	Ranking of Different Glasses Using Glass No. 2 as Unity From Corning Test.	88
A.20	Comparison of Chemical Durability for Various Glasses From Corning Test	89
A.21	Glasses Tested by Corning	91
A.22	Composition of Simulated Nuclear Waste Included in Waste Glass Tests at Corning.	92
A.23	Natural Geochemical Environments	92
A.24	Experimental Parameters of Corning Test	93
A.25	Corning Glass Grain Results - Acetic (pH 2.9)	95
A.26	Corning Glass Grain Results - Deionized Water (pH 7)	96
A.27	Corning Glass Grain Results - CaCO ₃ (pH 9.3).	97
A.28	Summary of Interpreted Results for all Glasses of Corning Test	98
A.29	Plate Test Results for Glasses A-E (55°C - 2 days)	100

ACKNOWLEDGMENTS

We are grateful to Dr. D. G. Schweitzer whose suggestion on the need for an in-depth assessment of the subject instigated this review and whose guidance and effort made this task possible.

Our gratitude is extended to the BNL Nuclear Waste Management Division staff for their critical reading of the manuscript. We especially thank Drs. P. Soo and S. Davis for their many valuable critiques and suggestions. Finally, we wish to express our sincere appreciation to Ms. Katherine Becker, Ms. Grace Searles and Ms. S. Moore for their efforts and patience in the preparation of this report.

GLASS CORROSION - A REVIEW

1. INTRODUCTION

The predominant effort in the development of a waste form for the containment of radioactive waste is encapsulation in glass.

Glass in contact with water is a "worst case" scenario that assumes nuclear waste repository flooding in which the glass will be subjected to various types of chemical and mechanical damage. The main thrust in waste form development centers on the performance of the waste form as a barrier to radionuclide release. A thorough understanding of the physical and chemical properties of the waste form as well as its probable behavior in a variety of aqueous environments are prerequisites to the assessment of waste form integrity over geological time.

Given the lack of any existing comprehensive reviews, the purpose of this report is to outline the mechanisms of glass corrosion under various laboratory and field conditions through a compilation of current data. Emphasis is given to commercial and nuclear waste borosilicate glasses since these are the primary candidate compositions for nuclear waste encapsulation. The data presented will be relevant to either a direct loading of waste in a glass matrix or to a waste form design utilizing sacrificial glass layers. Other glass types are included for the purpose of comparison and for those instances where these tend to illustrate various processes of glass corrosion common to all glass compositions. Within each section of the report, processes are discussed pertinent to any attempt at long-term prediction of glass corrosion.

The inherent radiation environment of the nuclear waste package is another factor to be considered for the assessment of the integrity of glassy waste forms. A brief summary of the radiation effect and its consequences are also presented.

Since data on most of the processes discussed in the text are not currently available, solubility and leaching data for commercial and waste borosilicate glasses are presented as a separate appendix to this report.

This review will form the basis of our evaluation of glassy and alternative waste forms in BNL's waste package overview and test development tasks for the NRC's Nuclear Waste Management Technical Support in the Development of Nuclear Waste Form Criteria.

2. GENERAL CORROSION

General corrosion is a major mode of leaching in glass. In the discussion that follows we will first summarize the models for dissolution kinetics and corrosion mechanisms. More specifically, the solution effects and the effects of various glass characteristics are critically evaluated for commercial and nuclear waste borosilicate glass. The variables under consideration in evaluating solution effects include solution composition, pH, flow rate, temperature, pressure, and reprecipitation. The discussion of glass characteristics includes composition, phase separation, surface area to volume ratio, surface stress, cracks, surface finish, and matrix inhomogeneity.

Cation selectivity in ion exchange and diffusion of gas and ions are reviewed separately since both characteristics are important to the assessment of radioisotope migration and gas generation over geologic time. Finally, consideration is given to corrosion by weathering particularly by the vapor phase since this is likely condition to be encountered in actual repository environments.

2.1 Kinetic Law

There is general consensus that in a static condition stage 1, dealkalinization reactions occur with a square root time dependence at low to intermediate pH values while the appearance of a stage 2, network dissolution reaction occurs with a linear time dependence at high pH. The fractional power relation between the amount of alkali removed Q and the time t , therefore, may be expressed in the form:

$$Q = a\sqrt{t} + bt \quad (1)$$

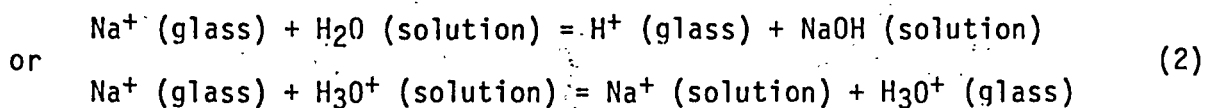
where a and b are appropriate constants. No comprehensive mechanistic studies are available at the present time to explain this relation. The square root indicates a diffusion controlled reaction and the linear relation reflects an interface controlled reaction. The relation is more or less empirical in nature. Most of the experiments are reconcilable with an overall rate process which varies with ' t ' at short times and low temperatures, and ' t^2 ' at long times and high temperatures. Examples include the work done by Berger⁽¹⁾ on glass powders, by Douglas and El-Shamy^(2,3) on alkali-oxide silica and soda-lime silica glasses, and by PNL⁽⁴⁾ on PNL 72-68 glass.

Although there has been considerable controversy over the transition between the square root to linear time regimes, as well as in the extent of the transition and the origin of it, it is generally acknowledged that the change from diffusion controlled stage 1 to interface controlled stage 2 primarily depends on the time required for the pH to reach a value of 9-10. It has been observed that the long transition period occurs only when glass powders are corroded. In powdered glass, concentration-cell effects locally increase the surface-area-to-volume ratios causing a rapid increase in the pH surrounding many of the glass particles.

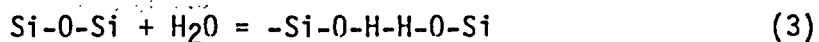
The formulation of leach kinetics through the use of empirical or semi-empirical equations is based on several assumptions such as homogeneous leaching, the preservation of leachant composition, surface area and mechanical integrity. In real situations, these factors should be incorporated into the formulations.

2.2 Reaction Mechanism and Kinetic Models

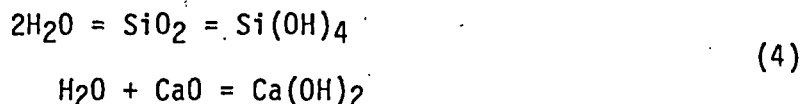
At least three different stages are involved in the reaction of water with a silicate glass containing alkali ions: The first is ion exchange of hydronium (H_3O^+) or hydrogen ions from the water with alkali ions in the glass; the second is the partial hydration of the silicon-oxygen network of the glass; and the third is the dissolution of the glass into the contacting solution. Either or both of the first two steps can be absent, depending upon glass composition or solution pH, and the third is absent when the glass reacts with water vapor instead of liquid water or a solution. The initial exchange of alkali ions in the glass and hydrogen or hydronium ions from water can be described^(5,6) as follows:



In this layer of partial exchange the network structure of the glass is intact and the only change is the replacement of one ion by another. Closer to the glass surface the network can become partially hydrated through the reaction of silicon-oxygen bonds with water:⁽⁵⁾



This partial hydration leads to a more open structure than in the original glass; ions from solution and water molecules can penetrate through this partially hydrated or gel layer with mobilities much higher than in the glass network which remains intact. At extended times of reaction, silicon and other glass constituents dissolve as follows:⁽⁵⁾



The dissolved species are ionized further. Sometimes, hydration involves stress generation in the hydrated layer causing swelling, contraction, cracking or peeling of the layer.

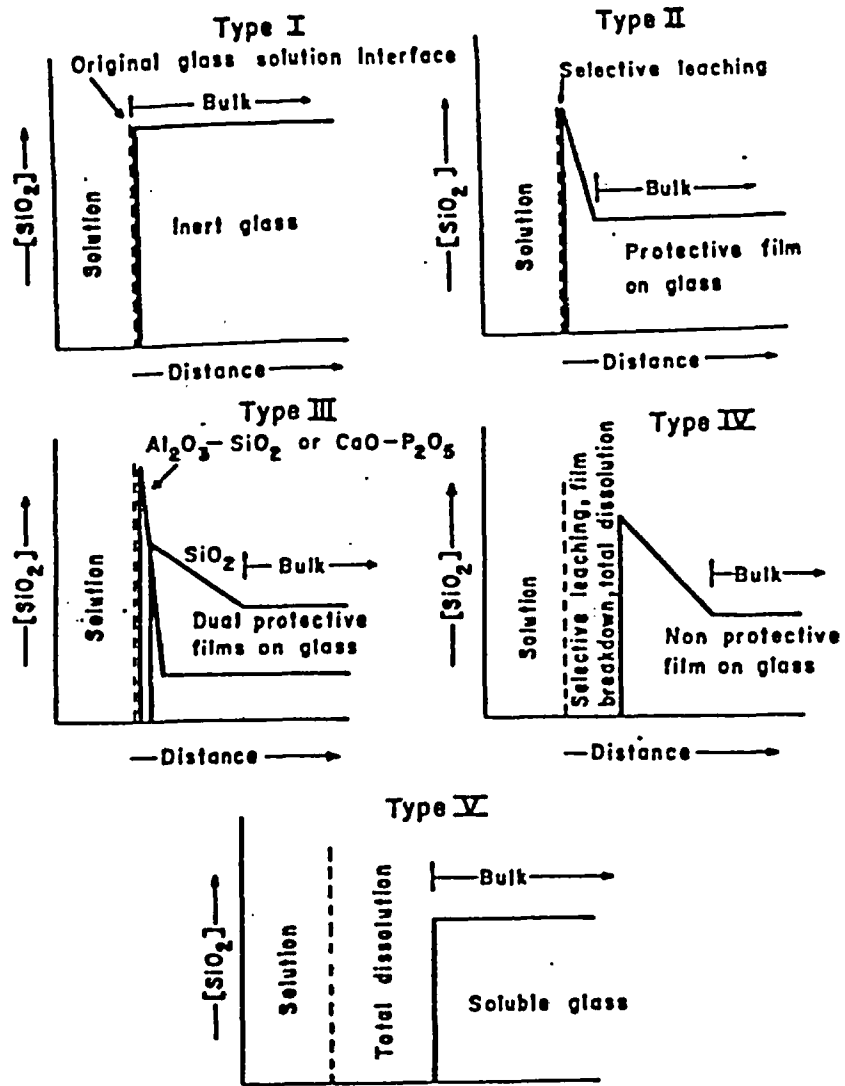


Figure 2.1 Five types of surfaces developed during the leaching of silicate glasses. (7,8)

In more complicated systems, the absence of one or more steps described above leads to another classification of corrosion modes in view of the apparent overall dissolution. The glass may: (1) react with the corrosive materials to form new compounds on the surface; (2) be preferentially dissolved leaving a leached surface layer; (3) be totally dissolved continuously exposing fresh glass. Workers at the University of Florida^(7,8) extended this concept to five types of surfaces (Figure 2.1) of a silicate glass and correlated these to its durability. A type I surface has undergone only a thin, $<50\text{\AA}$, surface layer hydration. Vitreous silica exposed to neutral pH solutions has a type I surface. A type II surface possesses a silica-rich protective film due to selective alkali ion removal. A glass with this type of surface is reasonably durable. Two layers of protective surface films are characteristic of type III. Such glasses are very durable in both acid and alkali solutions. Type IV glass surfaces also have a silica-rich film but the silica concentration is insufficient to protect the glass from rapid attack by dealcalization of network dissolution, resulting in poor durability. A glass of type V undergoes uniform attack losing considerable quantities of ions into solution.

A. Paul⁽⁹⁾ proposed the importance of the thermodynamic stability as well as conventionally studied kinetic stability. The relative influence of either of these two factors on durability will depend on the nature of the test. For low temperature tests, the kinetic aspects will be predominant while thermodynamic considerations will be more important if the surface area of the glass sample exposed to the corroding medium is high, and/or the experiment is carried out at relatively high temperatures. Also, it is very likely that steady potentials will be obtained with conventional glass electrodes within a short time such that the kinetic barrier would not appear to play any important role, at least at the surface of the glass. Paul calculated the stability of different oxides commonly used in glass making (SiO_2 , ZnO , PbO , Al_2O_3 , ZrO_2 , etc.) in aqueous solutions at different pH, and related the quantitative results to the corrosion behavior of various glass compositions. The important finding of this study is that the long-term chemical resistance of a glass may be determined by the thermodynamic activity and stability of its component oxides in aqueous solutions.

A quantitative prediction and interpretation of glass durability as a function of time needs comprehensive analytical models based on the qualitative and mechanistic observations described above. Doremus⁽⁵⁾ proposed a mathematical model in which the two steps of interdiffusion of ions and dissolution of the glass can be combined in a diffusion model where the surface of the glass is progressively removed. By solving the diffusion equations of a moving boundary, the model estimates the kinetics of the cumulative amount Q of ions diffusing out of the glass per unit area; square root of time law at early stages, linear time law at longer periods for a diffusion coefficient independent of composition, and approximately linear time law at longer times for a concentration-dependent diffusion coefficient. Obviously this model is oversimplified considering the many factors involved during the corrosion process such as changes in solution chemistry as well as various glass characteristics which will be discussed separately in later sections. In spite of the

simplification, the study presents important features in the long-term prediction of glass durability. As the corrosion system becomes complicated as in the case of a concentration-dependent diffusion coefficient, the kinetic equations will also be complicated. During the laboratory testing period, the kinetics can be approximated by a linear time law. However, for longer time extrapolation, the exact solution may exhibit significant discrepancy from the linear behavior. Thus, it may not be valid to use the simple apparent linear time law in the prediction of long-term glass durability. Also, the authors have found that even in a simple system it is necessary to make measurements over a range at least three to four orders of magnitude in time to obtain reliable values for the coefficients of \sqrt{t} and t of the kinetics, since it is easy to deceive oneself about the linearity of the plots of Q against t or \sqrt{t} . The interpretation of short-term laboratory data should take these facts into account.

A similar model was proposed by Godbee et al. (10,11) based on mass transport theory which assumes that diffusion through the solid is a rate-limiting process. They include factors arising from more complicated situation such as periodic leachant renewal, initial wash-off of active or contaminated surface, the rapid change of surface concentration as well as the moving boundary condition by surface dissolution. The calculated results show good agreement with the cumulative loss of radioactive isotopes leached by distilled water from waste borosilicate glass and cement. Similar models have been developed by Ewest, (12) for more ideal situations, and by Machiels, (13,14) including surface reaction and diffusion processes. Again it is pointed out that data fitting based on short-term laboratory tests may result in significant discrepancies when such models are applied to long-term predictions.

Workers at Catholic University of America (15-18) have attempted to calculate the cumulative mass release from the waste form over geologic time based on experimentally observed corrosion rates of glass. This model is the first attempt to include the flow conditions and the accompanying pH change of the leachate. The model is purely phenomenological in its assessment of leach rates in that it lacks a basic understanding of the corrosion mechanisms.

At the present time, more comprehensive models that would take into account the complex factors involved in real corrosion systems are not available for estimating glass durability. Due to a lack of basic data, it is perhaps too premature to attempt a complete formulation of corrosion kinetics for glass.

2.3 Solution Effects

2.3.1 Solution Composition

A small concentration of ions present in water or other aqueous solutions affects glass leachability in various ways. Preliminary studies by Hench, et

al.(19) have shown that leach rates in groundwater are greatly decreased from those in deionized water commonly used in laboratory experiments. During the leaching process, the pure solution will undergo compositional change as the rate of surface attack progresses until it reaches a steady-state value; concomitantly the solution will contain some fraction of the ions from the glass components. A significant fraction of the mixed alkali effect, for example, is due to solution ion effects (Mixed alkali effect: If a second alkali oxide, such as potassium, is added to a sodium silicate glass, the durability of the glass is increased; the presence of Na_2O and K_2O together serves to lower the rate of surface dealkalinization).

The influence of the salt compounds in improving durability has been investigated, indicating some of the effects of solution ions on the durability of glass.(4,7) The influence of the salt compounds on leaching are in decreasing order: CaCl_2 , ZnCl_2 , AlCl_3 . Two extremes, Ca^{2+} and Al^{3+} , will be described as follows: Ca^{2+} ions in solution improve the corrosion resistance of binary alkali-silicate glasses by a factor of 10 in comparison with pure water; for Al^{3+} ions (<25 ppm), glass dissolution increased due to a more rapid increase in dealkalinization and resultant solution pH. This is due to insufficient Al^{3+} ions to passivate active surface sites and incomplete formation of stable alumino-silicate surface complexes. At concentrations greater than 25 ppm Al^{3+} , the total dissolution of the glass is greatly reduced. Sufficient concentration of Al^{3+} in solution creates a dual protective film against extensive network dissolution. The rate of selective leaching or ion exchange is relatively unaffected by the presence of Al^{3+} in solution.

In brine solutions, the leach rates of waste glass are generally lower than in DI water and silicate water.(20) Alkaline elements released will enhance the durability because of resultant salinity increases. Cs and Mg, however, have an adverse effect. These changes, though, are well within an order of magnitude. Limited data exist on the effects of anions and organics in leachants. The oxidation potential (Eh) is also controlled by the small concentrations of the ions present in solution. For all practical purposes, Eh effects would tend to be insignificant under repository conditions.

2.3.2 Solution pH

There is a fundamental difference between chemical attack by water or acids and that of alkaline solutions. The former limit their action to the other constituents but have very little effect on silica, while the latter attacks all constituents, including silica. The general effect of pH of the solution on the relative rate of attack for a low expansion borosilicate glass is shown in Figure 2.2. The test was performed at a temperature of 95°C. Figure 2.3 shows the rate of attack for a borosilicate glass (Corning 7740) in 5% NaOH at 95°C. Below pH 7, alkali or alkaline earth ions are replaced by hydrogen or hydronium ions, but the silica matrix of the glass is unaffected. As the solution becomes more alkaline, the silicic acid formed by bulk

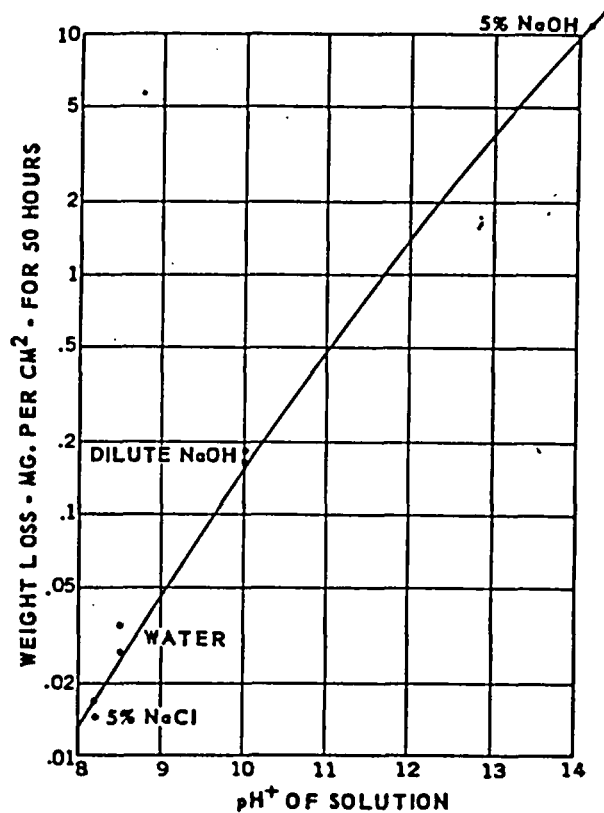


Figure 2.2 Durability of low-expansion borosilicate glass vs pH of the reagent at a temperature of 950C. (21)

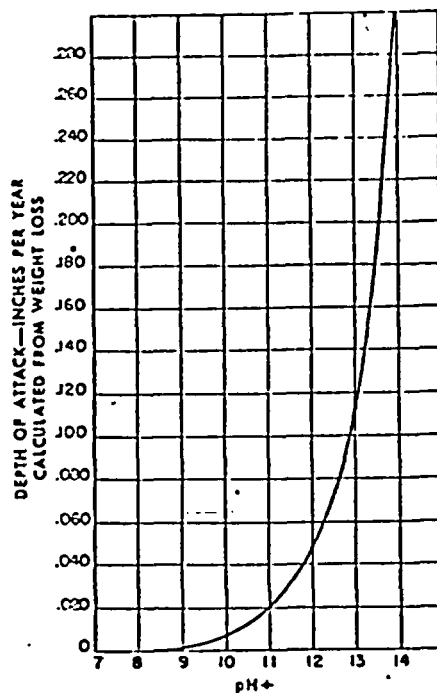


Figure 2.3 Rate of attack on Corning 7740 in 5% NaOH at 950C. (22)

bulk amorphous silica in water ionizes and dissolution becomes more rapid. Because of the ionization reactions, the solubility of amorphous silica increases sharply above a pH of about 9, leading to a sharp increase of the dissolution rate above this value. The dissolution of silicate glasses, therefore, shows a strong dependency on the solution pH. The dissolution rate is not influenced much by pH in neutral or acidic solutions because the dissolving species (non-ionized silicic acid) has a nearly constant solubility. In a static leaching condition, a transition occurs by the replacement of alkali ions to increase silica dissolution. Hench⁽¹⁹⁾ explained this transition in terms of typical surface structures (see Fig. 2.1); the change from a protective surface (type III) to a rapidly deteriorating surface (type IV or type V).

El-Shamy et al.⁽²³⁾ presented experimental data on the dependence on pH of the decomposition for a number of alkali oxide-silica and soda-lime-silica glasses. Typical examples are shown in Figures 2.4 and 2.5. Sodium extraction is indicated for S15 glass; silica removal is shown for P15 glass.

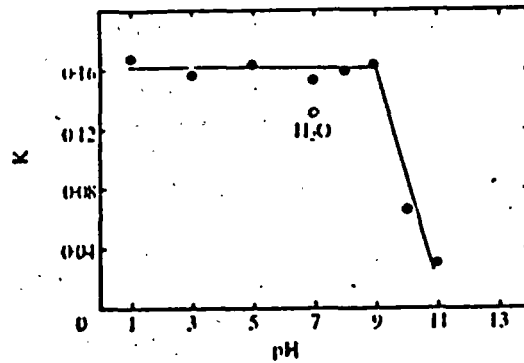


Figure 2.4 Dependence upon pH of the rate of extraction of sodium oxide $[mg\ g\text{-glass}^{-1} (\sqrt{\text{min}})^{-1}]$ from S15 glass at 35°C.⁽²³⁾

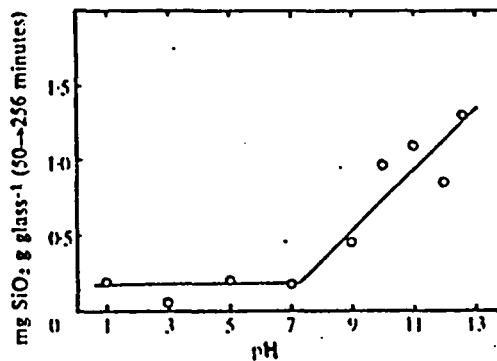


Figure 2.5 Dependence upon pH of the removal of silica from P15 glass at 35°C.⁽²³⁾

The addition of other constituents, such as lime, only slightly modified the typical shapes of the graphs. For more complicated commercial glasses, this general trend may still be valid with some modifications for the addition of multicomponents. The quantitative and detailed effects of these multicomponents are not known at the present time. Some examples are given below.

In alkaline solutions, boron oxide in Pyrex borosilicate glass does not influence, to any great extent, the rate of dissolution of the silicate lattice, while in some instances (7050 glass) it leads to reduced alkaline durability. Similarly, in 0010 glass a small amount of lead has little effect on durability, while in larger concentrations it reduces alkaline durability.

Certain ions in the glass can lead to preferential attack by acid solutions. Glasses containing substantial amounts of boron, aluminum, or lead, such as Corning 1720 and 7050, are much more rapidly attacked by acid than soda-lime glass, while Pyrex and vitreous silica glasses retain their durability. The high solubilities of boron, aluminum, and lead oxides in acid apparently lead to their deleterious influence on the durability of glass.

Such complications lead to the unexplainable pH dependence on the leach rates of U.K. borosilicate waste glass as shown in Figure 2.6⁽²⁴⁾. It can be seen that the leach rates are increased by low pH leachants. At high pH the leach rates are also increased. Similar results were also obtained for Savannah River Plant (SRP) borosilicate waste glass covering a wider range of pH than the U.K. study. The SRP results are shown in Figure 2.7 and 2.8.^(25,26)

Waste glasses usually contain less than 50 wt.% SiO₂ while commercial container glasses contain more than 70 wt.% SiO₂. This accounts for the difference in behavior at lower pH.⁽²⁷⁾ At high pH, the trend of leach rates generally follows that of commercial glasses. In actual repository conditions, the unbuffered solution would have little effect on the leach rate while a buffered solution may change the leach rates significantly as a result of the pH shift.

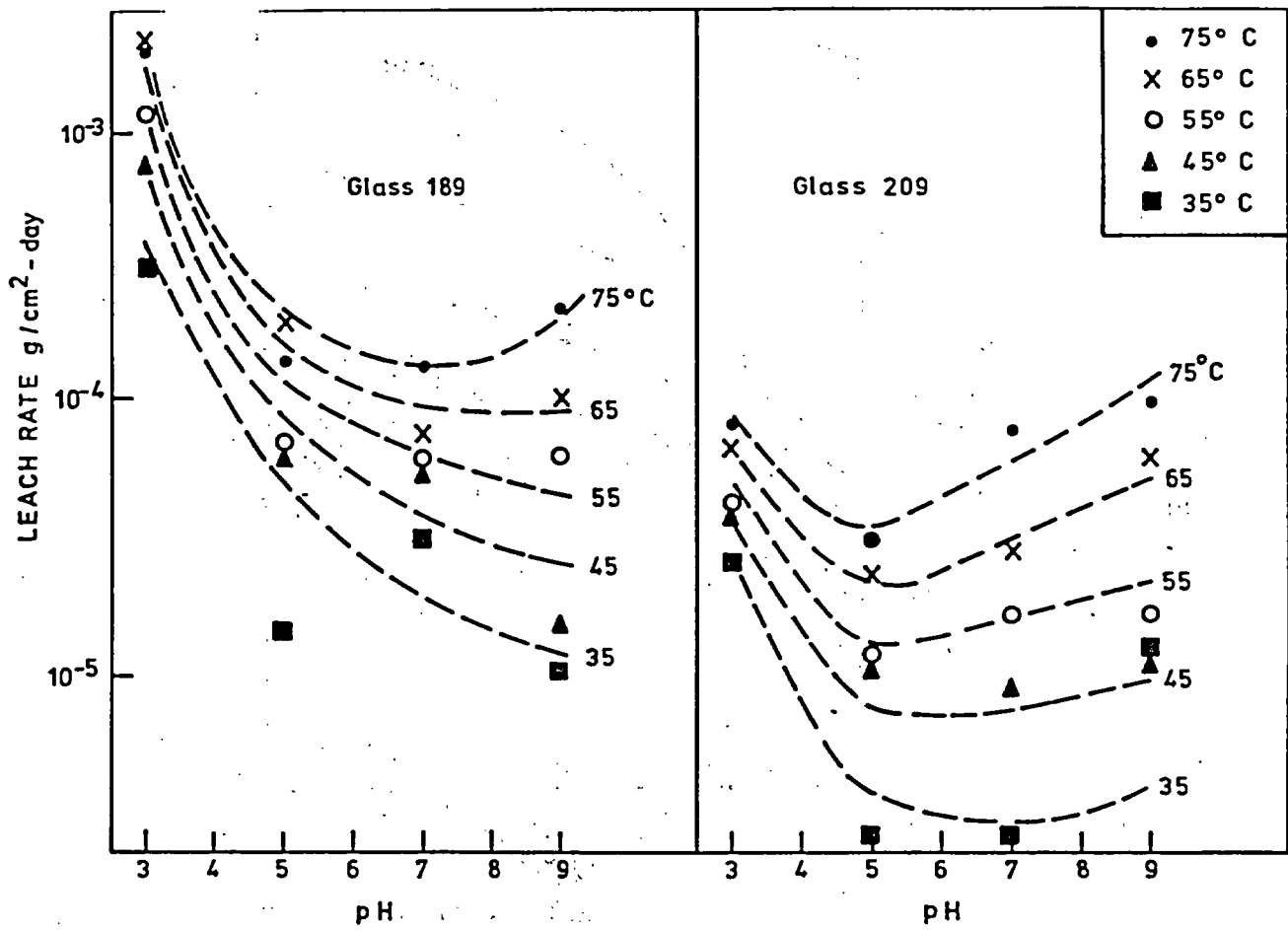


Figure 2.6 The effect of pH on the leach rate of glasses 189 and 209 at different temperatures.(24)

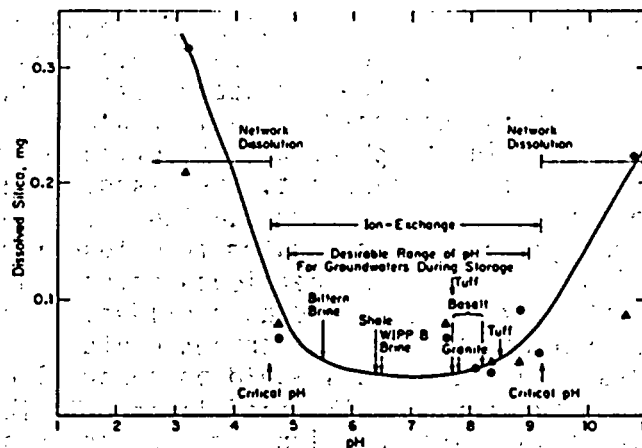


Figure 2.7 Silica dissolution vs pH curve of SRP glass.(25)

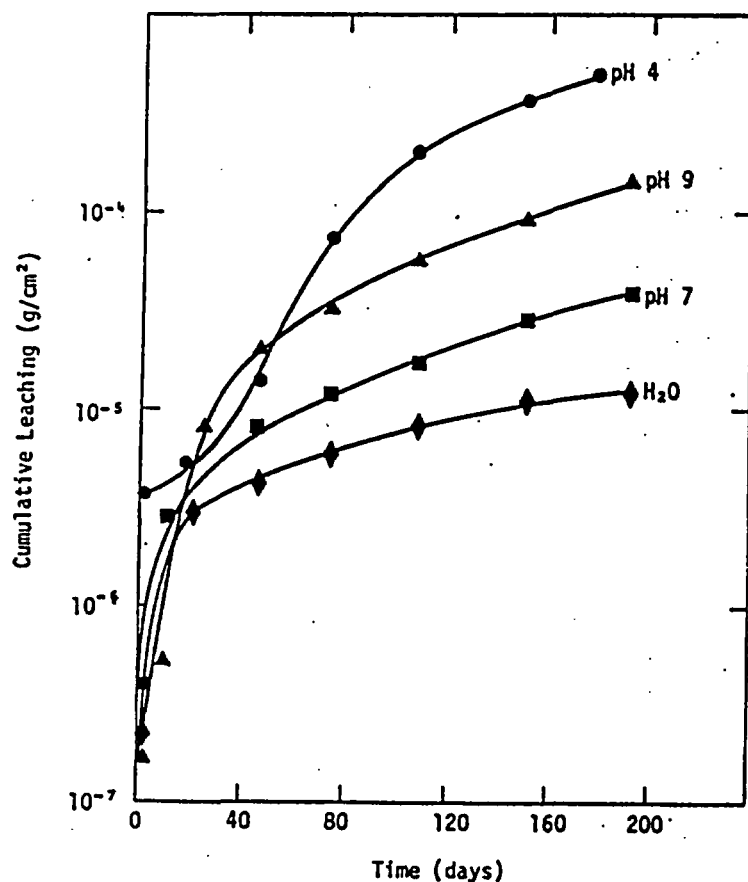


Figure 2.8 Cumulative leaching based on ^{90}Sr analysis of SRP glass. (26)

2.3.3 Flow Rate

The replenishment or flow of solutions has been reported as showing two opposite effects on the glass corrosion. In a leach test of $\text{K}_2\text{O-SiO}_2$ glass at 40°C (3), a marked increase in the extraction of silica was shown as the number of replenishments is decreased. The increase can be attributed to the evident accompanying rise in the pH of the attacking solution. If the flow rate is slower than the rate of replenishment, the dissolution rates will slow down as a result of the saturation of the surrounding medium by silica. (17) If the flow rate is high enough to keep the system from leaching saturation, this could account for conditions exhibiting higher leach rates. However, should reprecipitation of insoluble hydroxides, hydrates oxides, or silicates at high pH occur, radionuclide release to the environment could be saturated. (28) At very high flow rates, the leach rates would be controlled by the pH of the medium and the stability of the dealcalized layer. Taylor and Smith (21) reported a significant increase in weight loss under these erosive conditions.

Some leach data are available for the behavior of waste borosilicate glass subjected to different flow rates. Leach rates on British waste glasses⁽²⁴⁾ were obtained using a Soxhlet apparatus, heating in static water, and exposed to flowing (1×10^{-8} m³/sec) water. Duration of the tests was dependent on time sufficient to achieve a measurable weight loss. This varied from approximately one week at 100°C to several months at ambient temperature. Leach rates were obtained (Figures 2.9 and 2.10) over a range of temperatures. The figures point to higher leach rates in the Soxhlet method over the static. Glass 189 was doped with 5 weight percent ²³⁸Pu and stored. The results obtained in Soxhlet leach tests for yearly intervals are shown in Table 2.1. It is evident that higher leach rates are obtained using the Soxhlet method than in static tests. Under repository conditions, the slow flow rates would tend to have an insignificant affect on the leach rates as indicated by the above observations.

Table 2.1

Results of Soxhlet Tests of U.K. Glass for Yearly Intervals⁽²⁴⁾

Temperature (C°)		Total Dose Over 3 yrs Disintegra- tions per g	Leach Rates, (g/cm ² -day) at 100°C		
First yr	Subsequent yrs		After 1 yr	After 2 yrs	After 3 yrs
50	20	2.7×10^{18}	1.6×10^{-3}	2.3×10^{-3} 2.4×10^{-3}	2.3×10^{-3}
170	20	2.7×10^{18}	1.5×10^{-3}	2.3×10^{-3} 2.2×10^{-3}	2.6×10^{-3}

A-14

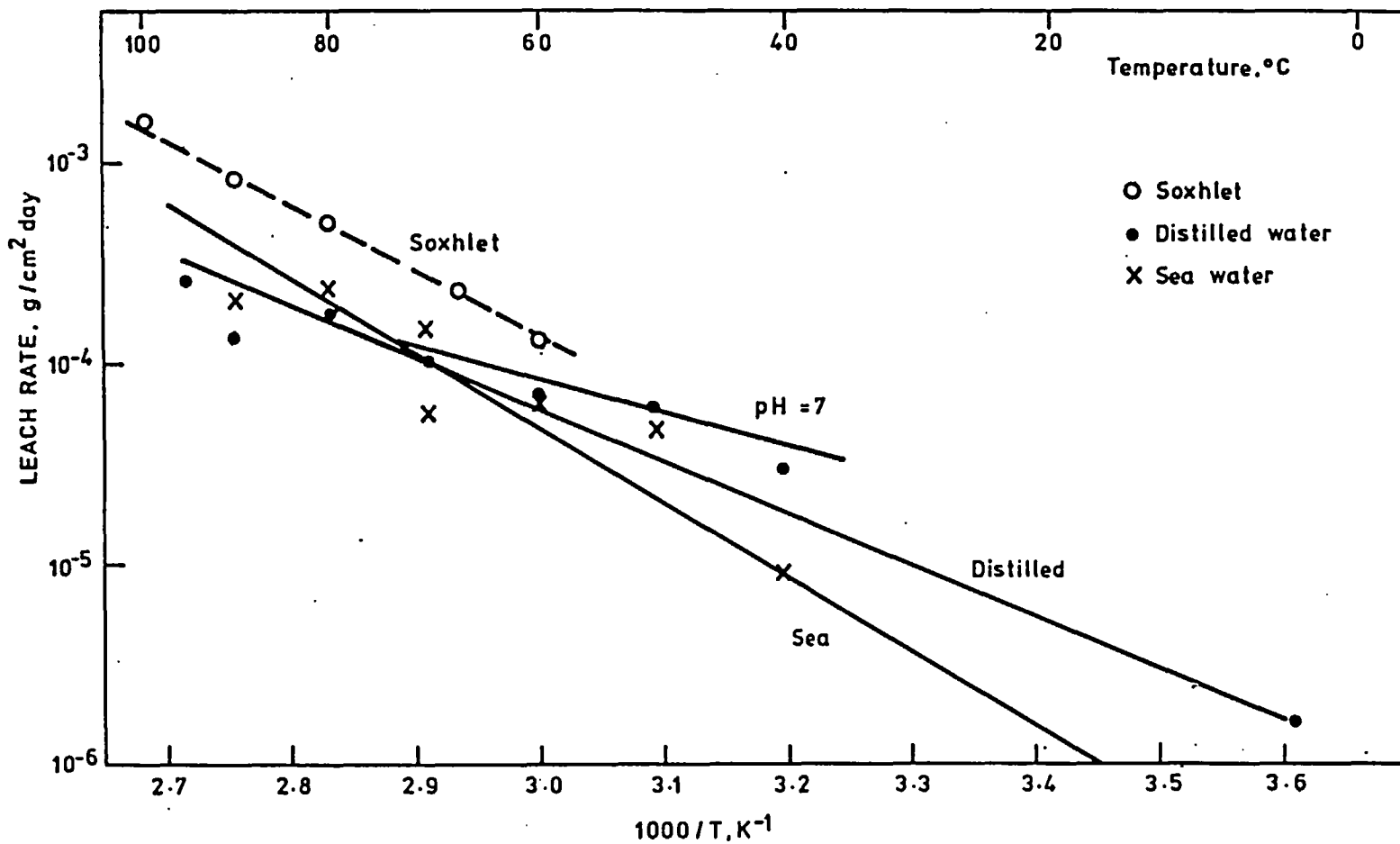


Figure 2.9 Soxhlet and static water leach rates for glass 189. The Soxhlet results for temperatures below 100°C were obtained by boiling the water under reduced pressure. The leach rates in flowing water (pH=7) are included for comparison. (24)

A-15

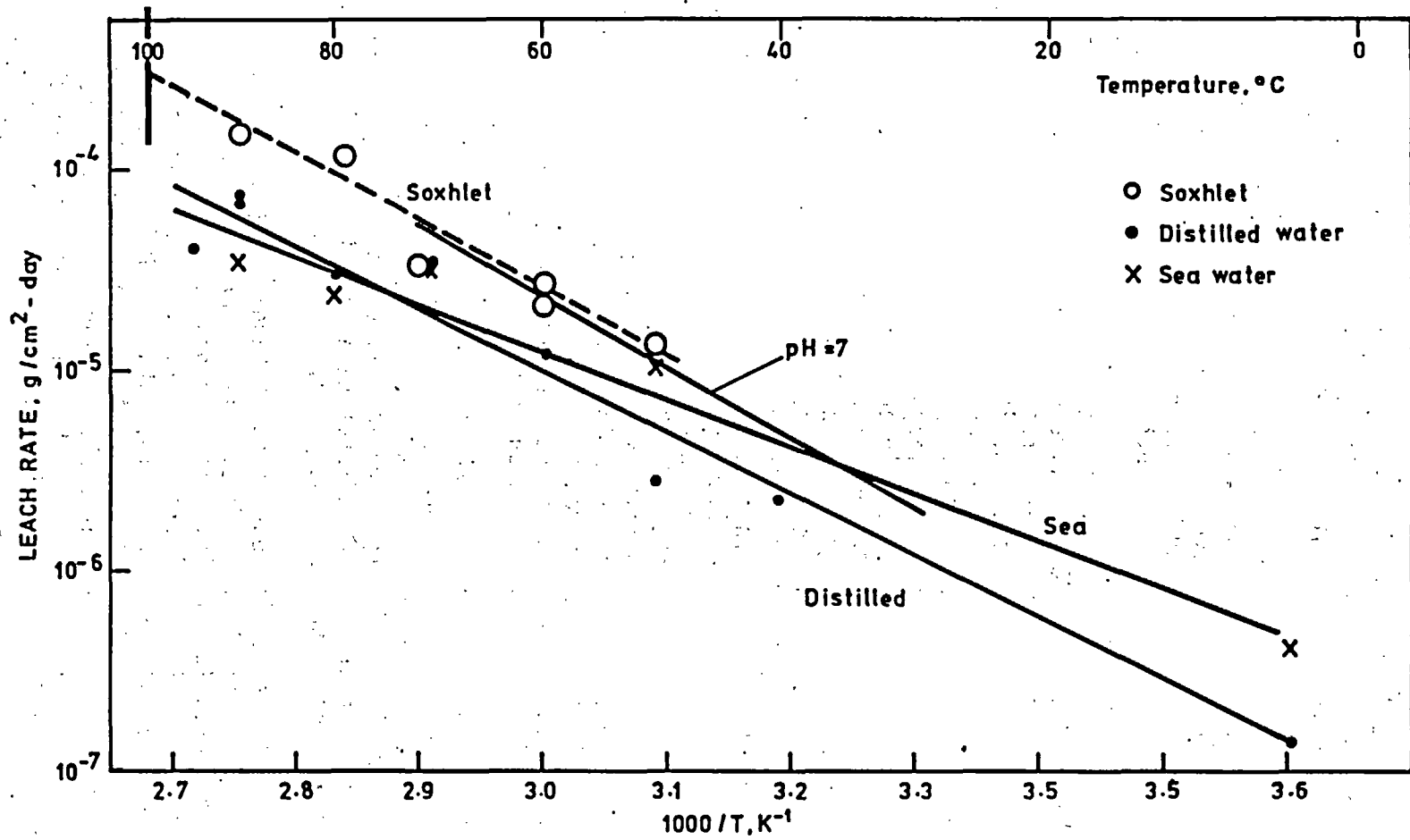


Figure 2.10 Soxhlet and static water leach rates for glass 209. The vertical line at 100°C shows the spread of 11 different Soxhlet results. (24)

2.3.4 Temperature and Hydrothermal Effects

The quantity of alkali extracted from a glass in a given period of time increases with increasing temperature. The type of reactions which control the release of radioisotopes in waste glass are also affected by temperature. For most silicate glasses, the quantity leached in a given time is nearly doubled for every 8°C to 15°C rise in temperature and the reaction rate increases by a factor of 10-100 for every 100°C increase in temperature, depending on the composition of the glass and the type of alkali ion. Some workers⁽⁹⁾ have attempted to express the temperature dependence of alkali extraction in terms of the Arrhenius equation. However, it is not easy to assign a single activation energy, since alkali extraction is always associated with pH changes and these depend not only on the quantity of alkali released but also on that of silica. Further, below approximately 80°C, a siliceous layer forms on a glass which acts to retard further leaching. Metasomatic reactions, in which new crystalline compounds form from some of the glass constituents, can also occur at the glass surface, particularly at elevated temperatures. Such complications make it difficult to theoretically define a single rate-determining step in a given temperature range. Nevertheless, for a large number of nuclear waste glasses, the apparent leach rate follows the single activation energy Arrhenius equation.⁽³⁰⁾ For PNL waste glass,⁽²⁹⁾ such an observation was made as shown in Figure 2.11; representative leach rates at 25°C are 1×10^{-6} to 1×10^{-5} g of glass/cm²-day. Representative leach rates at 40-50°C are 5×10^{-6} to 5×10^{-5} g of glass/cm²-day. Similar results for U.K. waste glass 189 and 209 were reported by measuring the leach rate over a range of temperatures using static and Soxhlet methods. The results are shown in Arrhenius plots in Figures 2.9 and 2.10.⁽²⁴⁾ White⁽³⁰⁾ has found the expected exponential increase in rate with temperature well up to the hydrothermal range. This is noteworthy for the assessment of waste glass durability since accelerated testing at high temperature may be a valid means for the simulation of leaching over geological time as a result of this single activation process. However, it is premature to define the leaching mechanism based on these activation analyses due to a lack of data and the system's complexity, which is described below.

In hydrothermal environments, the complexity is more significant since glass is altered rapidly if the temperature is sufficiently high. Although it is generally assumed that the maximum temperatures at which water will contact a solidified waste form in a repository are more likely to be in the range of 150°C, or less, substantial research efforts have been invested in hydrothermal reactions of waste glass in the last two years.

Hydrothermal effects were investigated at Sandia on a copper borosilicate glass (PNL 76-199) with simulated Barnwell fission product oxide waste.⁽³¹⁾ The tests were conducted in autoclaves for periods of 1 week to 3 months at 250°C and 16.5 MPa. The leach solutions used were: (1) deionized water; (2) high Mg⁺² (35,000 ppm) saturated brine; (3) saturated NaCl brine with low Mg⁺² (10 ppm); and (4) seawater. The rate of corrosion and cesium extraction increased in the order: deionized water < NaCl brine < MgCl₂ brine < seawater; lower pH values lead to higher cation solubilities. Gel layer cracking was reported in glass exposed to deionized water. Devitrification was evident but no crystalline phases were identified.

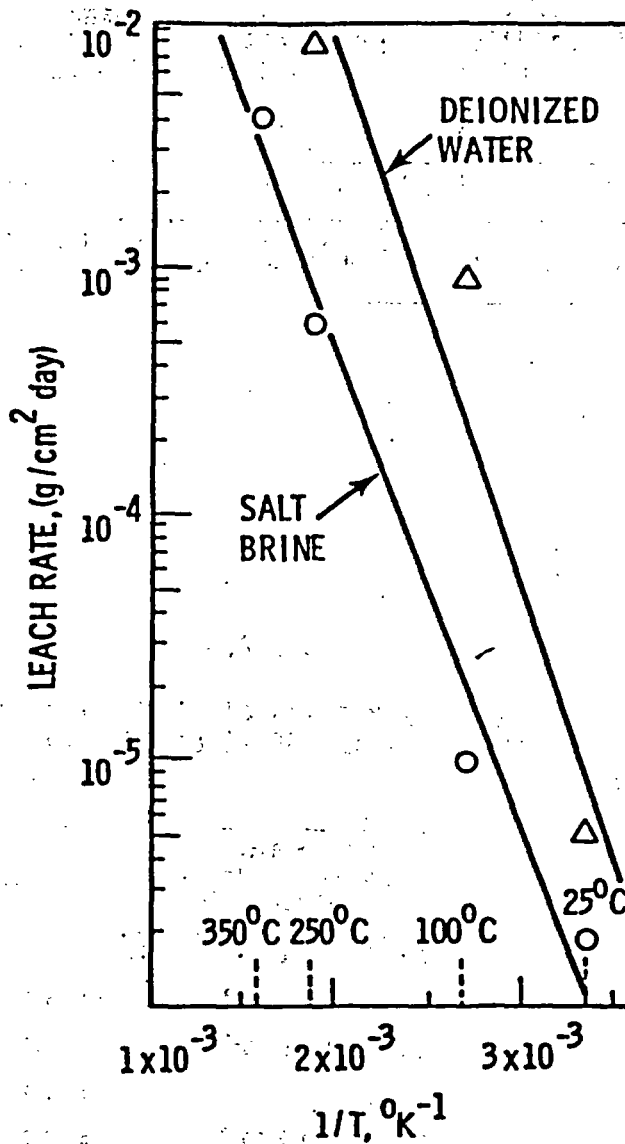


Figure 2.11 Leach rate of waste glass as a function of temperature. (29)

Tests conducted on PNL 76-68 glass at 300°C and 300 bars in deionized and artificial Hanford groundwater, resulted in the conversion of the glass sherds to crystalline and non-crystalline products plus dissolved species in a two week period. The major products were $(Cs, Na, Rb)_2(UO_2)_2(Si_2O_5) \cdot 4H_2O$ (wecksite) and pyroxene-like phases $(Na, Ca)(Fe, Zn, Ti)Si_2O_6$ (acmite, augites). High Na_2O and low SiO_2 may be responsible for the rapid alteration of the sample. The PNL results indicate that the alteration of the glass pellet was higher in deionized water than in brine by a factor of 10. (see Tables 2.2-2.4)

Table 2.2

Percent Element in Solution After Hydrothermal Treatment of 76-68 Glass⁽³²⁾
(4 Weeks at 300°C and 300 Bars)

	Cs	Sr	La	Nd	U	Zr	Na	Rb	Ca	Ba	Zn	Si	Mo	B	Fe	Ni	Cr
Defonized water	5.0	0.2	0.5	--	0.03	---	45	8.7	1.2	0.1	0.05	4.6	72	93	0.02	4.0	27
USGS MBT-6a brine	52	49	26	11	18	0.05	--	53	---	---	33	---	3	48	0.02	10.4	1.1

Table 2.3

Leachability Results of 76-68 Glass and
Super-Calcine SPC-4 at 350°C⁽³²⁾

Test	Material	Solution	Time	Leach Rate Based on Weight Loss (g/cm ² -d) ^a	Percent of Element in Solution ^b							
					Cs	Rb	Sr	Mo	Si	B	U	Zn
1	Glass 76-68	Brine	7 d	4.0 x 10 ⁻³	66	72	3.6	54	0.2	71	<0.1	0.5
2	Glass 76-68	Brine	7 d	4.6 x 10 ⁻³	80	82	3.4	59	0.2	73	<0.1	0.3
3	Glass 76-68	Brine	21 d	4.5 x 10 ⁻³	95	90	4.8	62	0.1	89	<0.1	0.3
4	Glass 76-68	Brine	21 d	c	70	96	3.4	c	0.1	89	0.2	0.6
5	Glass 76-68	Defonized Water	7 d	5.3 x 10 ⁻³	6	16	0.2	49	2.2	100	0.1	<0.1
6	Glass 76-68	Defonized Water	21 d	4.0 x 10 ⁻³	4	20	0.4	63	1.9	86	0.2	<0.1
A	Super- calcine SPC-4	Brine	3 d	c	46	80	3.3	0.6	0.5	c	c	c

^aWeight loss of a cylinder of material divided by its geometric surface area and time.

^bEach test included roughly 20% by weight of a solid cylinder and 80%-325 mesh powder. The majority of ions in solution were leached from the powder.

^cNot available or not present.

Table 2.4
Results of Scouting Autoclave Leach Tests
of Various Glasses, Ceramics and Minerals at 250°C(32)

Sample Material	Leach Rate, g/cm ² -day ^a		
	50 mL Brine Solution	150 mL Brine Solution	50 mL Deionized Water
Soda-lime-silica glass (NBS No. 710)	3 x 10 ⁻³		
Borosilicate glass (NBS No. 717)	5 x 10 ⁻⁴		
Waste glass 72-68	7 x 10 ⁻⁴		
Waste glass 76-68	2 x 10 ⁻⁴	2 x 10 ⁻³	8 x 10 ⁻³
Granite	6 x 10 ⁻⁴		
UO ₂ fuel pellet	2 x 10 ⁻⁴		
Alumina	2 x 10 ⁻⁴		
Sintered Supercalcine (SPC-2)		4 x 10 ⁻⁴	

^aSamples immersed in simulated WIPP "B" brine for 72 hr at 250°C and 1000 psi. Leach rate based upon weight loss and geometric surface area.

As a result of these tests the role of water under hydrothermal conditions may be described as follows:

- (a) Crystallization catalyst: acts to convert a Na-Fe rich glass into Na-Fe rich crystalline pyroxene-like phases
- (b) Solvent and transport medium: dissolves and transports Cs, Na, U, and Si from a glass at weeksite-like crystalline
- (c) Reactant: forming hydrated weeksite-like phase and a hydroxyapatite.

Additional research reported hydrothermal alteration of powdered sodium zinc borosilicate glass at temperatures up to 200°C.⁽³³⁾ Zincsilite is a major product in the alteration. The addition of ZnO was found to improve durability at 100°C through the formation of a Zn-rich alteration zone. ZnO is said to promote subliquidus immiscibility in borosilicate glasses.

Under hydrothermal conditions, alteration is a major variable influencing the enhanced leach rate. Since the alteration is accompanied by complications such as stress generation, a delineation of the mechanisms involved in hydrothermal leaching is not easily achieved.

2.3.5 Reprecipitation

The dissolved silica begins to recrystallize under prolonged leach conditions. Barkatt⁽³⁴⁾ observed the recrystallization of Pyrex glass in water at a pH of 9.5. It was further observed that multivalent ions and species are tightly bound to the matrix by the recrystallization process. Recrystallization has received recent attention as a result of its effect on the measurement of leach rates by solutions analysis. It is quite easy to distort leach data by ignoring the analysis of precipitates in solution. When, under what conditions, and to what extent precipitation takes place depends largely on the system. The controlling mechanisms and accompanying variables are only recent subjects requiring further investigation.

2.4 Effects of Various Glass Characteristics

2.4.1 Glass Composition

Before presenting specific illustrations of compositional effects on the chemical durability of commercial and waste borosilicate glass, we will briefly outline a general approach taken by Adams, et al. (35) to "force-frit" complex commercial glasses into a ternary description composed of network formers, B_2O_3 , and network modifiers. The sum of network formers is described as XO_2 which replaces SiO_2 in the ternary scheme and generally consists of additional oxides such as Al_2O_3 , ZrO_2 , TiO_2 , Fe_2O_3 , Cr_2O_3 , P_2O_5 , Y_2O_3 , MoO_3 , TeO_2 , La_2O_3 , CeO_2 , Pr_6O_{11} , Nb_2O_3 , Gd_2O_3 and Sm_2O_3 . Network formers are known to be relatively insoluble in water. The network modifiers include the sum of all alkali oxides, R_2O , such as Na_2O , K_2O and Li_2O . They generally weaken the networks and are readily soluble in water. The alkaline earths or divalent atoms, RO can be considered as part of XO_2 since they generally enhance water durability, or as part of the R_2O since the role of RO in the formation of crystallographic structures is similar to that of R_2O . RO includes oxides such as CaO , MgO , PbO , ZnO , BaO , SrO and NiO . In this study compositions of various commercial borosilicate glasses were plotted in the ternary system of $XO - B_2O_3 - R_2O (+RO)$ (Figure 2.12). Approximations were made for the lines of equivalent durabilities (isodurs) using a model based on the correlation between the integrity of crystallographic structure and the chemical durability. Numbers 1, 2, and 3 are in decreasing order of the chemical durability. Since their model is empirical in nature and supported by experimental data, the contour lines illustrate fairly well the general trend of the composition effect.

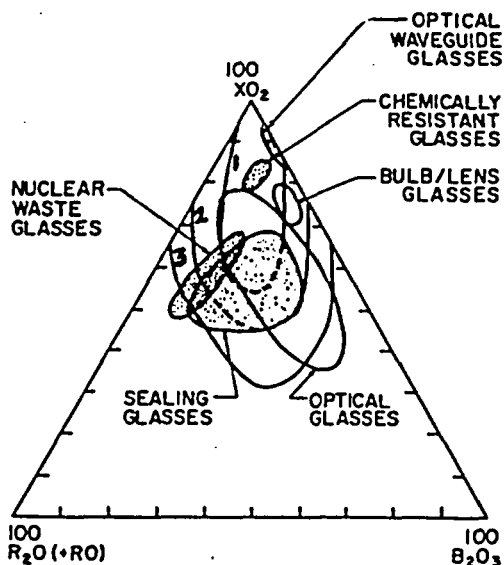


Figure 2.12 Commercial glass composition areas. (35)

The composition effect has been studied, qualitatively in most cases, (5,7,9,15,32,33) by considering whether the component: (1) is thermodynamically stable in a given pH-temperature range and affects the thermodynamic stability of other components; (2) affects the formation of insoluble surface film and concomitantly retards or accelerates the surface dissolution rate; (3) affects the diffusion rate of certain ions responsible for the observed dissolution rate (such ions include hydrogen ions, hydronium ions or other cations); (4) influences the solution chemistry, especially the pH; and (5) changes the crystallographic structure of the network leading to a change of dissolution rate. The studies vary from simple binary systems to complex multicomponent systems while the majority restrict their tests to room temperature. Nevertheless, as shown in the beginning of this section, the general trend can still be observed from room temperature to maximum 100°C for the borosilicate glass system. A summary of the effects of particular components is given below.

Network Formers

- SiO_2 : The stability of vitreous silica has been illustrated for a given pH range at room temperature as shown in Appendix A.1. The solubility or dissolution rate increases rapidly at pH above 9 by the increased ionization of silicic acid. The solubility increases linearly with temperature up to 200°C.
- Al_2O_3 : The addition of Al_2O_3 slightly increases alkaline durability and mechanical abrasion resistance. Presumably this improvement is attributed to: (1) decreased mobility of hydronium and alkali ions, (2) formation of a protective aluminosilicate film in a static condition, (3) the stabilization of calcium-silicate-rich film, and (4) the reduction of the effect of pH in the glass dissolution.
- ZrO_2 : A small amount of ZrO_2 (about 2 weight percent) increases acid and alkaline durability. The hydrated ZrO_2 surface is stable at all conceivable pH ranges and offers a very high activation barrier for the diffusion of other ionic species.
- TiO_2 : Similar to Al_2O_3 and ZrO_2 , TiO_2 is expected to increase in chemical durability. However, no measurements of ionic mobilities are available.
- P_2O_5 : An extensive investigation of corrosion reactions of an inert soda-lime-silica glass containing P_2O_5 has been conducted because of the incredible property of the glass to form a strong and stable bond with living bone. This is attributed to the formation of a stable calcium phosphate film when in contact with an aqueous environment (type III surface in Figure 2.1), occasionally accompanied by the formation of a fine-grained polycrystalline apatite mineral phase.

B₂O₃

B₂O₃ causes a reduction in the diffusion coefficient of alkali ions. In Pyrex borosilicate glass, the diffusion coefficient is low compared to other silicate glasses, including fused silica, and it also accelerates inert film formation as in the case of the P₂O₅-containing glass. The extracted B₂O₃ acts to neutralize the alkali and reduce the solution pH. These effects combine to increase glass durability.

Network Modifier: R₂O

As the amount of monovalent alkali element increases with the remaining constituents held in the same ratios, the rate of reaction with water increases. In static solutions this trend is primarily related to the increase in the total quantity of alkali in solution surrounding the glass. This leads to a progressively more alkaline solution and a rapid attack of the glass. The diffusion coefficient of alkali increases as the amount of alkali in the glass increases. This increased reaction rate has also been interpreted in terms of surface effects (type IV surfaces in Figure 2.1).

The relative durability "contribution" of ions among the R₂O group is in the order is Li₂O > Na₂O > K₂O. Their role in the formation of a durable SiO₂-film is reflected in this order. It has been observed that the hydronium ions have a higher mobility in potassium. Also, from the thermodynamic point of view, the absolute stability increases in the above order.

If a second alkali oxide, such as potassium, is added to a sodium glass, the durability of the glass is reported to increase. The increase is greatest when the molar ratio of alkali ions is about equal. This increase is a result of the "mixed-alkali" effect, in which the mobility of an alkali ion is reduced when another alkali ion is added, or when the second alkali aids film formation leading to a limited surface attack.

Network Modifier: RO

- CaO: The addition of calcium oxide improves the durability and reduces the extent of selective alkali leaching (up to approximately pH 10). It appears that the addition of calcium lowers the mobility of alkali and hydronium ions. When the alkali ions are lost during corrosion, they leave behind a much more stable CaO-SiO₂ rich film reducing the surface dissolution rate. However at high temperatures, CaO greatly weakens the glass network.
- MgO, SrO, BaO, CdO: These oxides of divalent metals give a similar enhancement of durability as CaO. SrO is known to provide a greater resistance to the destruction of the above-mentioned calcia-silicate surface film. The addition of BaO is reported to reduce the extent of selective alkali leaching.
- ZnO: ZnO addition to a silicate glass increases its chemical durability in the alkaline range up to approximately pH 13, and is

susceptible to vigorous alkaline attack above pH 13. Also, zinc-containing glass will be susceptible to acid attack up to approximately pH 5.5.

- PbO: It is generally known that lead oxide increases the alkaline durability and decreases the acidic durability.

The preceding discussion on the composition effects and the particular mechanisms involved was aimed at providing a brief summary on a complex subject. Most of the data presented were obtained for relatively simple systems (usually ternary components). As the number of components increase, the characteristics described should be modified to some extent, especially when nuclear waste is incorporated. Quantitative measurements relating to composition effects are scarce at the present time. One attempt made by PNL (37) centered on the effects of 26 oxides in a generic study of defense waste glass. Chemical durability was tested in acid and basic solutions, at RT and 99°C, in distilled water; percent weight loss was determined for each of the samples. Table 2.5 is a summary of the results which shows a general agreement with the summary of each component described previously. In addition, the effects of U₃O₈, MnO₂, Fe₂O₃ and NiO were observed. These types of studies are useful in determining the effect that a certain component may have in a specific glass composition.

Table 2.5
Summary of Defense Waste Glass Durability (37)

Oxide Components	Base Glass, wt%	Variation, wt%	Durability		
			99°C Distilled Water	pH-4	pH-9
Li ₂ O	3.0	0-6.0	++	++	0
Na ₂ O	13.9	5.0-15.0	++	++	0
K ₂ O	0	0-6.0	++	++	0
MgO	0	0-3.0	+	++	0
CaO	4.53	0-6.0	0	++	0
BaO	0	0-3.0	++	++	0
U ₃ O ₈	1.53	0-4.0	-	0	0
TiO ₂	7.5	0-10.0	-	--	0
MnO ₂	2.58	1.16-4.0	-	+	0
Fe ₂ O ₃	7.9	0.39-15.41	0	+	0
NiO	0.53	0-3.0	0	0	0
ZnO	0	0-7.0	++	++	0
B ₂ O ₃	7.50	5.0-15.0	0	++	0
Al ₂ O ₃	11.60	1.56-21.64	-	++	0
SiO ₂	39.4	---			0

0 indicates negligible change with increase in this component, + and - indicate increases or decreases, and ++ and -- indicate large increases and decreases with component increase.

A PNL study(38,39) on the generic effects of composition on waste glass properties was conducted where testing involved a systematic variation of glass components. The fitted models used in the prediction of glass properties are shown below. Figure 2.13 gives the predicted Soxhlet weight loss of a four component mixture including the defense waste calcine. The general trend is consistent with our previous summary with the exception of complications arising from the addition of B_2O_3 . However, as the number of glass components increases, complications are compounded due to interactions among the various components as shown in the test of the 11 components (Figure 2.14).

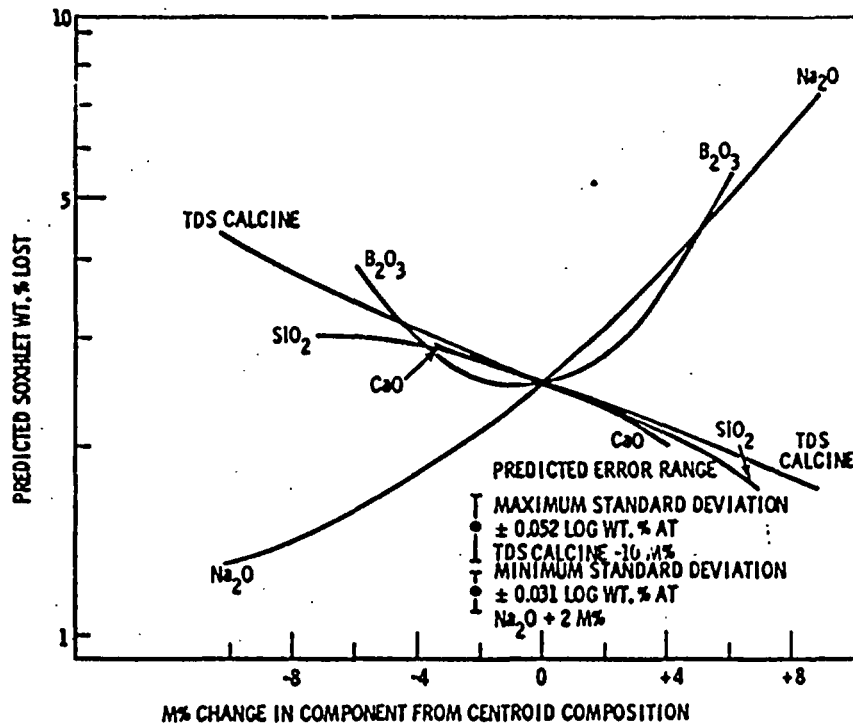


Figure 2.13 Effects of components of PNL four components glass on Soxhlet leach rate. (38,39)

This type of graphical presentation of compositional effects is useful in illustrating multicomponent effects such as in nuclear waste glass although experimental data are very limited at the present time.

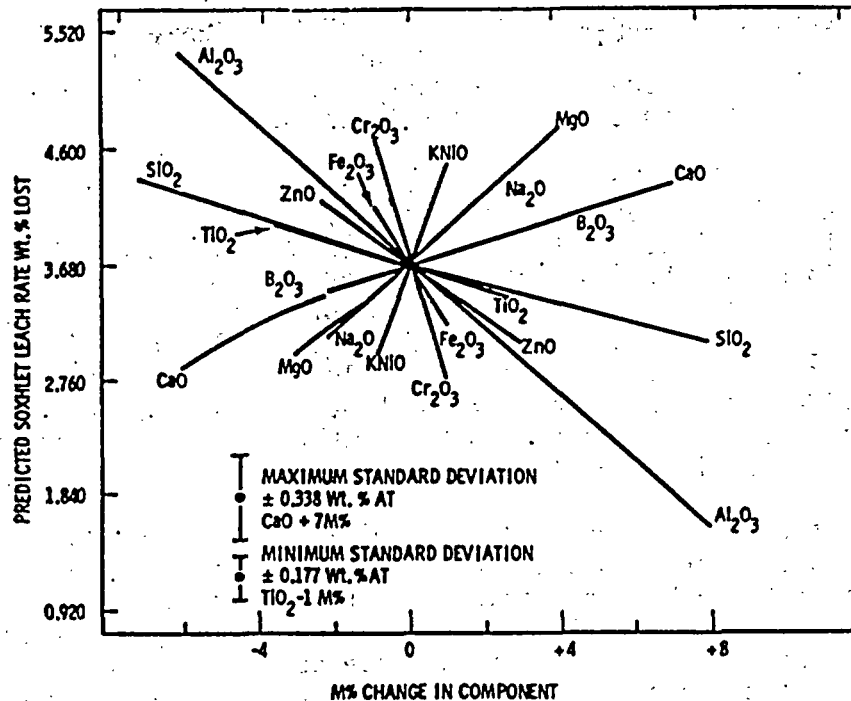


Figure 2.14 Soxhlet leach rate vs change in component from centroid of PNL 11 components glass^(38,39)

2.4.2 Phase Separation

The chemical durability of phase-separated glasses is closely related to the microstructure. The microstructure of phase-separated glasses may be classified into three types, namely (a) an interconnected microstructure; (b) chemically more durable (e.g., SiO₂ rich) phase particles dispersed in the chemically less durable (e.g., Na₂O-B₂O₃ rich) phase matrix; and (c) chemically less durable phase particles dispersed in the chemically more durable phase matrix. The chemical durability of glass deteriorates with phase separation when the glass exhibits microstructural types (a) and (b); chemical durability remains increased or relatively unchanged when the glass durability was found to depend primarily upon the composition of the chemically less durable phase.

The presence of phase separation in borosilicate glasses strongly influences their chemical durability. There is evidence that commercial Pyrex borosilicate glass separates into a disconnected sodium borosilicate phase in a silica-rich matrix, on a scale of 20Å or less, contributing to chemical durability. However, as Pyrex borosilicate is heated to 600°C or higher, its durability deteriorates as a continuous sodium borosilicate phase separates from a silica-rich phase. Previous studies by Skatulla et al.⁽⁴⁰⁾ for Pyrex-type glass have illustrated the phenomenon of decreased durability due to phase separation. Transitions in behavior between a discontinuous to a continuous microstructure also depend on the types of glass considered. For most commercial borosilicate glasses, the phase separated microstructure results in a reactivity of the glass akin to that of a high silica phase lead-

ing to high chemical durability. Sometimes even when the sodium borosilicate phase was continuous it could not be easily etched out because of the high pressure needed to force liquid water through capillaries 30 Å in diameter. However, as the interconnected microstructure becomes bigger, the soluble sodium borosilicate phase will be easily etched out.

The immiscibility boundaries of the system $\text{Na}_2\text{O}-\text{B}_2\text{O}_3-\text{SiO}_2$ have received the widest attention since this system is the basis of many commercial borosilicate glasses. An illustration by Haller, et al.⁽⁴¹⁾ is reproduced in Figure 2.15 where three boundary regions are observed at various temperature ranges. A variety of sodium borosilicate glasses containing up to about 10% Na_2O and from about 10% to 70% B_2O_3 (balance: SiO_2), can readily separate into two phases; other elements such as calcium oxide and aluminum oxide reduce the tendency to phase separation. Currently, several places in the U.S. are involved in research on the immiscibility gap for nuclear waste borosilicate glass.

The surface of commercial glasses will sometimes exhibit a slightly different composition from that of the bulk. This compositional difference can be accentuated through phase separation, resulting in a considerable difference in the chemical durability of the surface layer. One example⁽⁴²⁾ is commercial borosilicate glass with an interconnected microstructure having an excess Al_2O_3 concentration in the surface layer. Excess Al_2O_3 lowers the HF etch rate because of the lower extent of phase separation on surface.

Researchers have considered the possibility of increasing the driving force for crystallization by prior glass phase separation. However, there is no consensus on this point nor any experimental evidence for demonstration.

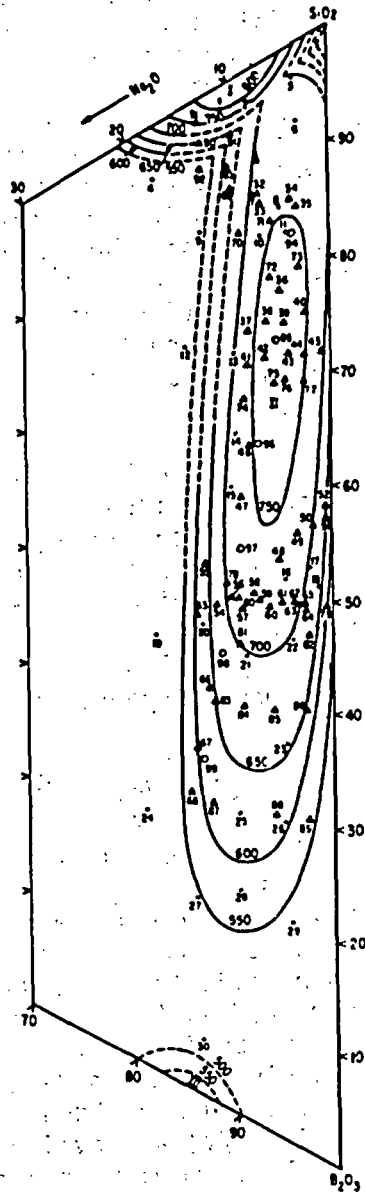


Figure 2.15 Immiscibility boundary of $\text{Na}_2\text{O}-\text{B}_2\text{O}_3-\text{SiO}_2$ glass system. (41)

2.4.3 Devitrification

The effects of devitrification on corrosion are dependent on the composition and the degree of devitrification. In a simple system such as 33L glass,⁽¹⁹⁾ 90% crystallization improved corrosion resistance considerably when tested for 120 hrs at 95°C. This is attributed to the absence of a compositional gradient across the phase boundaries between the glass and the crystals. However, in practical systems, the composition of the crystalline phase is different from that of the glass, leading to a measurable attack of the glass phase. In fact, PNL 72-68 which was devitrified at 700°C showed an increase in Soxhlet leach rate of nearly one order of magnitude.⁽¹⁹⁾ When the extent of devitrification is reduced, a very small change (less than a factor of 5) in leach rate was observed in 72-68 glass, and no difference was reported in 76-68, 77-107 and 77-260 glasses.⁽⁴³⁾ In nuclear waste repository conditions, the thermal devitrification rate is so low that the enhancement of the leach rate may not be significant: at most an increase of a factor of 10 which is well within the leach rate variations observed between waste glasses of different compositions.

There is a possibility that devitrification affects leach rate indirectly. PNL 76-68 glass in a hydrothermal environment (300°C and 300 bars water) showed that crystalline phases may be responsible for the subsequent glass fragmentation which increases the exposed surface area leading to an enhanced leach rate.⁽³²⁾ The formation of a zinc-rich alteration zone was reported as being composed of mainly zincsilite under hydrothermal conditions in sodium zinc borosilicate glass.⁽³³⁾ This alteration was presumed to be responsible for an improvement in durability. No comprehensive results are available at present on these indirect effects.

2.4.4 Glass Surface Area (SA) to Solution Volume (V) Ratio

Several investigations have firmly established that the corrosion rate increases as the SA/V ratio increases for static corrosion conditions. The data also show that increasing SA/V is a valid means of accelerating the rates of the static attack of glass surfaces. One example is given in Appendix A where the alkali extracted from borosilicate and soda-lime powder specimens with the areas of 7000 cm² was compared with the weight lost by plate glass specimens of 100 cm². For bulk glass surfaces, the quantity of a specified glass constituent in solution at a given time is directly proportional to the (SA/V) ratio, namely the constants, a and b of Equation 1 include the linear term (SA/V). No systematic data of (SA/V) are available for commercial borosilicate glass. The following is a summary of a recent study on nuclear waste borosilicate glass.

Under static leaching conditions, it was shown that the loss of alkali or alkaline earth species from glass to an aqueous media increases the solution pH and concomitantly leads to a transition from $t^{1/2}$ kinetics to t kinetics. The progressive increase in solution pH for PNL 72-68 under static leaching conditions at 120°C and 15 psi in distilled water is shown in Figure 2.16 for various (SA/V) ratios.⁽¹⁹⁾ It is shown that the increase of (SA/V)

as a function of (SA/V) ratios for various glasses including 72-68 glass at different temperatures. When the logarithm of the time required for the glass to reach a specified level of attack is plotted, similar features will be obtained. The surface attack becomes greatly accelerated at high (SA/V) ratios and only short times are needed to show surface deterioration. Additional data on nuclear waste glass are currently being generated in several laboratories.

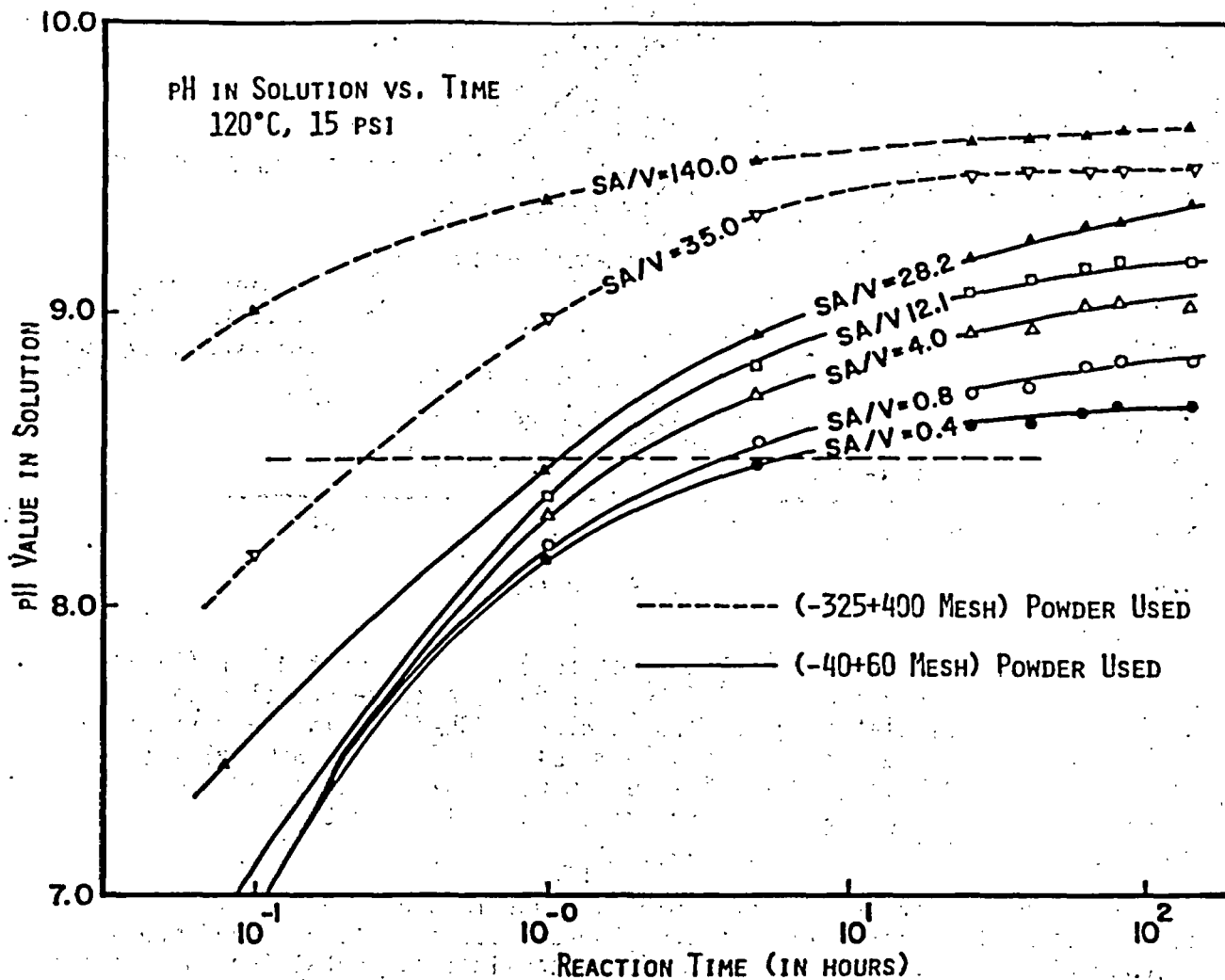


Figure 2.16 Solution pH vs exposure time for various surface area-to-solution volume ratios (SA/V). (19)

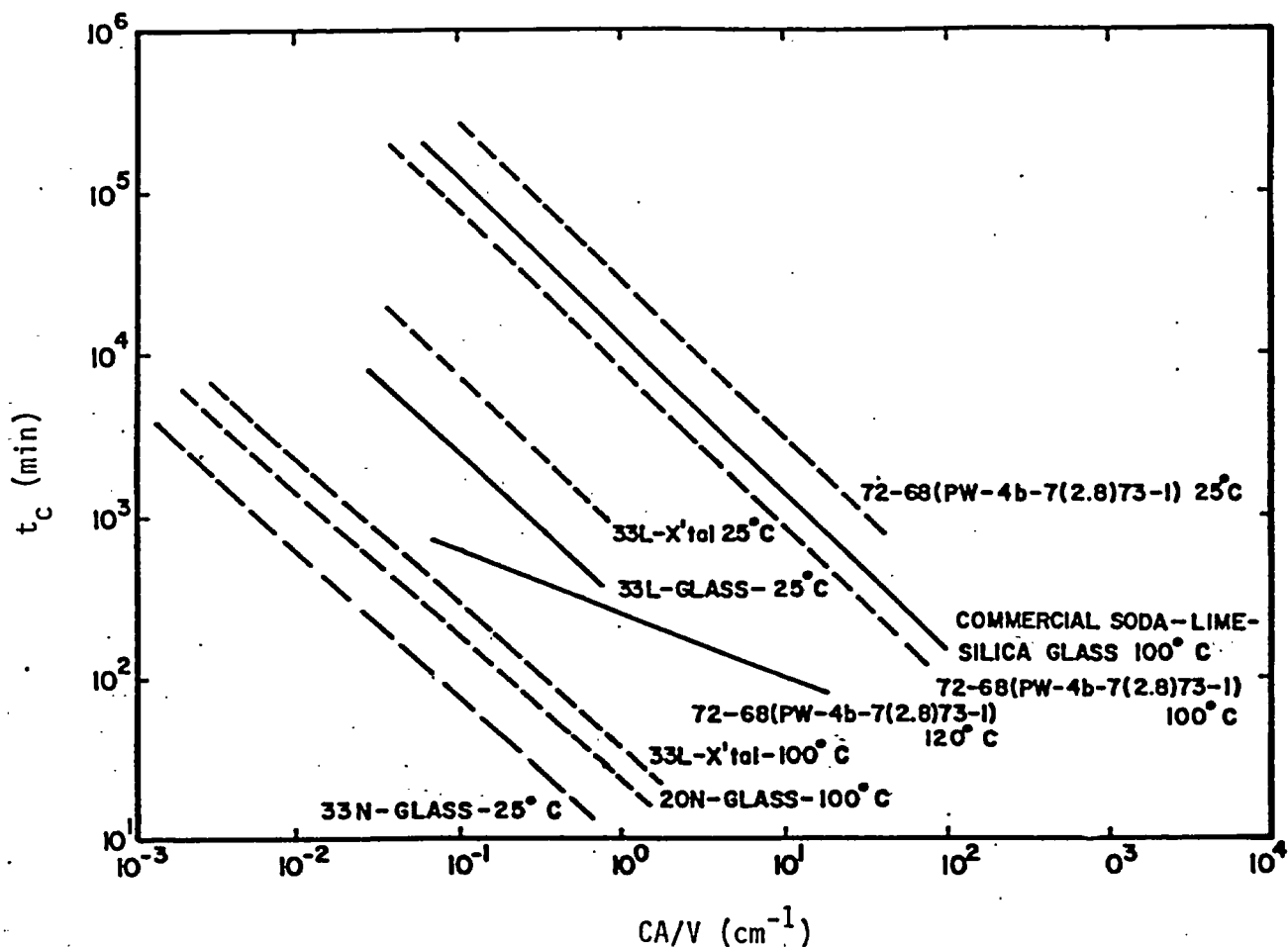


Figure 2.17 Changeover time in kinetics (t_c) as a function of (SA/V) for various materials. 72-68 is a zinc-borosilicate simulated nuclear waste glass; 33L-X'tal is the divitrified 33L glass; 33N is a 33 mole% Na_2O -67 mole% SiO_2 glass; 20N is a 20 mole% Na_2O -80 mole% SiO_2 glass; and the commercial soda lime glass is a glass container composition. (19)

Tests on powdered glass show complications in the determination of (SA/V) ratios arising from particle geometry, the surface area-time dependence and concentration cells. Particle shapes are complicated, containing sharp edges and even some porosity. The true surface area of these particles decreases with exposure time causing a corresponding decrease in (SA/V). During a static corrosion test, the glass grains settle to the bottom of the container, creating an agglomerate of particles containing concentration cells, and undoubtedly corroding in a manner different from that of the bulk glass surfaces due to local pH variations. Also film formation on smaller particles greatly alters the effective surface area for further reactions and this error becomes more severe the longer the exposure time until the smaller particles are totally dissolved. No quantitative data are now available for the dynamic determination of the effective (SA/V) ratios and its effect on leach rates.

2.4.5 Surface Stress

During the glass leaching process, the surface experiences stresses or swelling arising from hydration, ion exchange or crystallization. They subsequently lead to the spalling or peeling-off of surfaces before the congruent state is reached. For PNL 72-68 and 77-107 glasses leached using the IAEA technique of deionized water at 25°C with weekly changes of leach solution, the glasses exhibited cracked "mud flat" surfaces.⁽⁴³⁾ Surface disintegration was also observed in strontium alumoborosilicate glass by volatile Cs in the temperature range of 550°C-600°C for up to 300 hrs.⁽⁴⁴⁾ For the above mentioned surface deterioration conditions, the leach rate will rise abruptly due to cracking and partial or complete peeling off of the protective layer. The abrupt leach rate makes it difficult to predict the leaching kinetics of the type described by Equation (1).

Sometimes surface stress generated by the crystallization of the leached layer induces a catastrophic failure of the bulk glass by the propagation of the stress into the interior of the sample. This again will result in an unpredictable leach rate. Glass failure of this type will be discussed further in the section on static fatigue.

2.4.6 Cracking

Considerable controversy exists on the effects of microfracturing in glass leaching. PNL's study of partially devitrified ²⁴⁴Cm-doped waste borosilicate glass exhibited microfracturing with no accompanying measurable effect on leach rate.^(45,46) Other groups have, however, considered the significance of cracking.^(15,47) Recently, a more systematic simulation of cracking was performed by Perez, et al.⁽⁴⁸⁾ Cracks were simulated by stacking glass pellets with platinum wire spacers and holding them together with a stainless steel clamp. Their findings indicate that crack depth and crack width are important parameters with the possibility of a minimum crack depth limit required prior to enhanced leaching. In some cases, more than a factor of two increase in leach rate has been observed, as shown in Figure 2.18. It should be noted that for most cases, the increased cracked area does not appear to result in a proportional increase in leach rates. The importance of this work lies in its attempt to quantify the effects of cracks on the leach rate of glass. Further work is needed that would tie in this approach to the overall aspects of glass leaching.

2.4.7 Other Pretreatments

Surface chemical and structural variations can arise from a number of sources during the manufacture of glass. Variation in batch formulations including, forming procedures and environments, annealing conditions, subsequent hot end treatments, and exposure history, will affect the observed corrosion behavior during testing.

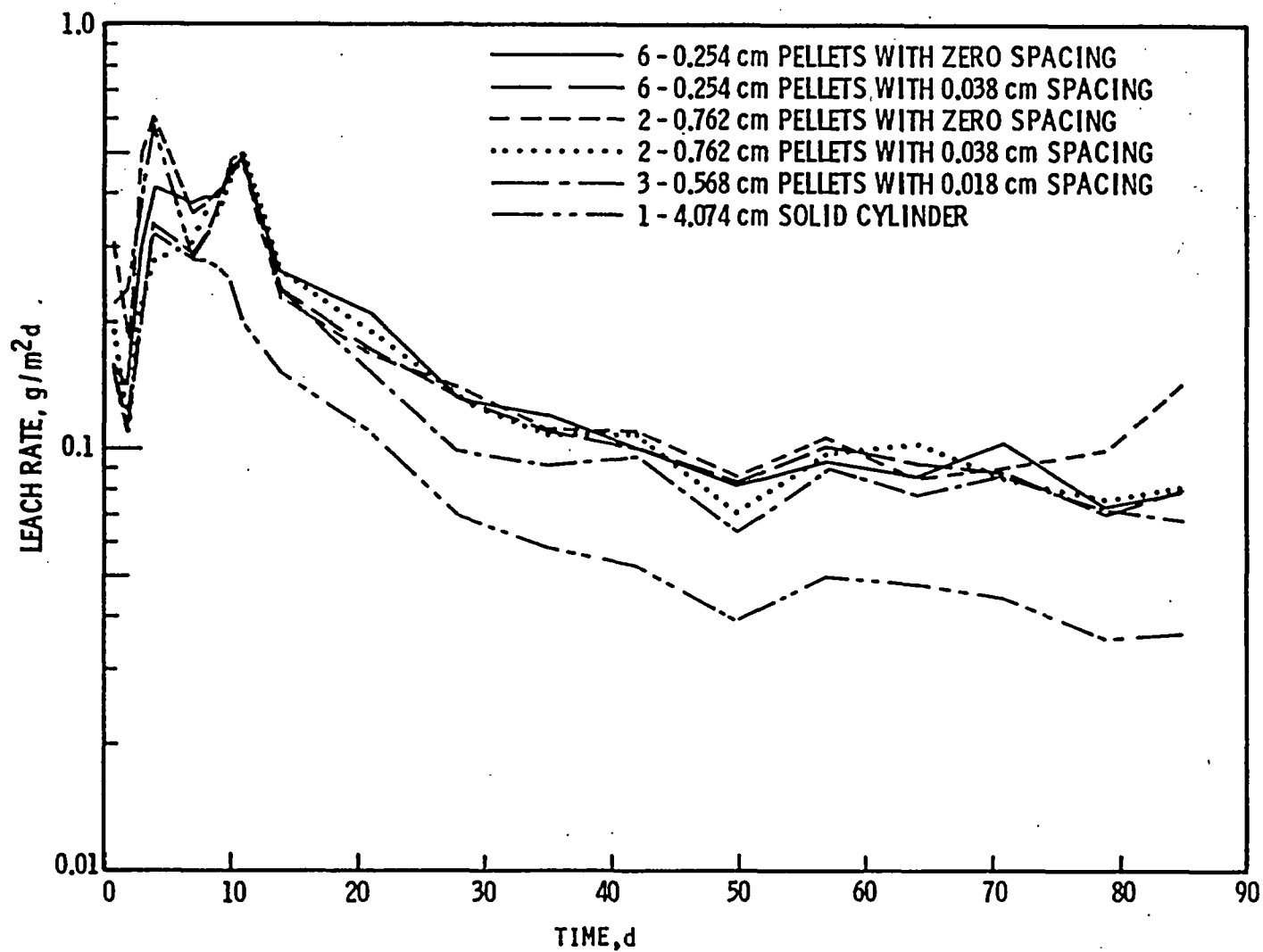


Figure 2.18 Leach rate (g-glass/m²-d) based on silicon vs time for 1.90-cm-diameter pellets (solid cylinder is an uncracked sample, and the rest are simulated cracked samples. (48))

Generally a more rapid reaction has been observed in the case of quenched glass with water compared to the annealed glass.^(5,49) This result can be understood from the higher ionic mobility in the quenched glass which has a lower density and a more open structure.^(49,50) However, the quantity of the enhancement is usually not significant being, at most within a few percent.⁽⁵¹⁾ In fact, for the ternary sodium borosilicate glass, no difference was observed between the rapidly quenched glass and the glass annealed for 2 1/2 hours at 600°C.⁽³⁵⁾

Glass homogeneity also affects leach rates. Inhomogeneity in this case mainly includes the quantity of undissolved constituents. Studies of 76-68 glass with several different thermal histories have shown that the best leach resistance was obtained from the glass exhibiting the best homogeneity.⁽¹⁹⁾ A quantitative assessment is not available at present.

Other variables such as surface roughness will also have an effect on leach rates. Sanders, et al. investigated this effect in a binary lithium glass by abrading the surface using various grit sizes.⁽⁵²⁾ Solution analysis showed that the initial rate of silica-rich film formation is most rapid for the smoothest surface. Evidence seems to indicate that surface roughness will also influence static fatigue behavior. Although complex processes are introduced by this parameter, it is clear that the extent of the roughness will have an influence on both the relative and total amounts of material removed from the surface of the glass.

2.5 Cation Selectivity and the Diffusion of Ions and Gases

Toxic radioisotopes may escape from the waste form by solid state diffusion. Cation selectivity and the diffusivity of ions and gas molecules are responsible for this process. What follows is a summary of the properties of diffusion and ion selectivity in glass.

Figure 2.19 shows a tabulation of the diffusion coefficient for monovalent sodium ions in various silicate glasses at 386°C.⁽⁶⁾ Note the range of 10^{-10} cm²/sec for Pyrex borosilicate glass, which gives a diffusion distance of approximately 1-2 cm for 1000 years. The distance, however, will decrease by orders of magnitude at temperatures below 100°C. Anions and cations of higher valence diffuse much more slowly than monovalent cations in glass. The self-diffusion coefficients of cations other than alkali ions measured at relatively low temperatures are summarized in Figure 2.20.⁽⁵³⁾ Unfortunately no data are available for borosilicate base glass, where the diffusivity changes by the relative amount of sodium borate phase and the continuous silica phase. As more sodium borate is added to the glass, the absolute value of the diffusivity decreases by the decrease of the effective area of the continuous silica phase. The quantitative amount of this change is not known. For the glassy materials suitable for the long-term storage of highly radioactive wastes, Ralkova⁽⁵⁴⁾ studied the diffusivity of ¹³⁷Cs and ⁹⁰Sr in alkali-lime-silicate glass and basalt. In the temperature range of 300°C-600°C, diffusivities were of the order of 10^{-13} - 10^{-11} cm²/sec in the basalt. Again data are not available for borosilicate base glasses.

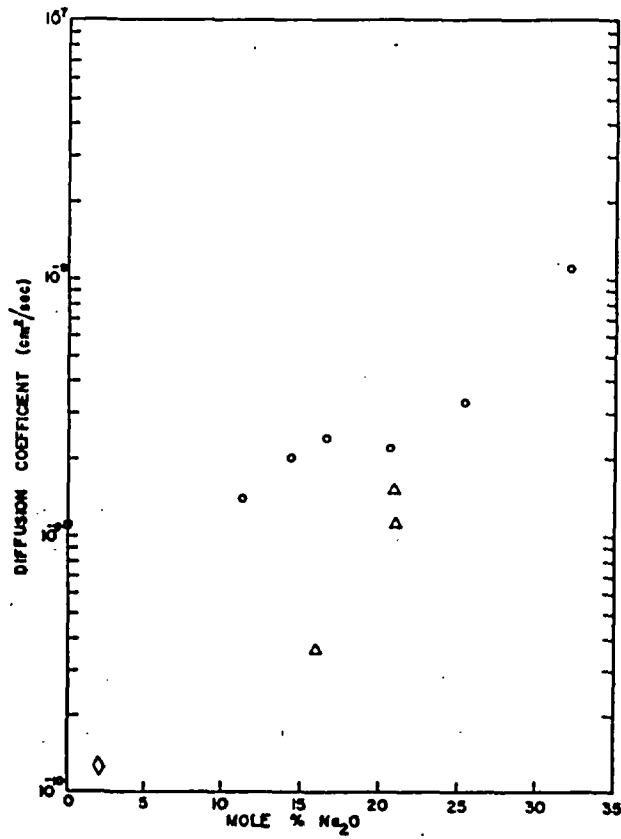


Figure 2.19 Diffusion coefficients of sodium in sodium silicate glasses at 386°C as a function of sodium concentration. ○, binary sodium silicates; Δ, sodium calcium silicates; □, fused silica; ◇, Pyrex borosilicate. (6)

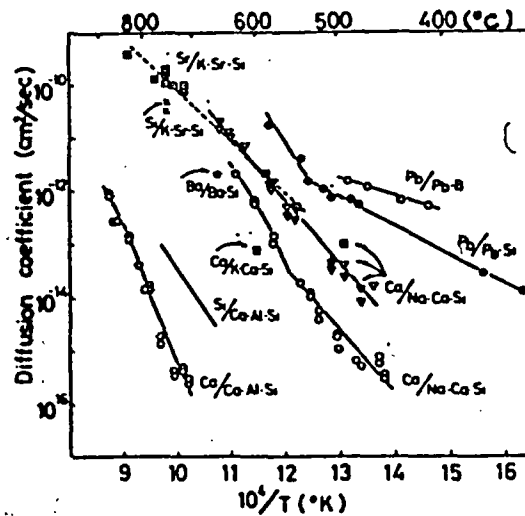


Figure 2.20 Self-diffusion coefficients of Ca^{2+} , Sr^{2+} , Ba^{2+} , Pb^{2+} , and Si^{4+} ions in various silicate and borate glasses. (53)

Some diffusion measurements for gases in sodium borosilicate glasses are summarized in Table 2.6. Gas diffusivities are in general higher than the cation diffusivities.

Table 2.6

Molecular Diffusion in Sodium Borosilicate Glass(55-57)

Glass	Gas	Diffusion Coeff. at 200°C
Pyrex	He	4.7×10^{-7}
"	D ₂	4.1×10^{-9}
Borosilicate*	He	5.0×10^{-8}
"	Ne	7.0×10^{-11}

(*60% SiO₂, 30.5% B₂O₃, 9.5% Na₂O)

The problem of relating glass composition to ion exchange has been studied extensively by Eisenman and co-workers.⁽⁵⁸⁾ The competing interactions of cations in dilute aqueous solutions are categorized as 11 sequences in a cation selectivity order. Table 2.7 shows the selectivity sequences, related in a definite way to the composition of the glass, which determines the field strength in the table. Data for silicate glasses without boron and aluminum fall to the lower end of the table, whereas the opposite is true for the borosilicates.

Table 2.7

Eisenman's Selectivity Orders Among the Alkali Ions(58)

I	Cs > Rb > K > Na > Li	
I	Cs > Rb > K > Na > Li	
IIa	Cs > K > Rb > Na > Li	or II Rb > Cs > K > Na > Li ^a
IIIa	K > Cs > Rb > Na > Li	or III Rb > K > Cs > Na > Li ^a
IV	K > Rb > Cs > Na > Li	
V	K > Rb > Na > Cs > Li	
VI	K > Na > Rb > Cs > Li	
VII	Na > K > Rb > Li > Cs	
IX	Na > K > Li > Rb > Cs	
X	Na > Li > K > Rb > Cs	
XI	Li > Na > K > Rb > Cs	

^aCalculated for closely spaced sites.

This basis will not be valid for glasses exhibiting phase separation, hydration, and before electrochemical properties are stabilized. The stabilization in certain cases may take long periods of time.

2.6 Weathering

Even though a water solution may be absent, chemical reaction can occur in the presence of water vapor in the atmosphere. Static and cyclic humidity must be taken into account when assessing glass durability. Corrosion will proceed if: (1) the products of ion exchange (notably alkali) remain on the surface; and (2) ambient conditions of relative humidity or temperature are disrupted.

Water adsorption tends to increase with time and humidity; alkali generation increases with time but varies with humidity. Other cations may enhance durability by decreasing the reactivity of the alkali such as Zn, Sr, Ba, Pb, Zr. Zr, for example, reacts to form a tight zirconium alkali-silicate protective layer increasing significantly acid and alkali durability.

Figures 2.21 through 2.25 and Table 2.8 show the results of tests conducted at Corning on the effects of humidity on various glass types.⁽⁵⁹⁾ The relative humidity (RH) ranged from 30-90%. Weathering effects have been observed down to 30% RH. Certain glasses can weather as much at 30% RH as at 90% RH. Weathering effects have been found to decrease (or slow down) with increasing RH by a dilution effect from adsorbed water.

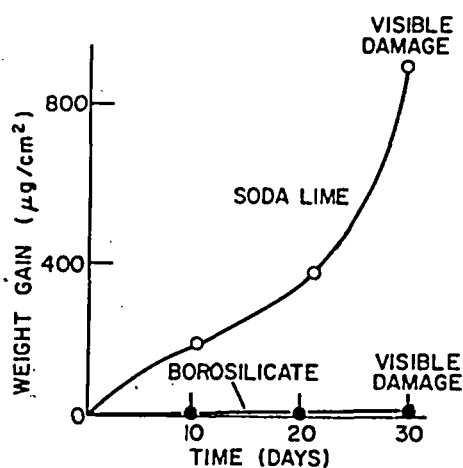


Figure 2.21 Weight change of soda-lime and moderately resistant borosilicate glass after weathering at 89% RH, 50°C.⁽⁵⁰⁾

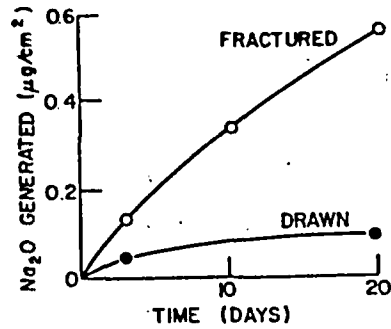


Figure 2.22 Na₂O on surface after weathering of moderately resistant borosilicate glass tubing at 98% RH, 50°C. (59)

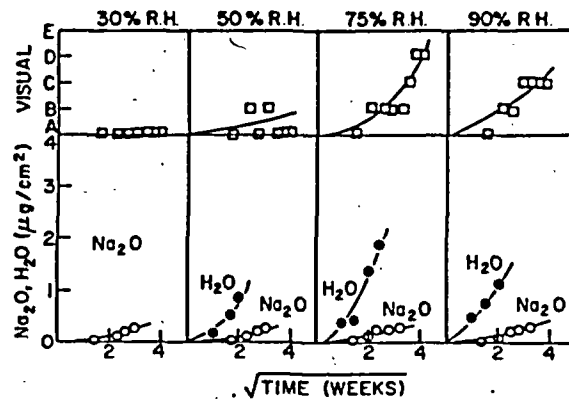


Figure 2.23 Visual appearance, Na₂O and H₂O generated on moderately resistant borosilicate glass tubing and power weather at different RH. (59)

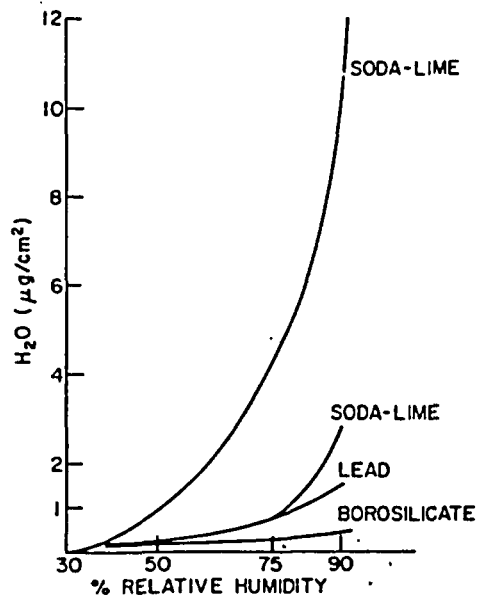


Figure 2.24 H_2O adsorbed on several glasses as a function of RH after 7 days. (59)

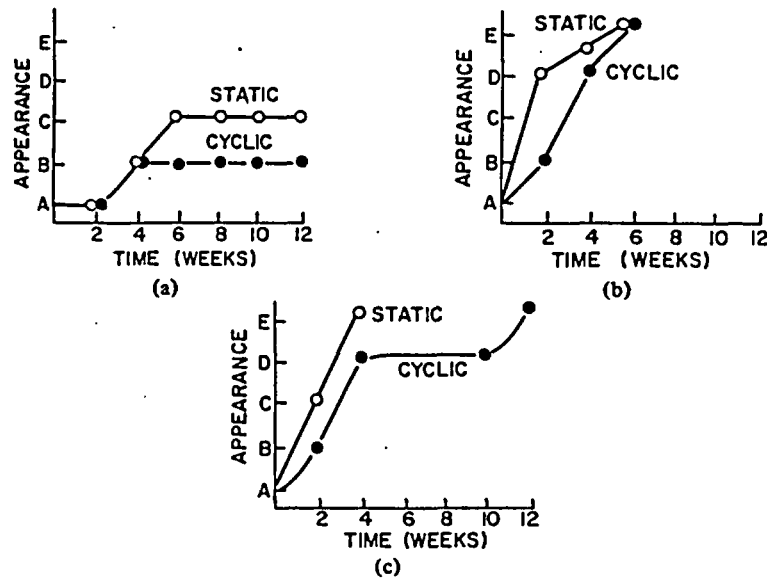


Figure 2.25 The effect of cyclic and static RH on visual appearance. (a) for borosilicate tubing, (b) for plate glass, (c) for soda-lime tubing. (59)

Table 2.8

Summary of Visible Damage and Generated Alkali on Various Glasses Weathered 14 Days at 98% RH, and 50°C⁽⁵⁶⁾

Glass Type	Visible Damage	Alkali Generated ($\mu\text{g}/\text{cm}^2$)
Alumino silicate	None	<0.01
Alkali borosilicate A	Barely detectable	0.01 to 0.05
Alkali borosilicate B	Slight	0.05 to 0.25
Alkali lead	Moderate	0.25 to 1.0
Soda lime A	Appreciable	1.0 to 5.0
Soda lime B	Severe	>5.0

Crizzling or spalling is a result of the adverse effects of weathering on glass surfaces. Spalling of the surface hydration layer may result where the alkali-depleted network is too weak to sustain stress. The protective layer will act as a barrier only as long as the high silica network remains intact.⁽⁶⁰⁾ At the Conasauga test site (Tennessee; shale) PNL 75-25 borosilicate glass, subjected to alternating wet-dry cycles, exhibited a 20 μm -thick layer showing network cracks and nonuniform penetration of corrosion into the underlying unaltered bulk glass.⁽⁶¹⁾ Spalling has been noted in a variety of archaeological glass compositions that have been subjected to alternate wet-dry cycles. This phenomenon came to the attention of conservators when glasses previously submerged were placed in dry environments for exhibit resulting in the spalling of the hydrated surface layer.⁽⁶²⁾

Since long-term weathering effects are quite difficult to duplicate under laboratory conditions for the geologic time periods under consideration in nuclear waste management issues, archaeological samples of weathered glass may provide insights into long-term durability.

Shaw,⁽⁶³⁾ using X-ray diffraction and differential thermal analysis, showed that the weathering crust on approximately 300 year-old buried potassium glass had a relatively high degree of crystallinity. Khy and Nauer⁽⁶⁴⁾ estimated the time period for the crystallization based on solid state transformation kinetics for the systems $\text{Na}_2\text{O}-\text{SiO}_2$ and $\text{Li}_2\text{O}-2\text{SiO}_2$ at 300 K. The $\text{Na}_2\text{O}-\text{SiO}_2$ system can be taken as resembling the compositional characteristics found in certain ancient glass forms due to a higher Na_2O and lower CaO content. Crystallization by homogeneous nucleation is beyond the range of archaeological consideration (approximately 10^{17} years). If the magnitude of acceleration as influenced by hydroxyl groups is taken into account, homogeneous nucleation will result at approximately 10^{14} years. Crystallization from heterogenous nucleation, assuming "worst case" conditions may occur in approximately 10^3 years. Since ancient glasses from periods greater than 10^3 years have survived a variety of different weathering environments, Khy and Nauer's assessment is not unrealistic and is confirmed by the long durability of ancient glass compositions.

Regarding the compositional effect on weathering of glass over geological time periods, analyses of 12th to 16th century glass showed that the most durable samples fell in the compositional range of 70-75% "SiO₂, low "R0" (10-40%) and notably low MgO (1.2-3.2%).⁽⁶⁵⁾ Conclusions based on the study of medieval glasses indicate that they do not weather noticeably during the 500-800 years of exposure provided the "SiO₂" content is greater than 60 mole percent. This seems to have been confirmed in additional studies by El-Shamy on K₂O-CaO-MgO-SiO₂ glasses.⁽⁶⁶⁾

X-ray fluorescence analysis coupled with SEM on medieval soda-lime glass and Roman soda-lime glass offer potentially useful insights for comparison into oxide depletion. The results of a profile study on the elemental composition of these glasses is presented in Table 2.9.⁽⁶⁷⁾ The surface alteration of these glasses was due to weathering processes as a result of near-surface burial.

Table 2.9
Profiles of Medieval and Roman Glasses⁽⁶⁷⁾

Oxide (Weight Percent)	Medieval Glass-YMG 1			Roman Glass-YMG 396		
	Surface: A	B	C	Surface: A	B	C
Na ₂ O	3.4	10.9	16.8	n.d.	11.4	18.9
MgO	0.9	0.8	0.8	1.0	0.4	0.4
Al ₂ O ₃	1.8	1.7	1.6	6.9	2.4	1.5
SiO ₂	65.9	63.7	68.7	63.8	60.4	70.2
P ₂ O ₅	0.8	0.7	0.9	0.4	0.2	0.3
K ₂ O	2.0	1.9	1.7	2.0	1.1	1.2
CaO	9.3	9.4	7.2	6.1	7.3	6.0
MnO	0.9	0.9	0.6	1.0	1.1	0.8
Fe ₂ O ₃	1.1	1.0	0.9	0.7	0.7	0.6
CuO	0.4	0.4	0.2	0.1	0.1	0.01
ZnO	0.05	0.05	0.03	0.04	0.04	0.03
PbO	0.8	0.8	0.6	0.2	0.2	0.1

n.d. = Not detected; detection limit reported <0.8 weight percent Na₂O.

A = Surface of sample - untreated.

B = Subsurface region approximately 200 μm below surface.

C = Approximately 500 μm below weathered surface; bulk composition.

If we assume that surface A represents the original surface with no detachment of weathered layers and that the depletion of Na₂O and SiO₂ have been uniform, the ratios of weight percent oxide loss to geologic time (approximately 800 yrs and approximately 1700 yrs for the Medieval and Roman glass, respectively) appear relatively close. Both samples were found in the same locality and we may assume that they were exposed to similar weathering conditions. The apparent uniformity in Na₂O/SiO₂ depletion may be

interpreted as indicative of a linear time dependence of glass dissolution. One of the oldest analyzed decomposed glass is a glass bead dating to approximately 1600 BC.⁽⁶⁸⁾ The weathering product was found to be impure hydrated silica. Results obtained by Geilmann⁽⁶⁹⁾ on medieval glasses confirm findings that alkalis and alkali earths are almost completely removed. Aluminum, iron, titanium, and several minor components remain or increase (reprecipitate) in concentration due to exchange or adsorption on the hydrated silica from soil or mineralized groundwater.

The complexity of the weathering process under burial conditions is evident through the examination of ancient glass. Investigations by Brill and Hood at Corning on weathering layers, suggested a periodic or cyclical accumulation of weathered crusts. The initial work involved the examination of ancient soda-lime-silica and potash-lime-silica compositions. Weathering layers (0.3-15 μm thick) tended to correspond to the approximate number of years that the object had been exposed to weathering. Initially seasonal variations (temperature, humidity or wet/dry periods) were suggested as the probable cause for such correlations. However, samples of ancient glass which had been submerged at sea also showed this pattern.⁽⁷⁰⁾ The layers seen in Figure 2.26 consist of almost pure amorphous silica. Similar results were obtained on borosilicate glasses involved with the production of Vycor-type glass at Corning.⁽⁷¹⁾ The correlation between the number of layers and the number of years of exposure has not been given an adequate explanation, although attempts have been made.^(72,73,74)

These studies also point out the nonuniformity of attack at the glass surface. Figure 2.27 shows a weathering 'plug' occurring beneath the amorphous weathering layers, possibly due to a high concentration of moisture at that point. The semi-circular areas at the top are also indicative of non-uniform weathering at the surface.⁽⁷²⁾ Decomposition begins at a large number of sites on the surface and proceeds into the bulk forming a series of alkali-depleted spherical layered shells which, at some point, will tend to coalesce parallel to the original surface.

The above review presents some evidence on the long-term integrity of various glasses. For a more quantitative study, a data base including profiling, devitrification, and weathering conditions is needed.

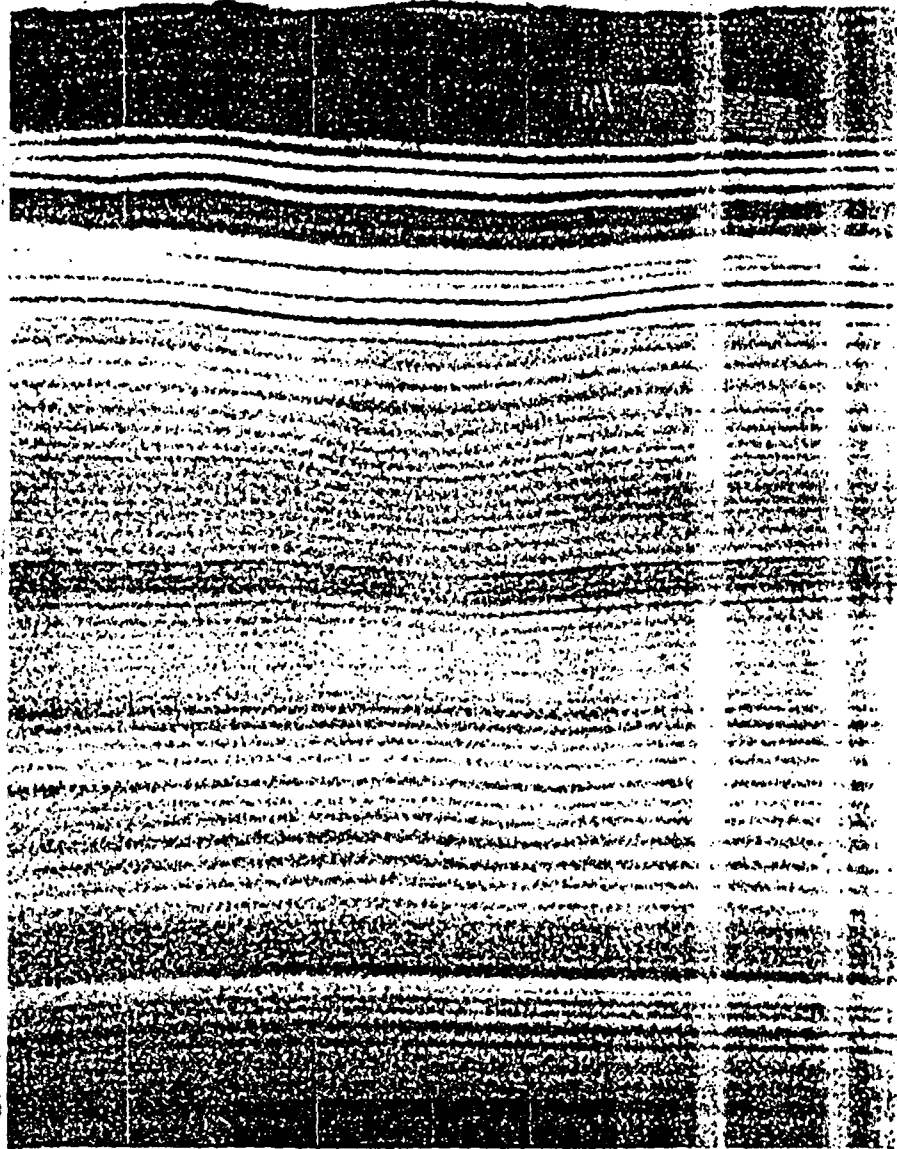


Figure 2.26 Cross section of the weathering crust on a 17th-century wine bottle (X750). Clear substance at top is the supporting plastic.⁽⁷⁰⁾



Figure 2.27 Enlarged (X50) section of a piece of window glass which had been buried for 288 years. The top surface was probably the outside of the window and there are 65 parallel layers at that surface before the 'plug' adds another 220 layers. Far fewer layers occur at this part of the lower surface. (72)

3. LOCAL CORROSION AND STATIC FATIGUE

There are insufficient data at the present time to draw any definitive conclusions on the importance of local corrosion in glass. The evidence seems to suggest that under laboratory conditions local corrosion, such as pitting, is no more severe than general corrosion.⁽⁵¹⁾ Although ancient glass exhibits local attack during weathering processes, experimental data on the effects of this phenomenon with respect to overall durability are not currently available.

Static fatigue, on the other hand, is known to be a very important mode of disintegration for glass in the presence of water. Cracks developed under static fatigue will increase the exposed surface area leading to a significant increase in the leach rate. Due to the importance of this phenomenon, static fatigue mechanisms, time to failure, and pertinent variables such as solution pH, humidity, temperature, pressure, compositions, matrix microstructure and surface flaws, require some discussion.

Static fatigue occurs only in the presence of water which reacts chemically with the strained bonds at the crack tip causing bond rupture. Therefore, static fatigue is a chemical process that involves a stress-enhanced chemical reaction between water and the highly stressed region near the crack tip. The general characteristics of static fatigue are as follows:

- static fatigue occurs generally in the presence of water;
- static fatigue can be detected for load times as short as 10^{-2} second;
- static fatigue is an activated process;
- static fatigue limit is observed in some cases.

3.1 Static Fatigue Mechanisms

Several proposed mechanisms by which the crack extension procedure occurs may be summarized as follows:

- **Chemical Corrosion:** Highly strained bonds at the crack tip are more susceptible to corrosive agents. The chemical reaction rate theory of Hillig and Charles^(75,76) and the multibarrier kinetic theory by Brown⁽⁷⁷⁾ are considered in assuming this mechanism.
- **Strain-Gradient Induced Diffusion:** This mechanism employs a strain-gradient induced diffusion of mobile ions yielding concentrations of such ions at positions in advance of the crack tip. Enrichment, with respect to these ions at the crack tip, reduces the local Si-O bond strength allowing crack advancement and apparently premature rupture. Gerberich and Stout⁽⁷⁸⁾, Cox⁽⁷⁹⁾, Hasselman, Stevens and Dutton^(80,81) proposed slightly different diffusion models.

- o Surface Energy Reduction: Orowan⁽⁸²⁾ attributed static fatigue to an adsorption-induced lowering of the glass surface energy, concomitantly leading to an easier crack growth.
- o Others: A model by Weidman and Holloway,⁽⁸³⁾ proposed that the growth of a plastic zone controls the rate of crack propagation. Fuller and Thomson⁽⁸⁴⁾ modeled a one-dimensional crack in two semi-infinite chains of atoms. Although these models explain certain features, such as a higher fracture energy than the surface energy, experimental evidence is needed to show that the adjustable parameters or uncertainties in each model can be eliminated.
- o Mechanism Predominance: Depending on the environment, the relative importance of each factor has been determined. For instance, in a corrosive environment chemical corrosion is likely to be the dominant process while the effectiveness of the environment for the reduction of surface energy will be predominant in the presence of noncorrosive environments.

3.2 Slow Crack Growth

From fracture mechanics studies, crack velocity v was found to be a function of a stress intensity factor K_I . For various glasses of different compositions, Figure 3.1 illustrates the K_I dependency in water environment.⁽⁸³⁾ Several expressions for this K_I dependency were developed. In general v is dependent on K_I exponentially. The most representative expression is given by

$$v = v_0 \exp[(-E^* + bK_I)/RT] \quad (5)$$

where v_0 , E^* and b are empirical constants representing, v_0 , the initial velocity; E^* , the activation energy without the applied stress.^(86,87,88) For borosilicate glass in water

$$E^* = 30.8 \text{ Kcal/mole}$$

$$b = 0.200 \text{ (m}^{5/2}\text{/mole)}$$

$$\ln v_0 = 3.5$$

3.3 The Law of Time to Failure

Generally, the time to failure depends on the magnitude and total duration of the load. The time to failure at a given stress level is inversely proportional to the n th power of the applied stress. The representative equation for the time to failure is given by

$$\ln(t/t_{1/2}) \approx -\beta \sigma_t (\sigma/\sigma_N)^{-1/2} \quad (6)$$

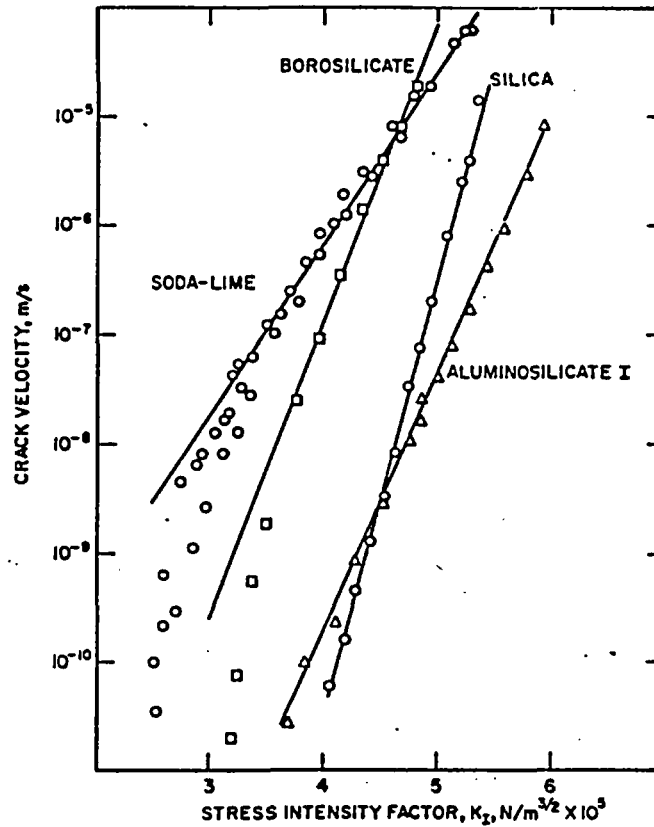


Figure 3.1 Effect of glass composition on crack propagation rate. Tested in water at 25°C. (85)

where $t_{1/2}$ is the failure time at $\sigma/\sigma_N = 1/2$, σ_t is found experimentally, t is time, σ is applied stress and σ_N is the failure stress at liquid nitrogen temperature. (89) For borosilicate glass with different surface treatments, the following parameters were derived experimentally in a water environment (Table 3.1). (6)

Table 3.1

Parameters for Various Glasses With Different Surface Treatments

Glass	Surface Treatment	Breaking stress	
		at 77°K (kpsi)	$\beta\sigma_t$
FN borosilicate	Abraded	11.0	31
FN borosilicate	Centerless ground	14.8	43
Pyrex	-	-	64

For the purpose of long-term prediction a simple calculation of the time to failure at zero applied stress is given as 5×10^6 years from a $1 \mu\text{m}$ crack which determines $t_{1/2}$ to be 2.14 seconds in water based on the formula of Wiederhorn and Bolz. (85,91) Various assessments at different stress levels and environmental conditions are possible and this will be a future research topic. In the above equations, the stress term can be converted into a fracture mechanics term by simple substitution resulting in a similar expression.

In practical design, a proofing test is used, and the time to failure, t_f , is usually expressed as

$$t_f = \sigma_a^{-2} f(\sigma_p/\sigma_a)$$

where σ_a is the service load, σ_p is a proof test load, and f is determined from measurements of K_{IC} , the critical stress intensity, and from crack growth data. (92-94) The data for borosilicate crown glass II is shown in Figure 3.2.

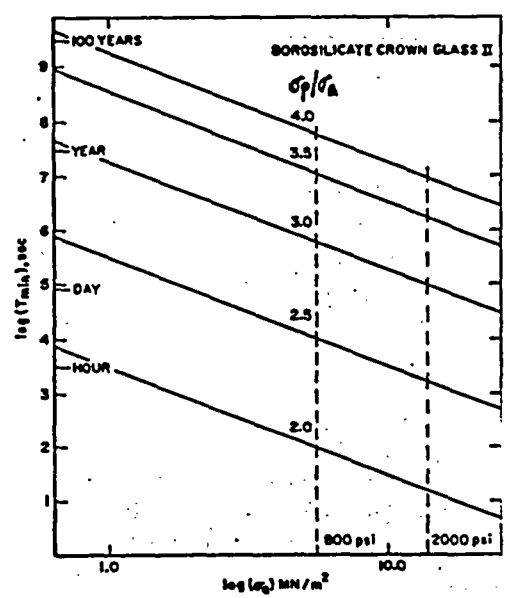


Figure 3.2 Proof test diagram for borosilicate crown glass II; minimum time to failure, T_{min} , given as a function of service stress, σ_a , and proof test ratio, σ_p/σ_a . (92,94)

From the practical viewpoint of a laboratory test, the critical stress intensity K_{IC} gives the material capability to carry a load in the presence of a given size of notch, or some other form of flaw or defect. The critical stress intensity factors for borosilicate glasses in vacuum are shown in Table 3.2

Table 3.2

Critical Stress Intensity Factor K_{IC} ($MN/m^{3/2}$) of Borosilicate Glass⁽⁹⁴⁾

Glass	Vacuum, DCB* No Preheat	Vacuum, DCB Preheat 300°C for 30 min.	Vacuum 3 Point Bend, No Preheat	Dry, N ₂ Gas <0.02% RH
Borosilicate	0.760±0.007	0.770±0.012	0.777±0.032	0.764±0.008
Borosilicate Crown, I	0.862±0.032	0.927±0.010	0.842±0.007	--
Borosilicate Crown, II	0.866±0.001	0.879±0.034	0.904±0.014	--

*DCB: Double Cantilever Beam.

However, when we consider geologic time periods, it is probable that cracking may develop even in the absence of applied stress (see Equation 6) during the corrosion process. One such example is shown in the study of cracks induced in a stress-free alkali silicate bottle after a few weeks exposure to water.⁽⁹⁵⁾ Such failure possibility can always take place for all glasses over geologic time.

The static fatigue model should eventually include the effects of surface stress caused by surface crystallization, hydration, or spalling which will also lead to crack propagation during the corrosion process. Therefore, the realistic prediction of time to failure will be much more complicated than the above simple equations which were derived from fracture mechanics and are basically empirical in nature.

3.4 Effects of Environmental Interaction

3.4.1 Solution pH

It was determined that the pH of the aqueous environments has a significant effect on the strength of glass. In high pH solutions (above 13), the strength of glass was greater, while in low pH solutions (below 1), the strength was less than in neutral solutions. In strong alkali solutions, samples will not be susceptible to cracking when the corrosion rate proceeds

faster than the crack velocity.⁽⁹⁵⁾ In the middle range of pH, the strength is nearly constant. For silicate glass, the slope of the crack velocity versus stress intensity factor was found to decrease as the pH increases. Wiederhorn⁽⁸⁷⁾ rederived the crack velocity equation in the Charles and Hillig model, including $[\text{OH}]^-$ ion concentrations, and found that the velocity is proportional to the nth power of the $[\text{OH}]^-$ ion concentration.

When water is the corrosive agent, the effect of a wide pH variation is important since the crack tip solution is rapidly modified by the glass and contains significant concentrations of elements that are normally present in the glass composition. Wiederhorn⁽⁹⁶⁾ further stated that high alkali glasses result in basic solutions at the crack tip, whereas low alkali glasses have crack tip solutions that are mildly acidic. This local pH change is determined by a dynamic balance between the ion-exchange and ion-diffusion processes. This local pH influences the slope and the shape of the universal fatigue curves.

3.4.2 Humidity

Humidity will hydrate the surfaces of some glasses causing them to swell, thus creating local stresses at a flow tip which will propagate cracks. The crack velocity is found to be proportional to the relative humidity by a theoretical analysis.^(97,98) The time to failure for older glass was found to be an inverse exponential function of the relative humidity.⁽⁹⁹⁾ These are valid when other parameters governing the crack growth or the time to failure are fixed. Quantitative data for borosilicate glasses are not available at the present time.

3.4.3 Temperature and Pressure

Glasses of poor chemical durability tend to crack at lower temperatures; concomitantly, the reverse is true at very high temperatures. The crack growth velocity and the time to failure have been expressed in an Arrhenius-type equation relating to temperature. For borosilicate glass, the activation energy for the crack velocity is reported in the previous section on fracture mechanics. The characteristic time to failure, $t_{1/2}$, is simplified to be a linear function of temperature.⁽⁸⁵⁾

As for pressure dependency, high pressure is known to have no effect on static fatigue in the range of 6 to 7 Kbar.⁽¹⁰⁰⁾

3.4.4 Glass Composition

Both the crack velocity and the time to failure change as the composition changes.

Systematic studies on composition effects or data pertaining to borosilicate glass per se are not available at the present time.

3.4.5 Flaws

The delayed failure curves for a number of glasses were quite sensitive to surface finish. Generally as the flaw size increases, the time to failure decreases. There is no report on the limitation of flaw size, below which no failure occurs. For optical fiber glass, the failure origin was found even though flaw sizes are much less than $1\ \mu\text{m}$.⁽⁹⁸⁾ Since $t_{1/2}$ is also a function of flaw size, universal fatigue curves are obtained when the time to failure is normalized in most cases. The fracture mechanics study illustrates the quantitative prediction of the dependency of flaw size on the time to failure or $t_{1/2}$.

3.4.6 Microstructure and Plastic Deformation

Phase separation is reported to increase the crack growth rate.⁽⁹⁸⁾ The plastic deformation is believed to play no role in the fracture process. However, very little quantitative data is available concerning these properties.

Static fatigue data for nuclear waste glass are not available at the present time. Several laboratories, including the National Bureau of Standards, have recently begun formal studies on this subject.

4. RADIATION EFFECTS

This section will briefly summarize the anticipated radiation effects on leaching and overall integrity of glass based on experimental work on commercial and nuclear waste glass. A more detailed review is due to appear in the BNL literature.⁽²⁰⁾

In waste glass, alpha, beta, gamma-rays, and transmutation effects are expected to exist.⁽²⁸⁾ Recently, Walker, et al.⁽¹⁰¹⁾ reported on a preliminary study involving borosilicate glass leaching during ^{60}Co gamma, ^{244}Cm alpha, and ^{90}Sr beta radiation. Leach rate was increased within a factor of 2 by gamma radiation presumably due to the leachant pH change by radiolysis, while no significant effects were observed for alpha or beta radiation. To date, transmutation effects on glass leaching have not been reported in the literature. Studies on crystalline waste forms⁽¹⁰²⁾ seem to indicate that the effect may not be significant. Indirect effects involving differential swelling and compaction have been observed in partially devitrified glass by alpha and gamma radiation leading to microfracturing. The concomitant increase of surface area will enhance the leach rate quite significantly⁽¹⁰³⁾. Similar effects are expected as a result of transmutations. The concentration of transmuted atoms may be large enough to form a second phase causing stress generation at the interface. No experimental evidence has been reported to date on this topic.

In a design utilizing commercial glass in a sacrificial capacity to encapsulate the nuclear waste glass, beta and gamma radiation effects are anticipated. Following the results of Walker, et al.,⁽¹⁰¹⁾ it appears that only the gamma radiation would affect the leach rate. An indirect effect may involve stress generation between the sacrificial layer and the waste glass from differential compaction and swelling. This stress may lead to microfracturing resulting in increased leach rate due to increased surface area.⁽¹⁰³⁾

Dose rates under repository conditions are assumed to be generally slower than under laboratory conditions reducing the above mentioned radiation effects. Given the limited experimental data, it becomes quite difficult to assess the effects of radiation on the integrity of glass over geological time. However, we feel that the radiolysis effect is quite minor and the fracture process can be avoided by a proper design of the waste form⁽¹⁰³⁾ which would preserve the integrity even in the presence of radiation.

5. LONG-TERM PREDICTION MODELS

All the efforts reviewed up to this point were aimed at predicting the durability of glass over geological time. The numerous complications and uncertainties in the preceding sections suggest that it is quite premature to generate a comprehensive model for prediction. Nevertheless, researchers have attempted to develop a method for long-range prediction of the durability of nuclear waste storage materials based on several hypotheses.

Hench⁽⁴⁾ emphasized a graphical method based on the analyses of laboratory tests, field tests, and natural analog materials by plotting material loss through leaching as a function of time. The best and worst cases are used for the upper and lower limit of the plot. For example, the accelerated leach rate by hydrothermal conditions is a factor controlling the worst case. It was admitted, however, that there are so many uncertainties involved, it is almost impossible to construct any specific chart at the present time. For instance, a study of natural analogs, especially in relation to laboratory tests, has only recently begun. Several scenarios of film dissolution and rupture behavior presented by workers at Catholic University⁽¹⁵⁾ offer additional proposals for the prediction of long-term durability.

Current attempts at modeling face severe shortcomings by their recourse to a limited number of variables. As shown in the previous sections, the interacting variables are complex and require a more sophisticated and realistic treatment if they are to offer any predictive advantage at all.

6. CONCLUSIONS AND RECOMMENDATIONS

We have reviewed various chemical and mechanical processes for the degradation of glass. Such processes are often translated into formulas or models for the prediction of long-term durability. Attempts have been made at constructing predictive models for borosilicate glass in a water environment based on experimental data. Since current efforts in this area are valid only under very limited circumstances it is inevitable that we conclude our review on a qualitative note.

From the experimental results on the leaching of binary systems, the diffusion controlled dealcalization is predominant in the beginning with a square root time dependence while the appearance of network dissolution occurs with a linear time dependence following the diffusion process. However, the development of the time laws for this process is still too idealized and a linear extrapolation of those kinetics to geological time is, therefore, quite oversimplified at present. In the case of multicomponent systems even such simple kinetics are not currently available.

Solution and environmental variables such as temperature and pressure will have a direct effect on the durability of glass. As dealcalization proceeds, the nature of the solution will change. The solution composition effects are difficult to discern since these are interrelated to pH change and passive film formation at the glass surface. Typical reactions in simple systems involve silica network dissolution in high alkaline solutions and lower leach rates in neutral and acidic environments. Multicomponent glass systems also exhibit greater durability in acidic environments. Changes in pH, precipitation, and the effects of erosion resulting from variations in flow rates may result in unpredictable leach rates. The single activation process, observed in many commercial and nuclear waste glasses, offers a method of accelerating conditions at high temperatures to simulate long-term corrosion effects. For hydrothermal conditions, the alteration product resulting from glass-solution interaction is one of the most important variables determining the leach rate. A thorough understanding of the role played by the altered zone is needed in order to adequately identify the mechanisms involved in the corrosion process.

Glass composition is one of the most important factors determining the leach rate. Generally, network formers and divalent modifiers increase durability while monovalent modifiers have the opposite effect. The effects of phase separation on leaching is dependent on the microstructure and can either enhance or retard durability. The ratio of solid surface area to solution volume is another important parameter effecting leach rates. However, the difficulty in the determination of the total surface area makes the exact formulation of this parameter extremely difficult. As parameters having secondary effects on the leaching process, partial devitrification, internal stress, surface roughness, and local inhomogeneity contribute to changes in the leach rate. No quantitative data on the contribution of these parameters are available at the present time.

Toxic radioisotopes may escape from the waste form by solid state diffusion. Tabulations of gas and ionic diffusivity in glass indicate that such events are very unlikely under repository conditions.

In glass, local corrosion is not any more severe than general corrosion. Static fatigue, however, should be recognized as an important mode of disintegration over geological time. From the well-defined fracture mechanics, it is known that there is a fatigue limit for borosilicate glass below which no cracking occurs; however, changes at the microstructural level may modify the fatigue limit hypothesis. Modifications may arise due to surface stress, solution pH, humidity, temperature, pressure, compositional and microstructural inhomogeneity.

Radiation would probably not affect the leach rate by more than one order of magnitude as a result of radiolysis. An indirect effect such as microfracturing may be avoided by a proper design of the multibarrier glassy waste form.

Typical values for the dissolution rate of waste borosilicate glass range from 10^{-7} to 10^{-4} g/cm²-d, varying depending on the component. From the data at hand on the chemical and mechanical aspects of glass durability, and given an adequate design incorporating sacrificial layers and a proper burial site selection, waste form integrity, at least for the first thousand years, is achievable. It is still premature to attempt quantifying material released from glass over geological time since major uncertainties exist in the identification of the various mechanisms involved in glass leaching. Several research topics which would contribute to our understanding of long-term corrosion are presented below:

- Study the effects of groundwater ions on the selective leaching and passive film formation.
- Study pH effects on nuclear waste glass--seek to explain why acidic solutions affect leaching in binary glass differently from leaching in multicomponent systems;
- Study the flow rate effect in multicomponent systems thoroughly, especially the relative change of solution pH, reprecipitation, and passive film formation;
- Verify the single activated process by the measurement of leach rate as a function of temperature systematically for multicomponent systems;
- Study the surface chemistry of the alteration zone during leaching, especially during hydrothermal reactions. Surface-sensitive tools such as ESCA and AES are useful and should be adopted;
- More sensitive analytic tools, such as neutron activation analysis, should be used in the analysis of the leachate;
- Study the optimization in tailoring the glass composition for best leach resistance along with a formulation of the mechanisms involved, especially in multicomponent systems incorporating nuclear waste;

- Study the optimum microstructure for high leach resistance based on the principle of phase separation;
- Develop valid means of defining and measuring the surface area of powdered and cracked samples. Local pH change and corrosion cell formation in powdered samples should be thoroughly understood;
- Partial devitrification, surface roughness and local inhomogeneity should be studied more quantitatively;
- Measure ionic and gas diffusivity in glass at ambient temperatures; especially the diffusivity of fission products in nuclear waste glass;
- Study the wet-dry cycle effect on glass and compare the results to natural and archaeological analogs;
- Use a more mechanistic approach in understanding static fatigue--the effects of surface stress on crystallization is one example as opposed to relying on the well defined artificial stress intensity. More quantitative studies of the effects of pH, humidity, temperature, pressure and glass composition are needed, especially in the area of nuclear waste glass development;
- In radiation effects, α -radiolysis, and radiation induced cracking and pH change should be studied.
- Study of natural analogs and ancient glass requires a more systematic approach if they are to offer insights into long-term durability;
- More sophisticated and comprehensive modeling of glass corrosion processes are needed. Computerized code generation may be a necessary step in the assessment of the complex processes and in the area of long-term prediction of glass durability.

7. REFERENCES

1. L. Holland, "Chapter 3. Surface Chemistry and Corrosion of Glass," in The Properties of Glass Surfaces, Wiley, NY; (1964).
2. R. W. Douglas and T. M. El-Shamy, Jour. Amer. Ceramic Soc. 50, 1 (1967).
3. T. M. El-Shamy and R. W. Douglas, Glass Technology 13, 77 (1972).
4. L. L. Hench, D. E. Clark, and E. L. Yen-Bower, "Surface Leaching of Glasses and Glass Ceramics," in High-Level Radioactive Solid Waste Forms, NUREG/CP-0005, (1978) 199.
5. R. H. Doremus, "Chemical Durability in Glass," in M. Tomozawa and R. H. Doremus, Eds., Treatise on Materials Science and Technology, Vol. 17, Academic Press, NY, (1979).
6. R. H. Doremus, Glass Science, Wiley, NY, (1973).
7. L. L. Hench, "Physical Chemistry of Glass Surfaces," in Proceedings of the XIth International Congress on Glass (1977) 343.
8. L. L. Hench, Jour. Non-Crystalline Solids 19, 27 (1975).
9. A. Paul, Jour. Materials Science 12, 2246 (1977).
10. H. W. Godbee, et al., Nuclear and Chemical Waste Management 1, 29 (1980).
11. H. W. Godbee and D. S. Joy, "Assessment of the Loss of Radioactive Isotopes From Waste Solids to the Environment. Part 1. Background and Theory," ORNL-TM-4333, (1974).
12. E. Ewest, "Calculations of Radioactivity Release Due to Leaching of Vitrified HLW," in G. J. McCarthy, Ed., Scientific Basis for Nuclear Waste Management, Vol. 1, Plenum, NY, (1979).
13. A. J. Machiels, "Prediction of Initial Leach Rates of Glass Waste Forms," in Proceedings of the International Conference on World Nuclear Energy, Transactions of the American Nuclear Society, (1980).
14. A. J. Machiels, "Short-Term Leaching Behavior of Waste Forms," Proceedings, Workshop on Alternate Nuclear Waste Forms and Interactions in Geologic Media, Gatlinburg, TN, (1980).
15. A. Barkatt, et al., "Stability of Fixation Solids for High-Level Radioactive Wastes," in High-Level Radioactive Solid Waste Forms, NUREG/CP-0005 (1978) 105.
16. P. B. Macedo, et al., "Porous Glass Matrix Method for Encapsulating High-Level Nuclear Wastes," in Ceramics in Nuclear Waste Management, Cincinnati, CONF-790420 (1979) 321.

17. P. B. Macedo, A. Barkatt, and J. H. Simmons, "A Flow Model for the Kinetics of Dissolution of Nuclear Waste Glasses," Proceedings of ORNL Conf. on the Leachability of Radioactive Solids, Gatlinburg, TN (1980).
18. T.-M. Ahn, R. Dayal, and K. J. Swyler, "Chemical Durability and Structural Stability of Molecular Stuffed Glass-An Evaluation," BNL memorandum (1980).
19. L. L. Hench, D. E. Clark, and E. L. Yen-Bower, Nuclear and Chemical Waste Management, 1 (1980) 59.
20. R. Dayal, et al., "Nuclear Waste Management Technical Support in the Development of Nuclear Waste Form Criteria for the NRC, Task 1: Waste Package Overview," NUREG/CR-2333, Vol. 1, BNL-NUREG-51458, February 1982.
21. E. B. Shand, Glass Engineering Handbook, McGraw-Hill, NY, (1958).
22. M. E. Nordberg, "Chemical Durability," Corning Glass Works, unpublished manuscript.
23. T. M. El-Shamy, J. Lewins, and R. W. Douglas, Glass Technology 13, 81 (1972).
24. K. A. Boulton, et al., "The Leaching of Radioactive Waste Storage Glasses," in Reference 16.
25. J. W. Wiley and S. M. Plodinec, Proceedings of the 1980 National Waste Terminal Storage Program Information Meeting, ONWI-212, (1980), p. 110.
26. J. W. Wiley, et al., "Glass as a Matrix for SRP High-Level Defense Waste, DPST-79-294, (1980), p. 31.
27. J. E. Mendel et al., "MCC, A State-of-the Art Review of Materials Properties of Nuclear Waste Forms", MCC Report, PNL-3802, UC-70, (1981).
28. T.M. Ahn, et al., "Nuclear Waste Management Technical Support in the Development of Nuclear Waste Form Criteria for the NRC, Task 4: Test Development Review," NUREG/CR-2333, Vol. 4, BNL-NUREG-51458, February 1982.
29. J. E. Mendel, et al., Nuclear and Chemical Waste Management 1, 17 (1980).
30. W. B. White, "Dissolution of Crystalline Waste Forms II. The Role of Temperature in the Dissolution Process," in Reference 17.
31. J. W. Braithwaite and S. K. Johnstone, "Chemical Durability and Characterization of Nuclear Waste Forms in Hydrothermal Environment," In Reference 16.

32. J. H. Westsik, Jr. and R. P. Turcotte, "Hydrothermal Glass Reactions in Salt Brine," in Reference 12.
33. G. G. Strathdee, N. S. McIntyre, and P. Taylor, "Development of Alumino-Silicate and Borosilicate Glasses as Matrices for CANDU HLW," in Reference 14.
34. A. Barkatt, et al., "Static and Dynamic Tests for the Chemical Durability of Nuclear Waste Glass," to be published.
35. P. B. Adams and D. L. Evans, "Chemical Durability of Borate Glasses," in L. D. Pye, V. D. Frechette, and N. J. Kreidl, Edited, Borate Glasses: Structure, Properties, Applications, Plenum, NY, (1978).
36. A. M. Filbert and M. L. Hair, "Surface Chemistry and Corrosion of Glass," in M. G. Fontana and R. W. Staehle, Eds., Advances in Corrosion Science and Technology, Vol. 5, Plenum, NY, (1976).
37. G. B. Mellinger and L. A. Chick, "Effects of Composition on Waste Glass Properties," in Reference 16.
38. W. A. Ross and J. E. Mendel, "Annual Report on the Development and Characterization of Solidified Forms for HLW," PNL-3060, (1979).
39. J. L. McElroy, et al., "Quarterly Progress Report-Research and Development Activities-HLW Immobilization Program, April 1 through June 1979," PNL-3050-2, (1979).
40. W. Skatulla, W. Vogel, and H. Wessel, Silikattechnik 9, 323 (1958).
41. W. Haller, et al., Jour. Amer. Ceramic Society 53, 34 (1970)
42. M. Tomozawa, "Phase Separation in Glass," in Reference 1.
43. J. W. Wald and J. H. Westsik, Jr., "Devitrification and Leaching Effects in HLW Glass-Comparison of Simulated and Fully Radioactive Waste Glass," in Reference 16.
44. L. F. Shumitskaya, et al., Izvestiya Akademii Nauk USSR, 12, 88 (1976).
45. W. J. Weber, et al., "Radiation Effects in Vitreous and Devitrified Simulated Waste Glass," in Reference 14.
46. J. L. McElroy, et al., "Quarterly Progress Report-Research and Development Activities-HLW Immobilization Program, January through March 1979," PNL-3050-1, (1979).
47. S. C. Slate, "Stresses and Cracking in HLW Glass," PNL-SA-7369, (1978).

48. J. M. Perez, Jr. and J. H. Westsik, Jr., "Effects of Cracks on Glass-Leaching," paper presented at the ORNL Conf. on the Leachability of Radioactive Solids, Gatlinburg, TN, December (1980).
49. G. W. Morey, The Properties of Glass, Reinhold, NY, (1954).
50. R. J. Charles, Jour. Amer. Ceramic Society 45, 105 (1962).
51. P. B. Adams, personal communication.
52. D. M. Sanders and L. L. Hench, Ceramic Bulletin 52, 666 (1973).
53. R. Terai and R. Hayami, Jour. of Non-Crystalline Solids 18, 217 (1975).
54. J. Ralkova, Glass Technology 6, 40 (1965).
55. K. N. Woods and R. H. Doremus, Phys. Chem. Glass 12, 69 (1971).
56. H. M. Laska, R. H. Doremus, and P. J. Jargensen, Jour. Chem. Phys. 50, 135 (1969).
57. W. A. Rogers, R. S. Burlitz, and D. Alpert, Jour. Appl. Phys. 25, 868 (1954).
58. G. Eisemann, Ed., Glass Electrodes for Hydrogen and Other Cations, Dekker, NY (1967).
59. H. V. Walters and P. B. Adams, Jour. of Non-Crystalline Solids 19, 183 (1975).
60. P. B. Adams, "Chemistry of Nuclear Waste Glass Reaction: Problems and Potential of Prediction," in Reference 12.
61. Proceedings of the National Waste Terminal Storage Program Information Meeting, Oct. 31-Nov. 1, ONWI-62, (1979), 114.
62. M. F. Kaplan, "Ancient Materials Data as a Basis for Waste Form Integrity Projections," The Analytic Science Corp, TR-1749-1, (1979).
63. G. Shaw, New Scientist 27, 290 (1965).
64. E. Khy and G. Nauer, Jour. of Non-Crystalline Solids 29, 207 (1978).
65. R. G. Newton, Jour. of Glass Studies 17, 161 (1975).
66. T. M. El-Shamy, Phys. and Chem. of Glasses 14, 1 (1973).
67. G. A. Cox and A. M. Pollard, Archaeometry 19, 45 (1977).
68. E. R. Caley, Analyses of Ancient Glass, 1790-1957: A Comprehensive and Critical Survey, Corning Museum of Glass (1962).

69. W. Geilmann, *Glastech. Berlin* 29, 145 (1956).
70. R. H. Brill, *Scientific American* 209, 120 (1963).
71. R. H. Brill and H. P. Hood, *Nature* 189, 12 (1961).
72. R. G. Newton, *Glass Technology* 7, 22 (1966).
73. R. G. Newton, *Glass Technology* 10, 40 (1969).
74. R. G. Newton, *Archaeometry* 13, 1 (1971).
75. C. L. Quackenbush and V. D. Frechette, "Slow Fracture of Glass in Alkanes and Other Liquids," in V. D. Frechette, et al., Surfaces and Interfaces of Glass and Ceramics, Materials Research Volume 7, Plenum, NY, (1974).
76. R. J. Charles, *Jour. Appl. Phys.* 29, 1549 (1958).
77. S. D. Brown, in R. C. Breddt, D. P. H. Hasselman, and E. F. Lange, Eds., Fracture Mechanics of Ceramics, Vol. 4, Plenum, NY, (1978), 597.
78. W. W. Bergerich and M. Stout, *Jour. Amer. Ceramic Society* 58, 222 (1976).
79. S. M. Cox, *Phys. Chem. of Glass* 10, 226 (1969).
80. D. P. H. Hasselman, in J. J. Burke, N. L. Reed, and V. Weiss, Eds., Surface and Interface, Syracuse Univ. Press, (1970).
81. R. N. Stevens and R. Dutton, *Mater. Sci. Eng.* 8, 220 (1971).
82. E. Orowan, *Nature* 154, 341 (1944).
83. G. W. Weidman and D. G. Holloway, *Phys. Chem. of Glasses* 15, 68 (1974).
84. E. R. Fuller and R. M. Thomson, in Reference 74, p. 507.
85. S. M. Wiederhorn and C. H. Bolz, *Jour. Amer. Ceramic Society* 53, 543 (1970).
86. S. M. Wiederhorn, "Environmental Stress Corrosion Cracking of Glass," *Corrosion Fatigue, NACE-2* (1972), 731.
87. S. M. Wiederhorn, *Jour. Amer. Ceramic Society* 55, 81 (1972).
88. S. M. Wiedherhorn, E. R. Fuller, Jr., and R. M. Thomson, "Micromechanics of Crack Growth in Ceramics and Glasses in Corrosive Environments," NBSIR 80-2023 (1980).
89. W. B. Hillig and R. J. Charles, in V. F. Jackey, Ed., High Strength Materials, Wiley, NY (1965).

90. J. E. Burke, et al., in W. W. Kriegel and H. Palmour, Eds., Ceramics in Severe Environments, Plenum, NY (1971).
91. S. M. Wiederhorn and H. Johnson, Jour. Amer. Ceramic Society 56, 192 (1973).
92. S. M. Wiederhorn, "Strength of Glass-A Fracture Mechanics Approach," Proceedings of the 10th Internat. Congress on Glass Ceramic Society of Japan (1974).
93. S. M. Wiederhorn, A. G. Evans, E. R. Fuller, and H. Johnson, Jour. Amer. Ceramic Society 57, 319 (1974).
94. S. M. Wiederhorn, A. G. Evans, and D. E. Roberts, "A Fracture Mechanics Study of the Skylab Windows," in R. C. Bradt, D. P. H. Hasselman, and F. F. Lange, Eds., Fracture Mechanics of Ceramics, Vol. 2, Plenum, NY, (1974).
95. P. B. Adams, "Crack Propagation in Annealed Glass During Exposure to Water," in Reference 89.
96. S. M. Wiederhorn, "Mechanisms of Subcritical Crack Growth in Glass," in Reference 91.
97. S. M. Wiederhorn, Jour. Amer. Ceramic Society 50, 40 (1967).
98. S. W. Freiman, "Fracture Mechanics of Glass," in D. R. Uhlmann and N. J. Kreidl, Eds., Glass Science and Technology, Vol. 5, Academic Press, NY, (1980).
99. R. R. Tummala, Jour. of Non-Crystalline Solids 19, 263 (1975).
100. S. M. Wiederhorn and H. Johnson, Jour. Amer. Ceramic Society 54, 585 (1971).
101. D. D. Walker, M. D. Dukes, M. J. Poldinec, and N. E. Bibler, "Effect of Radiation on Leaching of Borosilicate Glass Containing Defense High Level Nuclear Waste," SRL, presented at the 181st National Meeting of ACS, March (1981).
102. W. J. Weber, J. W. Wald, and W. J. Gray, "Radiation Effects in Crystalline High-Level Nuclear Waste Solids," presented at Materials Research Society Annual Meeting, November (1980).
103. T. M. Ahn and K. J. Swyler, "An Analysis of Radiation Induced Stress in High Level Waste," BNL Memorandum (1981).

APPENDIX A

SOLUBILITY AND LEACH DATA FOR COMMERCIAL AND WASTE BOROSILICATE GLASS

This appendix is a compilation of available solubility and leach or corrosion data for commercial and waste borosilicate glasses that have been subjected to a water environment. Other glass compositions are also considered for the purposes of comparison.

A.1 Solubility and Kinetic Data for Commercial Borosilicate Glass

Silica is almost insoluble in water at 25°C at neutral pH with the solubility at about 0.012 weight percent.⁽¹⁾ The dissolved species has been identified as unionized monomeric silicic acid, Si(OH)₄. Solubility is approximately constant at pH values from 1 to 8. Above pH 8, the solubility rises sharply because of the ionization of the molecular silicic acid. Between 25°C and 200°C, the solubility of amorphous silica in water increases linearly with temperature, being about 0.83 weight percent at 200°C. The addition of various glass components change the glass solubility in many ways. For instance, simple alkali silicate glasses are fairly soluble, but the addition of lime and certain other oxides tend to raise their resistance in water.

Cline, et al.⁽²⁾ attempted to measure the solubility of BK-7 borosilicate glass (composition not specified) in deionized water at 23°C for 48 hours but found it to be below detection (detection limit: 0.1 mg). At elevated temperatures, Nordberg⁽³⁾ prepared a classification of the water resistance for different glass compositions as shown in Table A.1. Glasses marked

Table A.1

Water Resistance of Glasses⁽³⁾
(After Nordberg)

Grading	Glass Type	Corning Glass Number
Excellent	Silica	7940
	96% Silica	7900
	Durable borosilicate	7740, 7331, 7800
	Aluminosilicate	1710, 1720, 1723
	High lead	8870
Good	Soda lime	0080
	Alkali lead	0010, 0120
	Lead borosilicate	7720
	Borosilicate sealing	7052, 7055
Fair to Poor	High alkali	----
	Borosilicate sealing	7040, 7050
	Calcium aluminate	----
	Phosphate	----
	Borate	----

Test Conditions: 120°C for 1 hr, 10 g of powdered glass (4060 mesh) in 100 cc of water.

excellent will normally be chemically resistant to water at temperatures under 100°C, whereas glasses classified fair to poor have limited application. Taylor and Smith⁽⁴⁾, using the glass compositions given in Table A.2, measured the weight of material extracted when distilled water was heated to 260°C in sealed glass tubes for six hours. The results are given in Figure A.1. Borosilicate glass A showed greater attack than the high lead glass E at static conditions. When the glasses were tested under erosive conditions in the form of tubular condensers exposed to escaping steam for 100 hours, the lead glass E lost 13 times as much glass as the borosilicate. However, even this borosilicate glass finally becomes deeply etched under erosive conditions.

Table A.2

Composition of Glasses Studied by Taylor and Smith⁽⁴⁾

	Percentage Composition					
	A	B	C	D	E	F
SiO ₂	81	73	72	63	35	60
R ₂ O ₃	2	1	1	1	--	3
Na ₂ O	4	17	13	7	--	8
K ₂ O	--	--	--	7	7	--
B ₂ O ₃	13	--	--	--	--	29
CaO	--	5	9	--	--	--
MgO	--	3	5	--	--	--
PbO	--	--	--	22	58	--

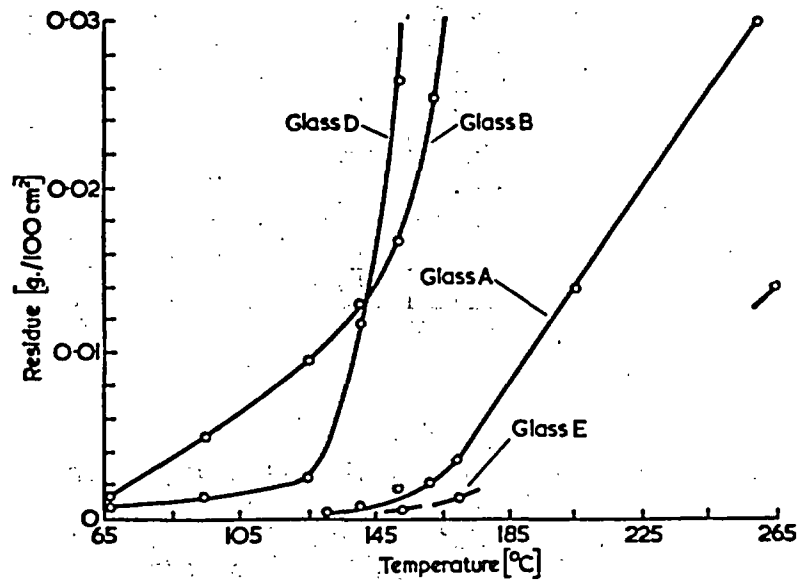


Figure A.1 Material removed at high temperatures from sealed glass tubes exposed to distilled water.⁽⁴⁾

Turner(5) and his co-workers conducted tests on a large number of British glasses and compared the results with similar tests on new Jena glassware. In one method a sample was subjected to the action of water boiling on a hot plate at such a rate that 200 cc was evaporated in two hours. In a second method, a sample was subjected to the action of water and steam in an autoclave at 183°C. The results are expressed as the loss in weight and the amount of Na₂O extracted. In resistance to attack by water at 100°C, the Jena glass and Pyrex chemically resistant glass offered the best results, while the Pyrex chemically resistant glass remained the most durable at 183°C.

Besides the material removed from sealed glass tubes at various temperatures shown in Figure A.1, Taylor and Smith (4) also reported the rates of attack by distilled water versus temperature on several glass compositions. Low-expansion borosilicate glass (D) was compared to soda-lime bulb glass (A), medium-lead electrical glass (B), and high-lead silicate glass (C). The compositions of these glasses are listed in Table A.2.

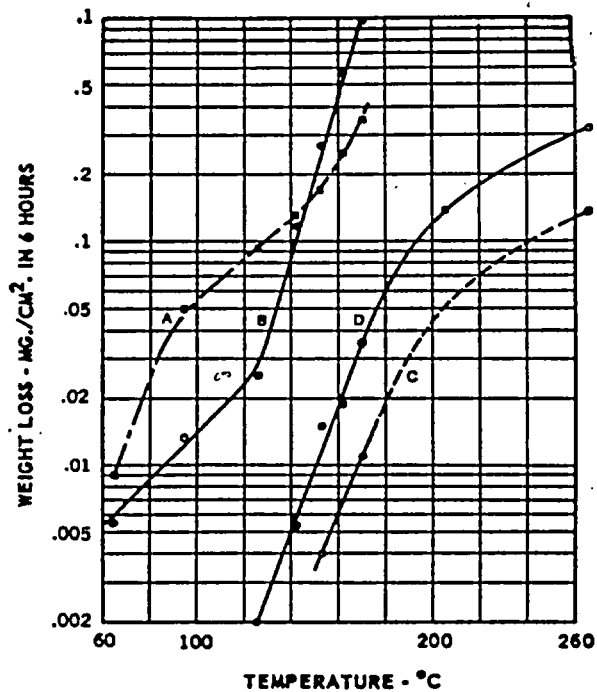


Figure A.2 Rates of attack by distilled water versus temperature on several glass compositions. A - Soda-lime bulb glass. B - Medium-lead electrical glass. C - High-lead silicate glass. D - Low-expansion borosilicate glass. (4)

Table A.3

Approximate Compositions of Glasses A, B, C, and D of Figure A.2

Designation	Percent									
	SiO ₂	Na ₂ O	K ₂ O	CaO	MgO	BaO	PbO	B ₂ O ₃	Al ₂ O ₃	
A. Soda-lime bulb glass	73.6	16	0.6	5.2	3.6					1
B. Medium-lead electrical glass	63	7.6	6	0.3	0.2		21	0.2	0.6	
C. High-lead silicate glass	35	7.2					58			
D. Low-expansion borosilicate	80.5	3.8	0.4				11.0	12.9	2.2	

As mentioned in the main text of this report, the effects of solution chemistry on glass solubility is a complex issue. Earlier work on this matter is illustrated by Figure A.3 which shows the amount of Na₂O dissolved from glass at 25°C and 90°C after 4 hrs. It is noted that the magnitude of alkali solubilities are similar for water and alkali solutions but different in acid solutions. The pH dependence is shown to be quite contrary to the conclusion of Section 1.3.2. The results must only be taken as generally indicative of the relative resistance of the glasses to alkali extraction. Thus after 4 hrs at 25°C in water, the soda lime glass B liberated more alkali than the sodium borosilicate glass F, but after 7 hrs glass A had taken the lead. In a more comprehensive study, Wichers⁽⁷⁾ tested the durability of three brands of flasks of borosilicate glass (Table A.4), varying somewhat in composition and general properties, and measured the total amount of substance removed from the glass in boiling water for 6 hrs as shown in Figure A.4 through A.6. The data were compared with tests in alkaline and acid reagents as well as nearly neutral reagents. No conclusion was drawn in this study.

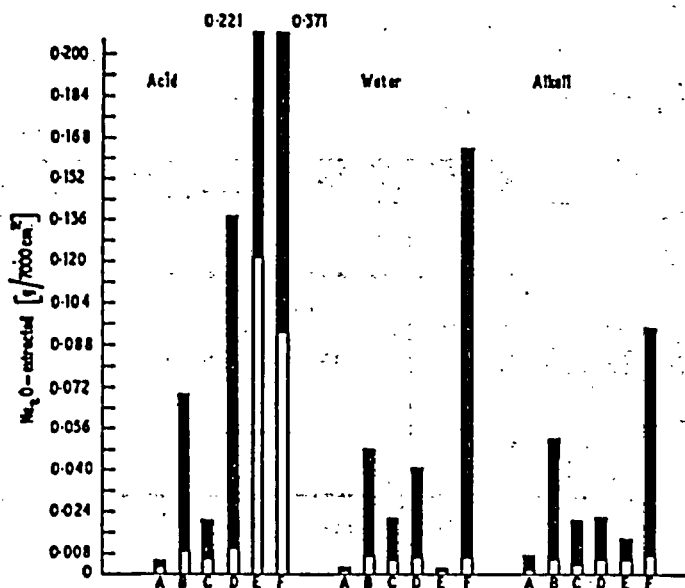


Figure A.3 Alkali extracted from glass powders at 25°C (double lines) and 90°C (solid black). Compositions are shown in Table A.2.⁽⁴⁾

Table A.4
Compositions of NBS Glasses (7)

Constituent	Glasbake (G)	Kimble (K)	Pyrex (P)	Vycor (V)
	Percent	Percent	Percent	Percent
SiO ₂	78.4	74.7	81.0	96.3
B ₂ O ₃	14.0	9.6	13.0	2.9
R ₂ O ₃	2.5	5.6	2.2	0.4
ZnO	n.d.	0.1	n.d.	n.d.
CaO	0.1	.9	neg.	neg.
BaO	n.d.	2.2	n.d.	n.d.
MgO	neg.	neg.	n.d.	n.d.
Na ₂ O	5.0	6.4	3.6	<0.02
K ₂ O	neg.	0.5	0.2	< .02
As ₂ O ₂	0.037	.027	.002	.005
Sb ₂ O ₂	.038	.009	n.d.	n.d.

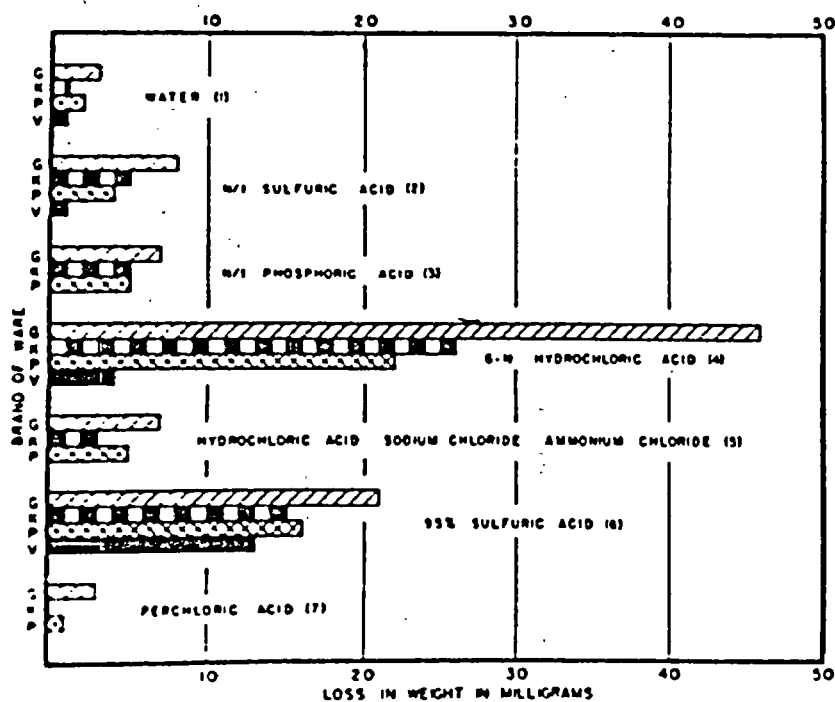


Figure A.4 Comparative resistance of NBS glasses to acid reagents and water. (7)

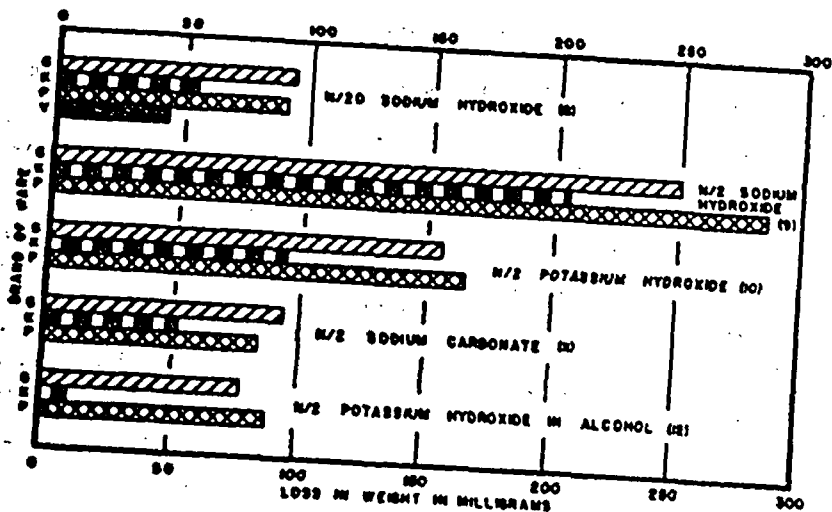


Figure A.5 Comparative resistance of NBS glasses to alkaline reagents. (7)

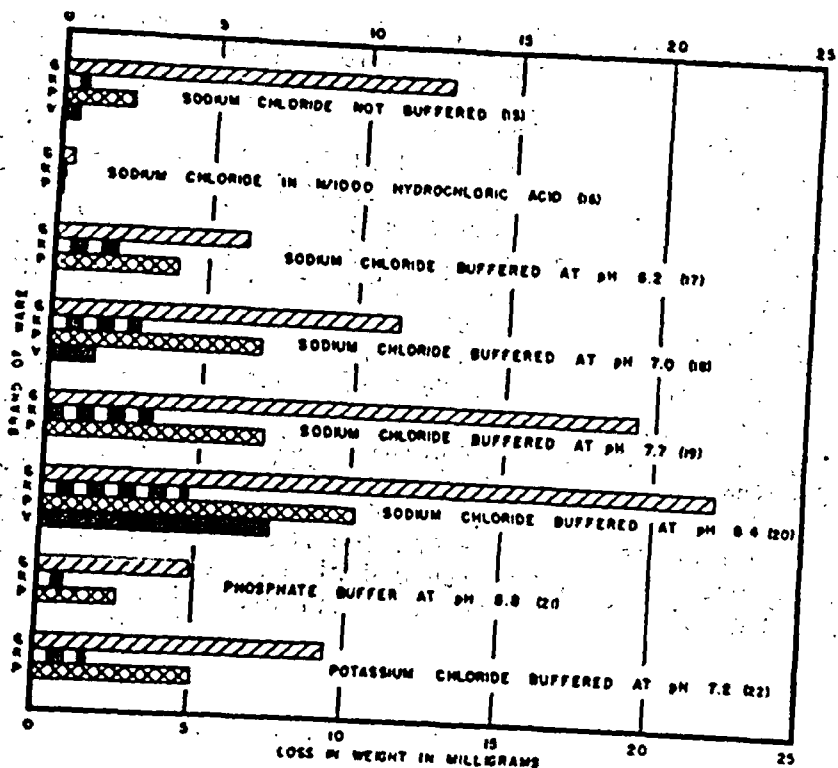


Figure A.6 Comparative resistance of NBS glasses to nearly neutral reagents. (7)

Holland⁽⁸⁾ measured the comparative loss of material from powder specimens (SA = 7000 cm²) with weight loss for plate glass (SA = 100 cm²) at 90°C.

Table A.5

Comparative Loss of Material With Varying Surface Areas⁽⁸⁾

	Plate Glass: 100 hrs, 90°C gm glass/100 cm ²			Powder: 4 hrs, 90°C gm Na ₂ O/7000 cm ²		
	H ₂ SO ₄	H ₂ O	NaOH	H ₂ SO ₄	H ₂ O	NaOH
Borosilicate:	0.00167	0.00184	0.00326	0.0047	0.0011	0.0062
Ratio:	0.9	1.0	18.6	4.27	1.0	5.64
Soda:	0.00164	0.00502	0.0517	0.0594	0.0434	0.0401
Ratio:	0.33	1.0	10.5	1.36	1.0	0.92

The results indicate that an effective increase of the total surface of the glasses significantly influence the total weight loss. The data on powder samples are comparable to that of plate glass although the powder samples were tested only for 4 hours while plate glass was tested for 100 hrs.

Workers at the Catholic University of America⁽⁹⁾ measured the leach rate on a borosilicate glass containing only sodium (0.44% Na₂O) for a period of 20 days at 22°C in distilled water (pH 5.7). The results of these measurements are presented in Figure A.7. The tests reported above show that the dissolution rates of both sodium and silica, as well as the ratio of sodium to silica in the dissolving materials, decline steadily in the course of exposure without showing any sign of rising again. However, in both cases the formation of a hydrated layer was not complete at the end of the test period. It appears that the ratio of sodium to silica in the dissolved material is still higher by an order of magnitude than the ratio in the solid glass. The only case where steady-state rates have been approached is when after 5 days, and up to at least 90 days of exposure, the rates of dissolution of both sodium and silica were observed to be constant with a sodium-to-silica ratio of 0.16:1 in the dissolved material compared with 0.096:1 in the solid glass. The findings that extremely long periods are required for the establishment of steady-state conditions is in agreement with results obtained in zinc borosilicate radwaste glass, where the rate of corrosion is observed to decline by about one order of magnitude during a period of 100 days of immersion in a neutral solution, and is still declining at the end of this period.

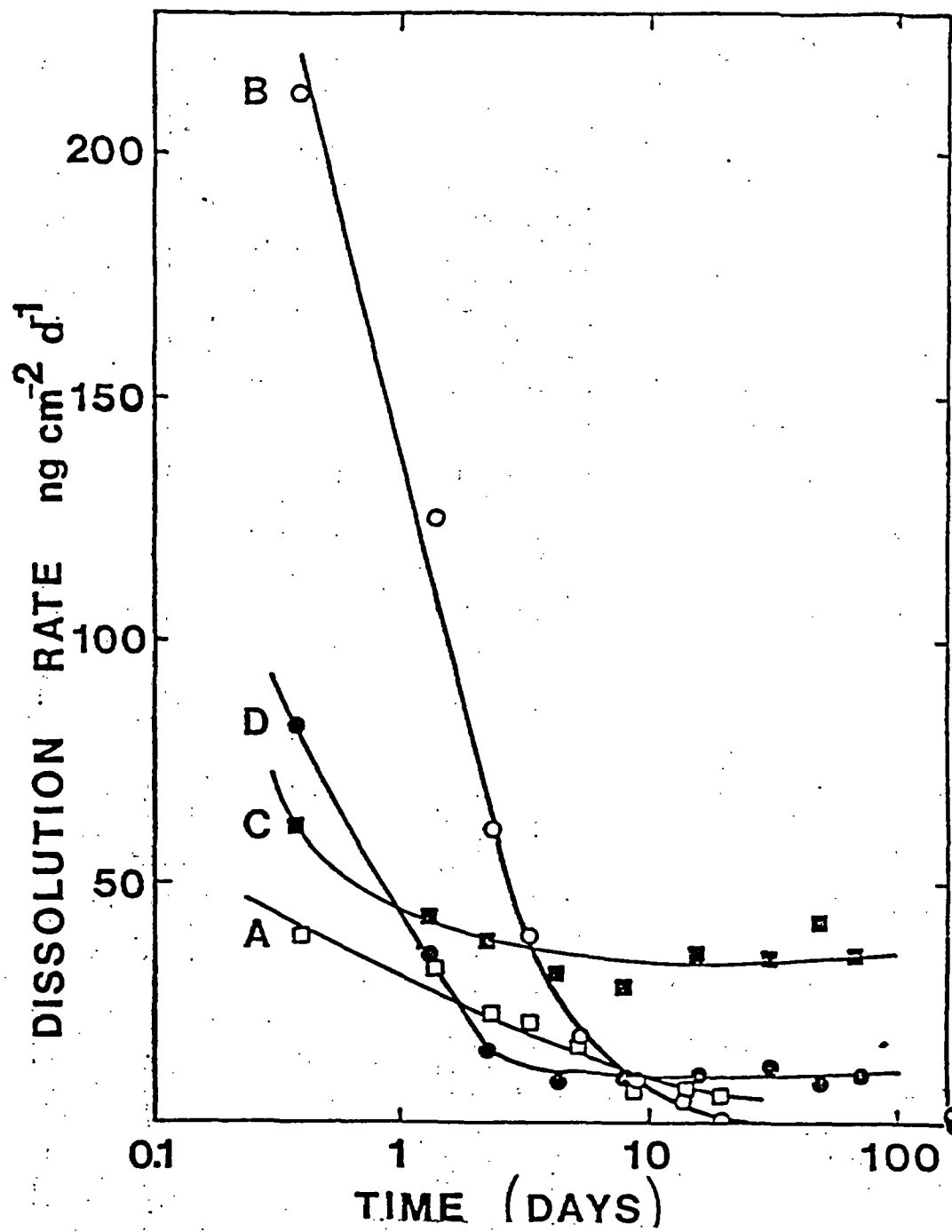


Figure A.7 Corrosion tests on borosilicate glasses in water.(9)

- A-dissolved SiO₂ from sodium glass at 22°C.
- B-dissolved Na from sodium glass at 22°C.
- C-dissolved SiO₂ from Pyrex glass at 70°C.
- D-dissolved Na from Pyrex glass at 70°C.

A.2 Waste Borosilicate Glass

The development of borosilicate glass for the encapsulation of nuclear waste by foreign and domestic laboratories continues to generate data on leaching and waste form characterization. The discussion that follows presents a brief summary of research efforts in this field. Since a unified approach to waste glass development is lacking, difficulties arise in the presentation of comparative results among the participant groups. Compositional differences in the waste glass product preclude any direct comparison while test methodologies vary from one laboratory to another. Given this independent approach to waste form development, it becomes rather difficult to draw any general conclusions concerning the glassy state for nuclear waste glass. In some instances, however, the evaluation of test results are aided by the inclusion of comparative material which allow for a certain "within-test" ranking of durability.

Simmons et al. tested the chemical durability of various waste glasses.⁽¹⁰⁾ Sample 1 (Figure A.8) is PNL's 76-68 glass with 33.0% PW-8a-2 simulated waste; sample 2 (Figure A.9) is a high silica glass formed by the Porous Glass Matrix Process (PGM) where the core is surrounded by a surface layer of glass free of waste components. Sample 3 is a low durability glass. Powders were used in the tests (355-250 μm fraction). The solution was deionized water; volume, 100 mL; surface area approximately 100 cm^2). The amounts of each component released to solution is shown in the following figures. The authors state that the pH of the solution was unchanged for the duration of the test.

The conclusion based on this study, is that high-silica glass is more durable than low silica compositions with the formation of a surface layer being a key variable in the overall durability of the glass. The crust is shown to be highly enriched in divalent ions. For the conditions described, cations with charge densities $>20 \text{ nm}^{-1}$ are expected to be readsorbed or undergo delayed leaching due to electrostatic interaction between cation and oxygen ion at the glass surface. The model tends to be oversimplistic and test conditions too mild to adequately test for long-term durability.

In long-term leaching of borosilicate glass reported by Scheffler, et al.,⁽¹¹⁾ the silica-rich layers were found to detach from the matrix as small particles. This was attributed to swelling of the silicate structure due to hydration. The surface gels formed in the presence of pure water or dilute NaCl swell up to 1 μm in thickness before detaching into solution. The swelling effect was not observed in saturated NaCl solutions. The average particle size of glass in water was in the order of $10^{-2} \mu\text{m}$. In tests at $23 \pm 1^\circ\text{C}$ in carnallite solution (H_2O -62.83%; MgSO_4 -2.04%; MgCl_2 -34.30%; KCl -0.62%; NaCl -0.21%), pure H_2O and 1MNaCl for a period of 80-240 days resulted in layers of 0.3 to 1.0 μm -thick. The report concluded that leaching behavior is characterized by successive periods of increasing and decreasing attack on the surface. The attack is not uniform in extent and duration. Over extended periods of time the attack proceeds as the average of successive layer detachments.

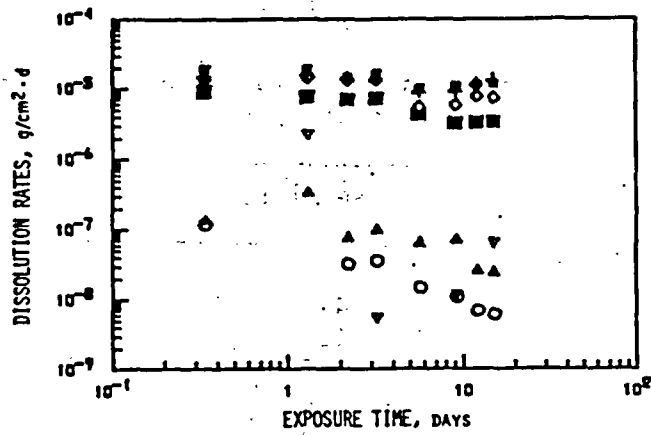


Figure A.8 Dissolution rates based on individual glass components for Sample 1 (borosilicate glass) at 70°C. ■, SiO₂; □, Na; +, Cs; ◇, Sr; ▽, Zn; ○, Fe; ▲, total Ln. (10)

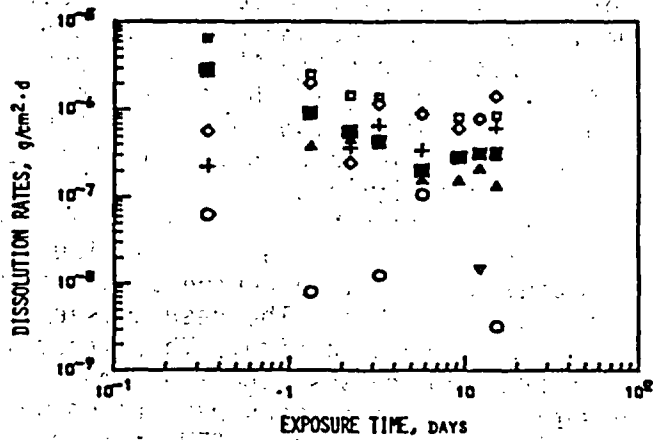


Figure A.9 Dissolution rates based on individual glass components for Sample 2 (high-silica PGM glass) at 70°C. ■, SiO₂; □, Na; +, Cs; ◇, Sr; ▽, Zn; ○, Fe; ▲, total Ln. (10)

Table A.6

Composition of Glass Used in German Leach Tests(11)
(in weight percent)

Oxide	Base Glass	HLW Glass
SiO ₂	50.5	40.2
TiO ₂	4.2	3.3
Al ₂ O ₃	1.4	1.1
B ₂ O ₃	13.6	10.8
CaO	2.8	2.2
Na ₂ O	27.5	21.9
Fission Products	---	16.68
Actinides	---	1.06

Alkali depletion is enhanced by higher temperatures. Tests using closed systems which tend to increase solution pH will alter the rate and mechanism of corrosion. Work performed by Lanza and Parnisari⁽¹²⁾ at temperatures of 30°, 80° and 100°C for periods up to 3600 hours on borosilicate glass with 20% simulated waste oxides. Tests at 30°C and 80°C were conducted in a Soxhlet type extraction apparatus with externally thermostated container. Tests at 100°C were conducted in an extraction in which the temperature was kept constant by the flow of water vapor. Two tests at 100°C used one system which kept the samples immersed in H₂O and one which kept the samples alternately wet and dry. Glass composition and simulated waste oxides are presented in Table A.7. Results obtained are shown in Table A.8 and Figures A.10 through A.13. In the worst cases the alkalis (particularly Na) are rapidly leached resulting in increased pH. In a replenished system, water composition and velocity are important parameters. The results seem to indicate a parabolic dependence of weight loss to time. The extraction of a sample for weighing purposes influences (increases) the leach rate. In a more recent work, Lanza and Parnisari⁽¹³⁾ reported measurements on weight loss and surface analysis, using EDX connected to an SEM, for the glass composition shown in Table A.9.

Table A.7

Parameters in Italian Waste Glass Research (12)
Glass Composition (80%)

<u>Comp.</u>	<u>Weight %</u>
SiO ₂	60
B ₂ O ₃	18.8
Al ₂ O ₃	6.2
Na ₂ O	15

Composition of Simulated Waste Oxide

<u>Oxide</u>	<u>Weight %</u>
K ₂ O	1.25
BaO	1.81
SrO	1.22
Fe ₂ O ₃	17.33
Cr ₂ O ₃	0.81
NiO	1.72
Na ₂ O	23.48
CuO	0.21
ZnO	0.17
La ₂ O ₃	2.23
CeO ₂	4.07
Pr ₆ O ₁₁	1.66
Nd ₂ O ₃	5.25
Sm ₂ O ₃	10.67
Y ₂ O ₃	6.85
ZrO ₂	5.67
MoO ₃	7.25
TeO ₂	0.82
CdO	0.11
SnO	0.07
UO ₂	7.33

Table A.8

Leaching Data (12) of Italian Glass

<u>Test</u>	<u>T°C</u>	<u>(gr/cm² d)</u>	<u>Observation</u>
1	30	4x10 ⁻⁷	
2	80	1.5x10 ⁻⁶	maximum value
2	80	3x10 ⁻⁶	minimum value
3	100	2x10 ⁻⁵	always full
4	100	4x10 ⁻⁵	partially full

A-74

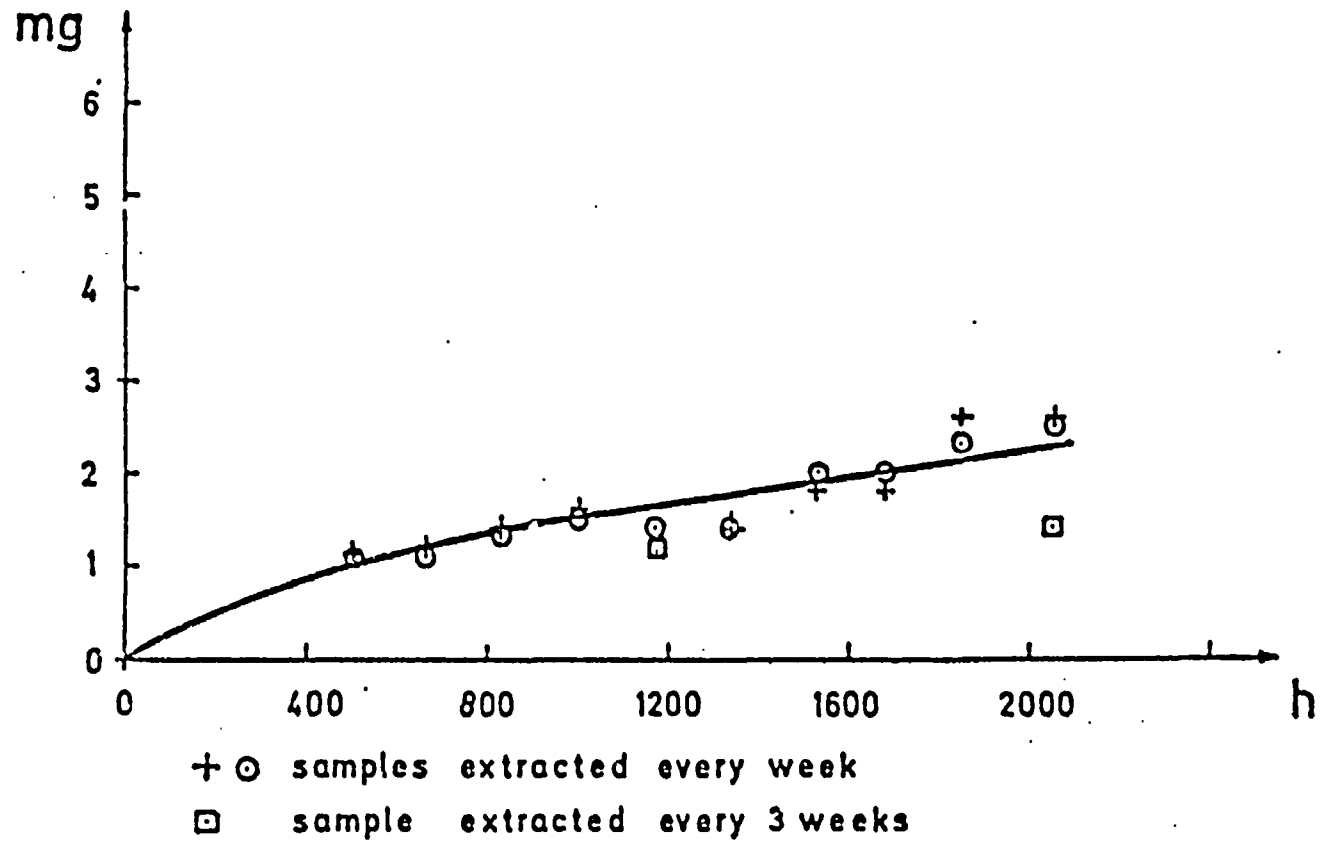


Figure A.10 Leach result of Italian glass at 30°C. (12)

A-75

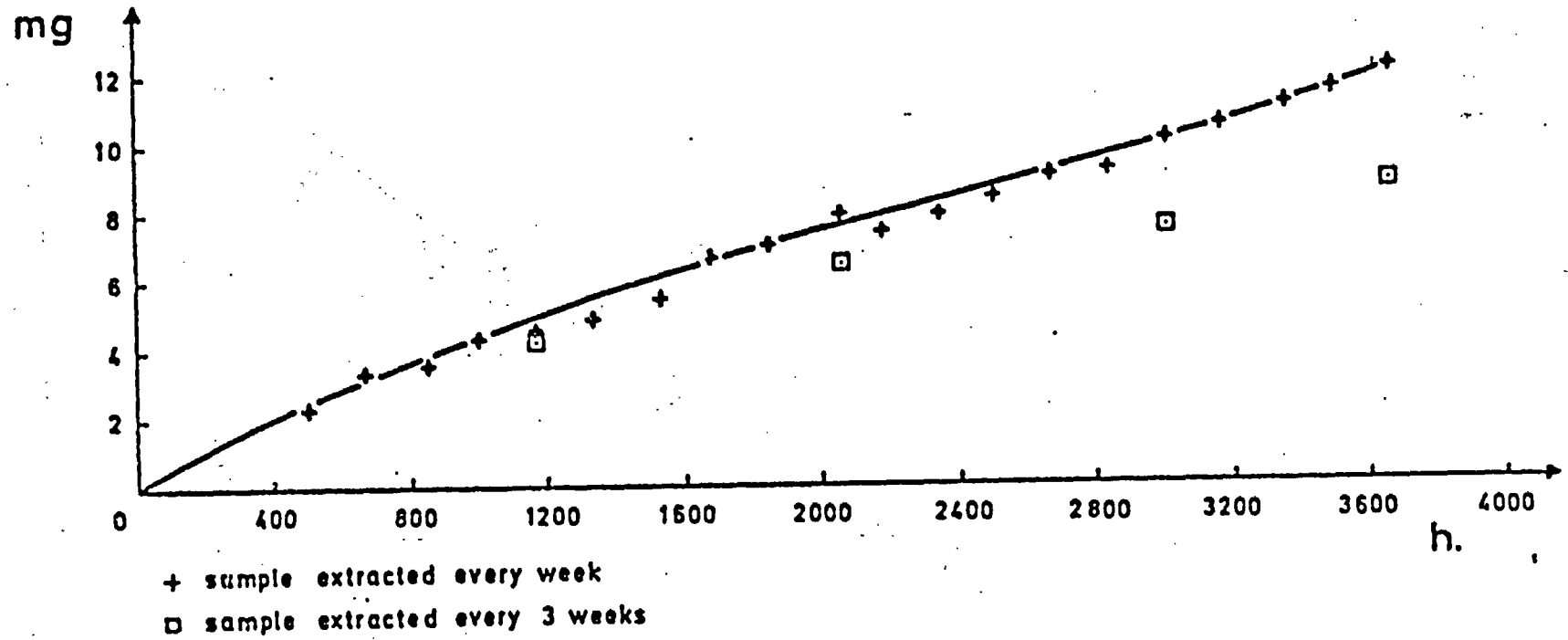


Figure A.11 Leach result of Italian glass at 80°C. (12)

A-76

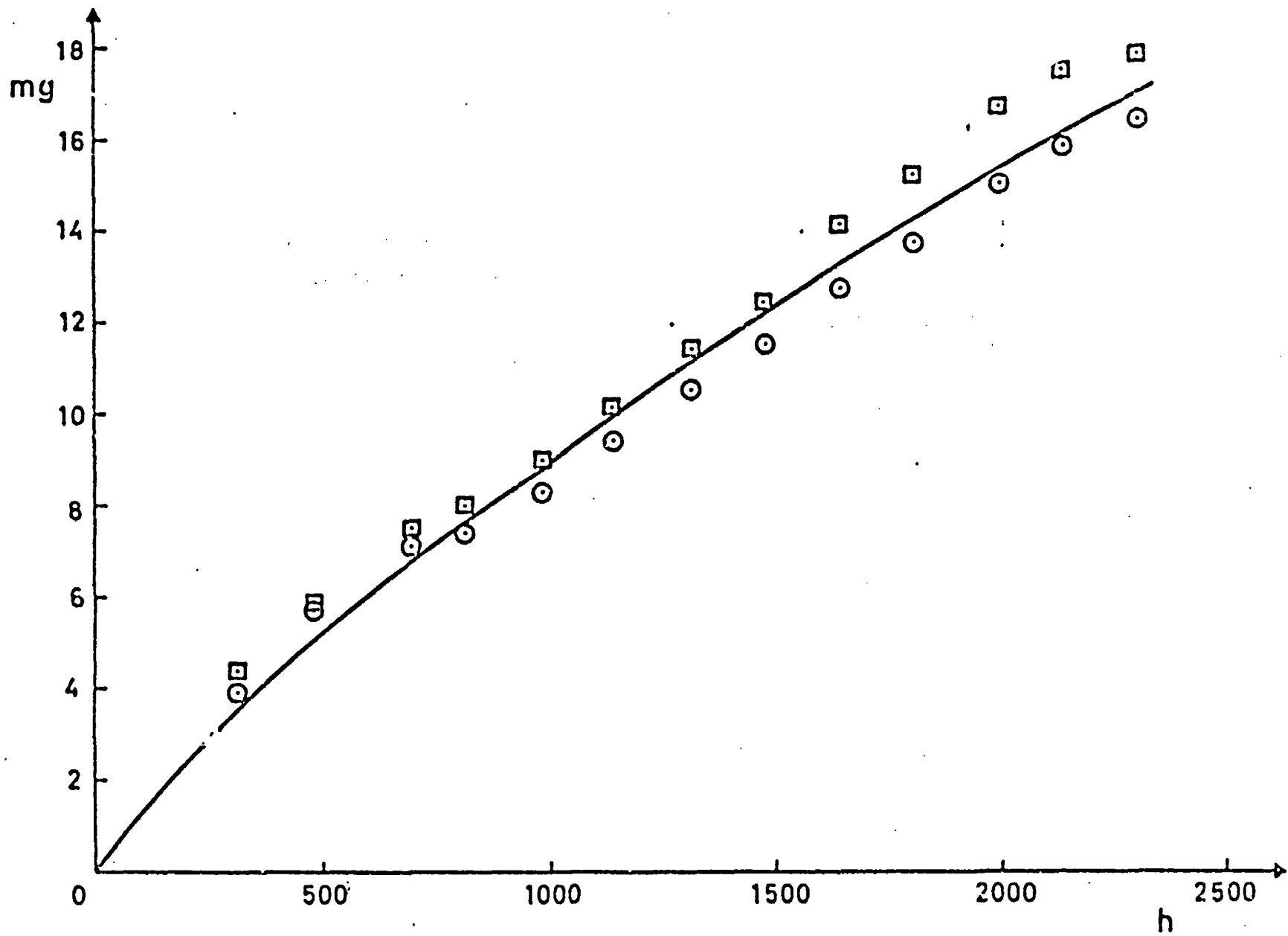


Figure A:12 Leach result of Italian glass at 100°C. (12)

A-77

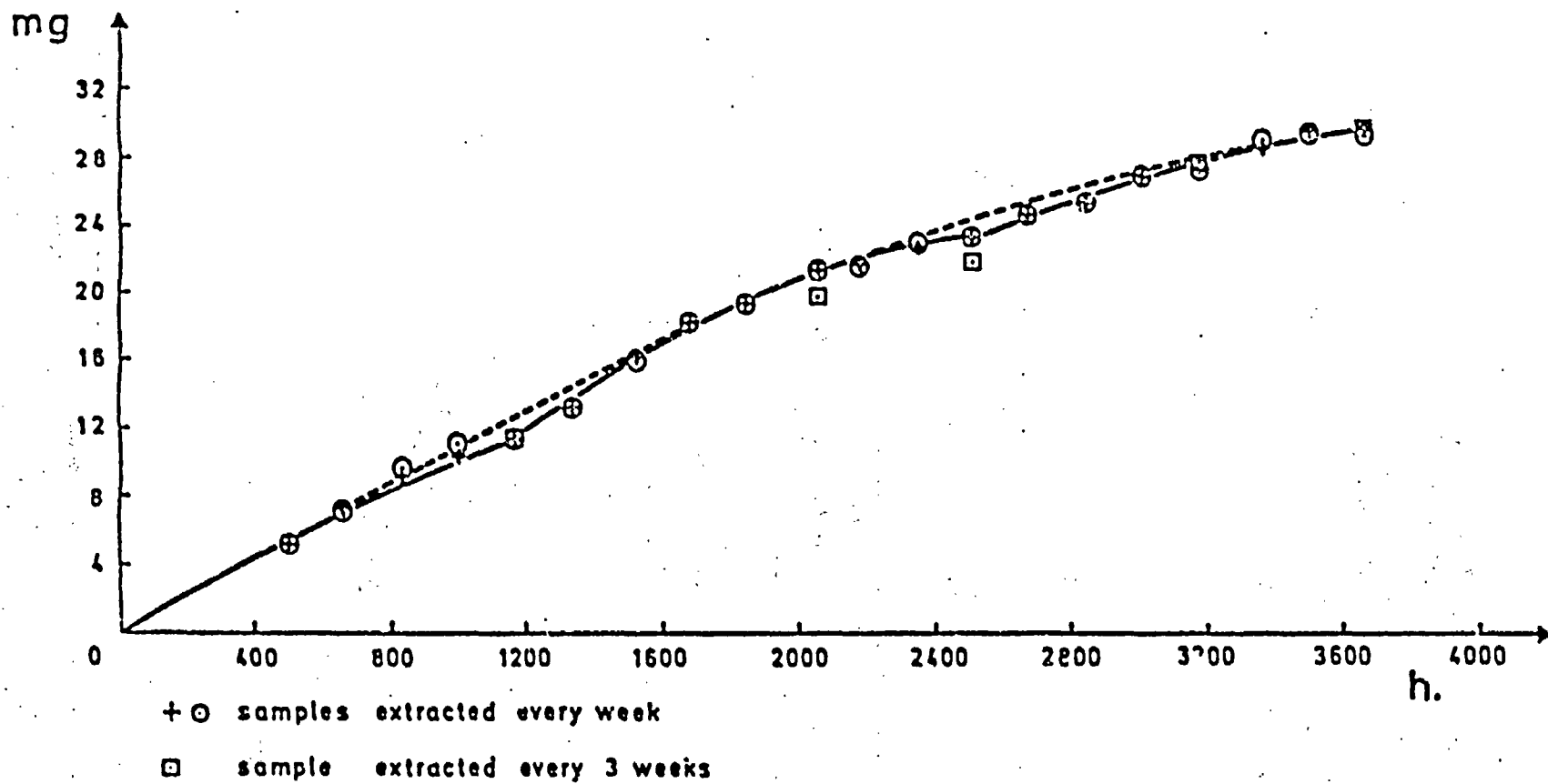


Figure A.13. Leach result of Italian glass at 100°C, water-vapor cycled.(12)

Table A.9

Additional Glass Compositions
Examined by Lanza and Parnisari⁽¹³⁾

Glass Composition			
Component	Wt.%	Component	Wt.%
SiO ₂	48	Sm ₂ O ₃	1.12
B ₂ O ₃	15	CeO ₂	0.76
Al ₂ O ₃	5	SnO ₂	0.03
Na ₂ O	18.49	ZrO ₂	1.06
SrO	0.22	MoO ₃	0.16
BaO	0.33	MnO ₃	1.35
Y ₂ O ₃	1.28	Fe ₂ O ₃	3.25
La ₂ O ₃	0.63	NiO	0.32
Pr ₂ O ₃	0.31	CuO	0.04
Nd ₂ O ₃	0.99	ZnO	0.03
		U ₃ O ₅	1.38

Temperatures: 50 and 80°C. Cast cylindrical samples of 10 mm diameter and 10 mm length.

Total weight loss as a function of time is shown in Figures A.14 and A.15.

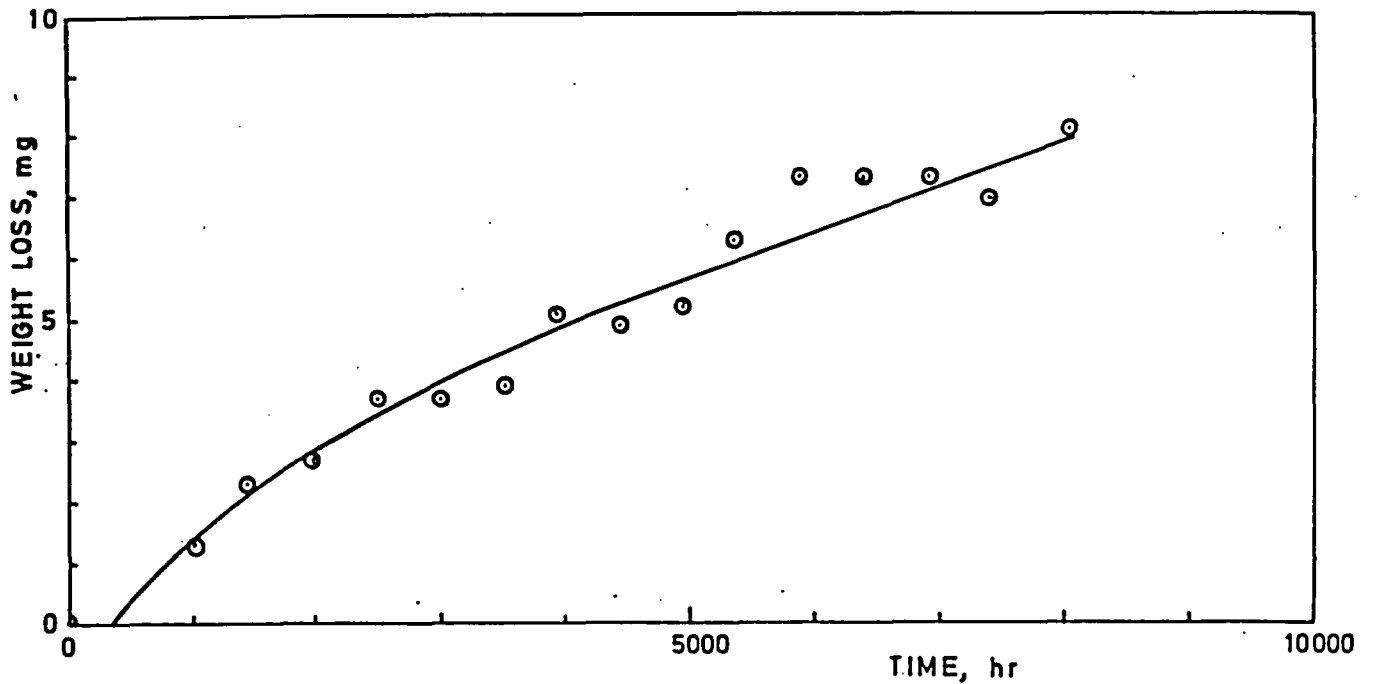


Figure A.14 Weight loss of Italian glass as a function of time
(T = 50°C).⁽¹³⁾

A-79

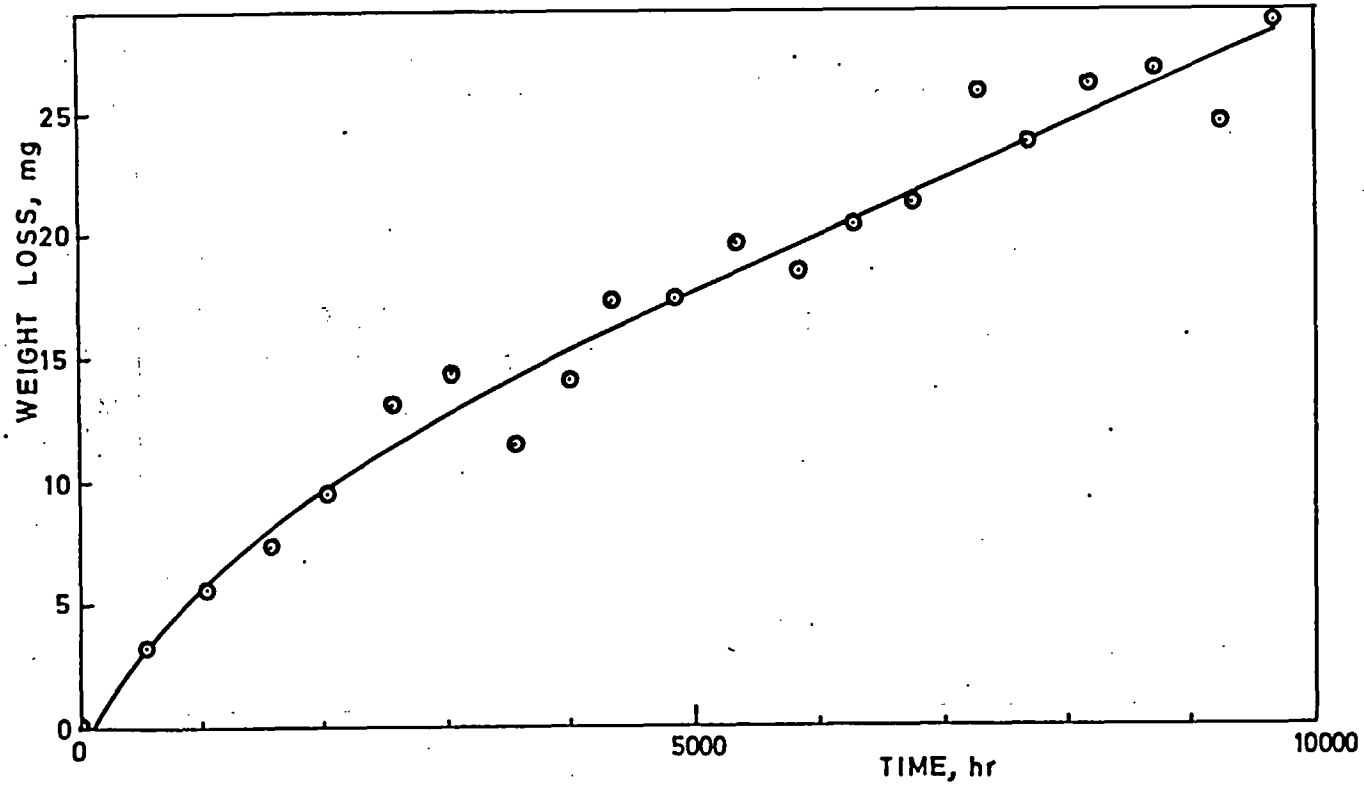


Figure A.15. Weight loss of Italian glass as a function of time ($T = 80^{\circ}\text{C}$). (13)

A-80

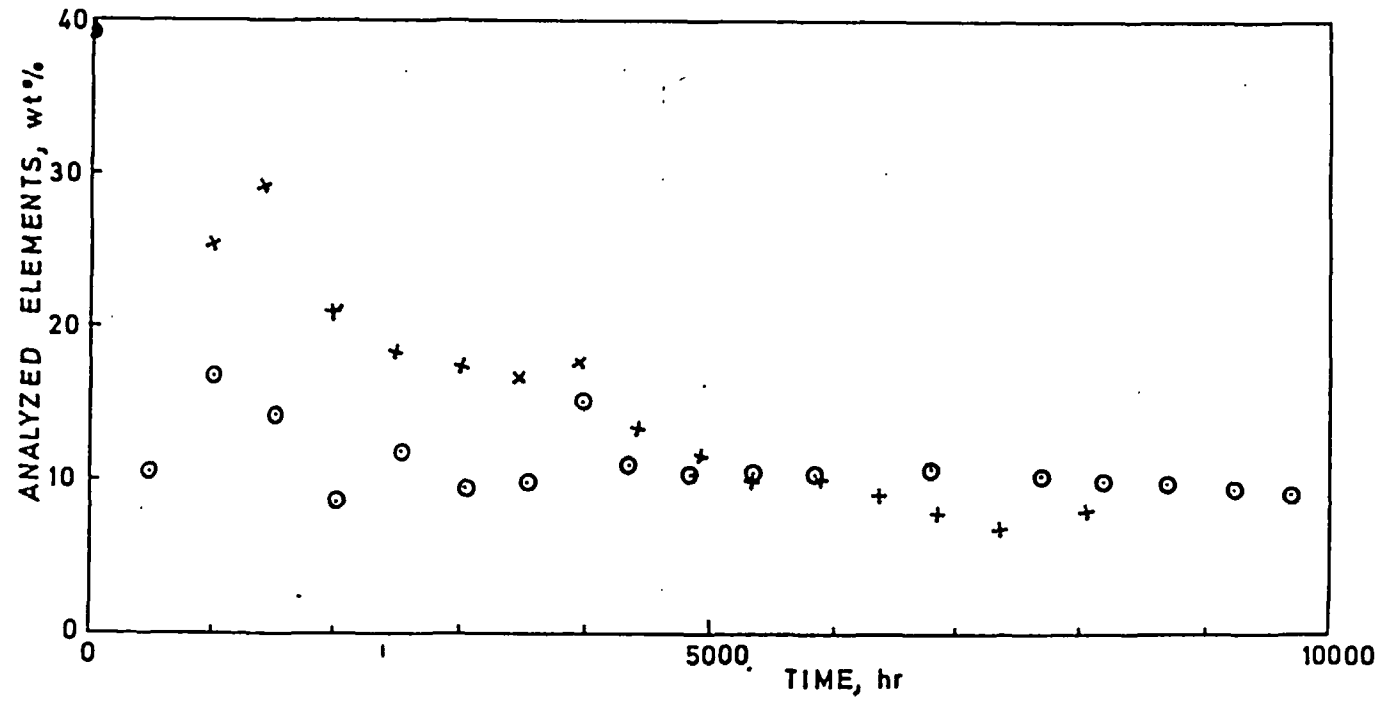


Figure A.16. Evolution of the total amount of the analyzed elements as a function of time in Italian glass (+ = 50°C, o = 80°C). (13)

Concentrations were obtained for Si, Na, Fe, Ni, Ce, and U. A plot showing total amount of cations as a function of time is presented in Figure A.16. The decrease in cation content of the surface gel may be attributed to surface hydration and H⁺ substitution as the reaction progresses through time. Table A.10 shows surface compositions based on the various leach times. It appears that after 9000 hrs (80°C) a steady state may have been reached. The conclusion of the authors is that periods longer than one year are needed to attain a linear time law.

Table A.10

Variations in Composition of the Surface Layer⁽¹³⁾ of Italian Glass

t, hr	Si/ Σ i, %	Na/ Σ i, %	Fe/ Σ i, %	Ni/ Σ i, %	Ce/ Σ i, %	U/ Σ i, %	T, °C
0	57.0	31.5	6.2	0.6	1.7	2.9	50
3024	49.4	15.6	21.3	2.2	5.2	6.4	50
5871	37.0	28.5	30.5	2.1	4.28	7.3	50
8055	36.3	24.2	24.0	1.4	5.4	8.6	50
0	57.0	31.5	6.2	0.6	1.7	2.9	80
3040	13.7	10.2	59.4	2.7	5.3	8.5	80
5864	24.2	13.0	48.4	2.1	2.3	9.8	80
9263	15.9	13.2	57.6	1.3	1.8	10.3	80

Corrosion behavior of glass 72-68 [PW-46-7(2.8)73.1], supplied by Battelle, was investigated in a variety of solutions by the Florida Group.⁽¹⁴⁾ Auger electron spectroscopy coupled with Argon ion milling and infrared reflection spectroscopy coupled with sequential polishing were used to determine the depth of the leached layers. The predominant processes proposed in the corrosion are selective leaching, primarily during the early stages, and network dissolution. Table A.11 shows the estimated thickness of the surface layer; Table A.12, the corrosion rates of the constituent elements. The lack of network stability in this glass may be due to the relatively small amount of silica (37.2 mol% SiO₂) which tends towards a weak silica film formation.

Table A.11

Estimated Thickness of Leached Layer^a
of 72-68 Glass⁽¹⁴⁾

Environment, 100°C	Time	Thickness of Leached Layer (μm) ^b
H ₂ O	10 hr	0
0.1M HCl	10 hr	22.6
	1 day	15.6
	2 days	13.6
0.1M NaOH	10 hr	1.2
	2 days	0.40

^aSA/V = 0.77 cm⁻¹.

^bDetermined from IRRS-sequential polishing technique.

Table A.12

Corrosion Rates of Elements From Nuclear Waste Glass 72-68
(Corrosion Temperature of 100°C and SA/V = 0.77 cm⁻¹)⁽¹⁴⁾

Solution	Actual Corrosion Time	g/cm ² -d ^{1/2}						
		Ba	Ca	Cs	Na	Si	Sr	Zn
H ₂ O	10 hr	NA			6.5x10 ⁻⁶	1.2x10 ⁻⁵		8.1x10 ⁻⁷
	2 days		4.9x10 ⁻⁷	4.9x10 ⁻⁶	6.9x10 ⁻⁶	4.6x10 ⁻⁶	2.8x10 ⁻⁷	6.4x10 ⁻⁷
	1 wk	2.4x10 ⁻⁶	2.2x10 ⁻⁶	1.1x10 ⁻⁷	6.8x10 ⁻⁷	1.4x10 ⁻⁶	2.2x10 ⁻⁷	9.8x10 ⁻⁷
0.1M HCl	10 hr	NA	2.4x10 ⁻⁴	2.4x10 ⁻⁴	4.5x10 ⁻⁴	1.5x10 ⁻⁴	3.8x10 ⁻⁴	2.7x10 ⁻³
	1 day	NA	1.4x10 ⁻⁴	5.2x10 ⁻⁴	2.9x10 ⁻⁴	8.8x10 ⁻⁵	2.0x10 ⁻⁴	1.9x10 ⁻³
	2 days	NA	1.2x10 ⁻⁴	1.3x10 ⁻⁴	2.2x10 ⁻⁴	6.9x10 ⁻⁵	1.8x10 ⁻⁴	1.3x10 ⁻³
	4 days	NA	9.1x10 ⁻⁵	9.1x10 ⁻⁵	2.3x10 ⁻⁴	3.0x10 ⁻⁵	5.5x10 ⁻⁵	8.4x10 ⁻⁴
	4 days	8.8x10 ⁻⁴	9.8x10 ⁻⁵	9.8x10 ⁻⁵	3.0x10 ⁻⁴	2.3x10 ⁻⁵	1.7x10 ⁻⁴	1.2x10 ⁻³
0.1M HNO ₃	1 wk	5.2x10 ⁻⁴	2.8x10 ⁻⁵	9.8x10 ⁻⁵	1.7x10 ⁻⁴	1.7x10 ⁻⁵	9.0x10 ⁻⁵	8.1x10 ⁻⁴
	1 wk	2.2x10 ⁻⁴	6.5x10 ⁻⁵	6.5x10 ⁻⁵	1.9x10 ⁻⁴	2.0x10 ⁻⁵	9.4x10 ⁻⁵	8.0x10 ⁻⁴
0.1M NaOH	10 hr	NA		1.9x10 ⁻⁵	NA	4.6x10 ⁻⁵	6.0x10 ⁻⁶	6.9x10 ⁻⁵
	2 days	NA		7.2x10 ⁻⁶	NA	7.9x10 ⁻⁶	6.5x10 ⁻⁷	1.3x10 ⁻⁵
	1 wk	9.5x10 ⁻⁶	2.4x10 ⁻⁷	9.3x10 ⁻⁶	NA	3.7x10 ⁻⁶	2.7x10 ⁻⁷	7.5x10 ⁻⁶

NA = not analyzed.

Leach studies conducted at Corning compared simulated nuclear waste glasses with obsidian glass.⁽¹⁵⁾ Tests were conducted on plates of 1.25-cm square and 0.32-cm thickness or grains under the following conditions:

- (1) pH 4: 42 to 60 mesh grains in 2.5% sodium acetate +7.0% acetic acid for 19 hrs at 25°C - results as weight loss.
- (2) Soxhlet test: 45 to 60 mesh in renewed distilled water, 24 hrs at 100°C - results as weight loss.
- (3) Strong base: plates in 5% NaOH, 6 hrs, 95°C - results as weight loss.
- (4) Weak base: plates in 0.02N Na₂CO₃, 6 hrs, 95°C - results as weight loss.
- (5) Strong acid: plates in 5% HCl, 24 hrs, 95°C - results as weight loss.
- (6) Distilled water: powder: 40 to 50 mesh grains, 4 hrs, 90°C - results as alkali extracted.
- (7) Acid: powder: 40 to 50 mesh grains in 0.02N H₂SO₄, 4 hrs, 90°C - results as alkali extracted.

Long-term tests at 30, 60 and 90°C were conducted, up to a year, on plate specimens immersed in distilled water in agitating constant temperature baths. Water was changed weekly for some of the samples. Table A.13 shows glass compositions of the test samples. Table A.14 ranks the materials relative to granite obsidian. Curves fit to the data for the waste glasses and the obsidians are shown in Figure A.17. Table A.15 shows the slopes for reaction rates derived from the various curves, recalculated as μm per year. The sodium extraction data is based on "Leach Depth" (LD) which indicates that sodium extraction or ion exchange has taken place to at least this depth. Test solutions were classified into two groups: (1) Lim RPB-limited reaction product buildup, and (2) Sig RPB-significant reaction product buildup.

It was noted that when there is no reaction product buildup as a result of increased temperature, the apparent activation energy does not change. Figure A.18 shows the log of LD vs inverse temperature after the Arrhenius expressions for glass R and Q at 20 weeks. Assuming linear dissolution rate for silica the range of reaction rates are given in Table A.16. Predicted rates are given in Table A.17.

Table A.13

Composition of Materials Studied at Corning⁽¹⁵⁾

Constituent	Natural Granite Obsidian, %	Synthetic Obsidian, %		Nuclear Waste Glass, %	
		Andesite	Basalt	Q	R
SiO ₂	74.6	60.1 (60.0)	49.7 (50.0)	38.1 (39.4)	40.1 (40.6)
TiO ₂		0.8	1.4		
Al ₂ O ₃	14.0	17.5	15.9	13.8	
Fe ₂ O ₃	2.0	6.6	11.9	5.2	11.3
MnO			0.3		
MgO		2.8	6.2	1.6	
CaO		5.1	9.1		2.0
Na ₂ O	3.8	3.7 (3.6)	3.2 (3.2)	17.3 (16.5)	13.0 (12.5)
K ₂ O	5.3	2.1	1.5		
P ₂ O ₅					0.5
ZrO ₂				0.4	1.9
CeO ₂				0.3	3.9
RuO ₂				0.3	
B ₂ O ₃				(17.1)	(9.4)
Cr ₂ O ₃				0.9	0.5
La ₂ O ₃				0.3	2.0
Cs ₂ O				0.3	0.5
NiO				0.6	0.6
MoO ₃				0.5	2.5
F				1.9	
Other					

Glass Q is Battelle's 76-101 (67 wt.%) with 33% PW-8a-2.
Glass R is the French SAN 55-20-20-F.22 waste glass.

Comparison of observed natural obsidian rates with predicted rates show 0.003 $\mu\text{m}/\text{yr}$ for granite obsidian at 30°C and 0.01 $\mu\text{m}/\text{yr}$ for basalt obsidian vs approximately 0.01 $\mu\text{m}/\text{yr}$ reported in this study.

A comparative summary of the Corning test results, including 7740 glass, is given in Tables A.18, A.19, and A.20.

Table A.14

Relative Values of Results for Standard Tests of Corning(15)

Test Type ^b	Relative Results ^a				
	Obsidians			Glasses	
	Granite	Andesite	Basalt	Q	R
Alkali					
Strong (3)	1	2	2	10	1
Weak (4)	1	2	32	6	1
Acid					
Strong (5)	1	5	1025	5050	5000
pH 4 (1)	1	53	567	43	7
Powder (7)	1	1	3	32	8
Water:					
Soxhlet (2)	1	4	25	62	37
Powder (6)	1	1	1	12	12

^aRelative results between samples but not between tests.

^bNumber in parentheses refers to test description as numbered in text.

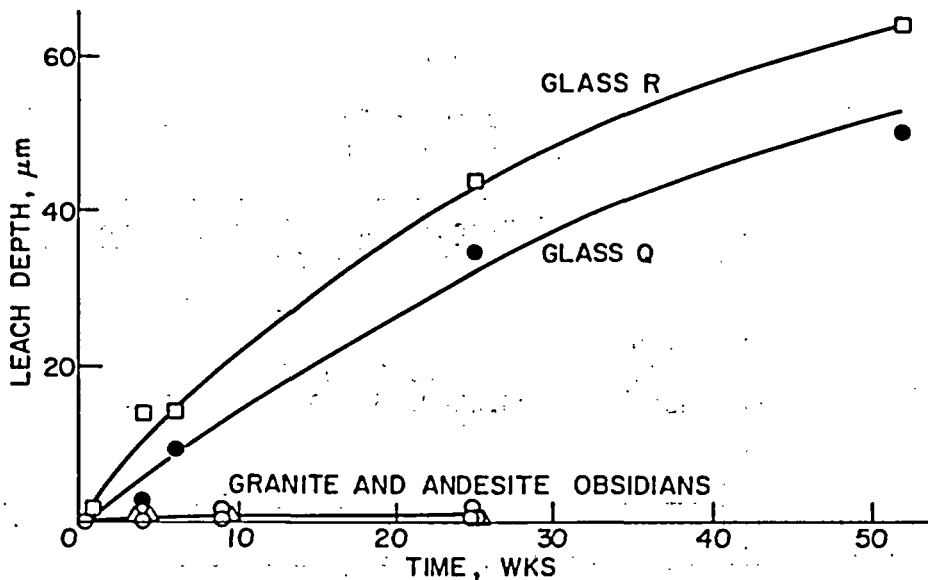


Figure A.17 Leach depth vs. time at 90°C when there is Lim RPB in water from Corning test.(15)

Table A.15

Sodium Reaction Rates (e.g., Slope of Curve) at 1 Week and 20 Weeks
From Corning Test⁽¹⁵⁾

Material	Reaction Extent ^a	Reaction Rate, $\mu\text{m}/\text{year}$						
		30°C	1 Week			20 Weeks		
			60°C	90°C	30°C	60°C	90°C	
Obsidian								
Granite	Lim RPB	<0.1	<1	1	<0.1	1	<1	
	Sig RPB	0.01	<0.1	<1	0.01	<0.1	<1	
Andesite	Lim RPB	<0.1	<1	1	<0.1	<1	1	
	Sig RPB	0.01	<0.1	<1	0.01	<0.1	<1	
Glass								
Q	Lim RPB	1	12	80	0.2	7	65	
	Sig RPB	1	3	10	0.04	1	3	
R	Lim RPB	1	40	140	1	15	65	
	Sig RPB	1	12	35	0.2	5	6	

^aEither limited (Lim) or significant (Sig) reaction product buildup (RPB).

Table A.16

Reaction Rate Ranges Based on SiO_2 Dissolution Results
of Corning Test⁽¹⁵⁾

Material	Reaction Rate Range, $\mu\text{m}/\text{year}$		
	30°C	60°C	90°C
Obsidian			
Granite	0.00-0.02	0.01-0.2	0.4-2
Andesite	0.00-0.06	0.4-4	0.4-9
Glass			
Q	0.02-0.2	0.6-6	1-25
R	0.02-1	2-16	1-40

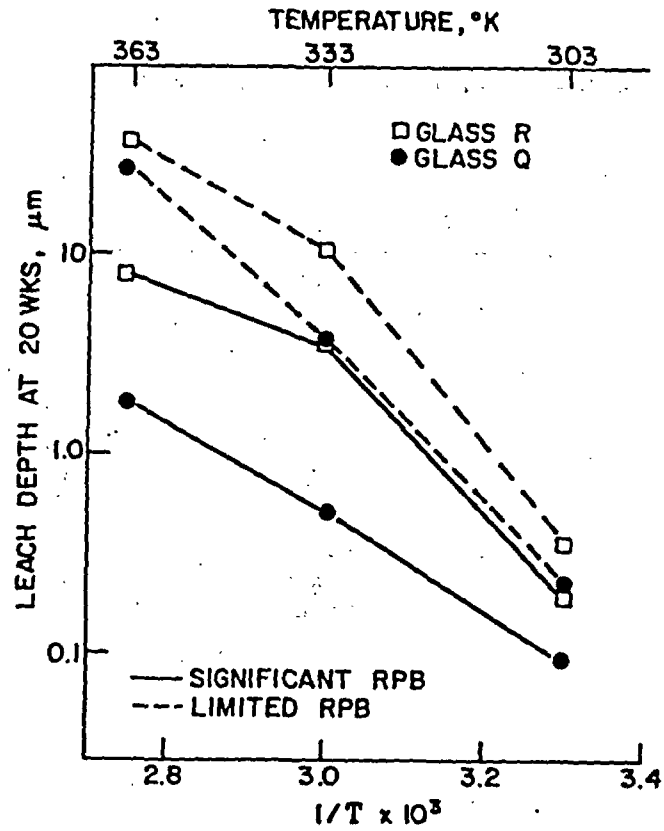


Figure A.18 Relevance of sodium data of Corning test to the Arrhenius expression. (15)

Table A.17

Predicted Reaction Rates of Corning Test (15)

	Microns per year		
	30°C	60°C	90°C
Obsidian			
Granite	0.01	<0.1	<1
Andesite	0.01	<0.1	<1
Basalt	0.01	0.1	<1
Glass			
Q	0.04	0.6	3
R	0.2	2	6

Table A.18

Comparison of Chemical Resistance From Corning Test(15)

Test	Test No.	Solvent	Time (hr)	Temp. (°C)	Units	Results for Glass Types			
						<u>1</u>	<u>2</u>	<u>3</u>	<u>4</u>
Acid Base	1	pH 9	19	25	%	0.0	0.0	0.0	0.0
	2	pH 4	19	25	%	17.0	1.6	1.3	0.2
Soxhlet	3	water	24	100	%	1.0	0.18	2.5	1.5
Plate	4	NaOH	6	95	mg/cm	1.1	1.1	6.7	0.7
	5	Na CO	6	95	mg/cm	1.6	0.1	0.3	0.05
	6	HCl	24	95	mg/cm	41.0	0.2	202.0	200.0

^aGlass 1 = 50% SiO₂ obsidian; glass 2 = 60% SiO₂ obsidian; glass 3 = SAN 55.20.20.20F.22 French composition; glass 4 = Battelle 67% 76-101, 33% PW-8a-2.

Table A.19

Ranking of Different Glasses Using Glass No. 2 as Unity From Corning Test(15)

Test	Approx. pH	Test No.	Result Compared to Glass No. 2 for			
			<u>Glass 1</u>	<u>Glass 2</u>	<u>Glass 3</u>	<u>Glass 4</u>
Acid	0.1	6	200	1	1000	1000
	4	2	10	1	0.8	0.1
Neutral	7	3	5	1	15	8
Base	9.5	5	16	1	3	0.5
	13	4	1	1	6	0.6

Table A.20

Comparison of Chemical Durability for Various Glasses From Corning Test(15)

Test	Natural Obsidian	7740 Glass	Synthetic Obsidian	Candidate Glasses French Battelle	
Plate -					
<u>Weight Loss (mg/cm²):</u>					
5% HCl ^a	0.05	0.01	0.2	202.	200.
5% NaOH ^b	0.8	1.0	1.1	6.7	0.7
0.02N Na ₂ CO ₃ ^b	0.05	0.1	0.1	0.3	0.05
Powder -					
<u>Alkali Extracted (%Na₂O)</u>					
0.02N H ₂ SO ₄ ^c	0.001	0.001	<0.001	0.012	0.012
Water ^c	0.003	0.005	0.003	0.097	0.025
a 24 hr at 95°C.					
b 6 hr at 95°C.					
c 4 hr at 90°C.					

The cyclic behavior of glass degradation is illustrated in a series of experiments by Kenna, et al. at Sandia⁽¹⁶⁾. Two zinc borosilicate glass samples, one prepared by PNL and one at Sandia, along with a hot pressed sodium titanate pellet, underwent Soxhlet leach tests for a 20 month period. The samples contained approximately 25 weight percent simulated high-level calcined waste. A quartz Soxhlet apparatus using deionized water (300 mL) at boiling temperatures was used for the samples and one empty quartz Soxhlet was run as a blank. Concentrations of Cs, Sr, Na, Mo, Zn, and Si in solution were determined by atomic absorption spectroscopy. Following two months of testing the glasses showed a gel layer (described as reddish-brown) which periodically broke off into solution. Results indicate that (1) the leaching behavior is not linear or uniform; (2) a periodic cycle of leaching is evident; (3) maxima for less mobile element (Mo) precedes mobile element (Cs) by approximately 1 month. The periodicity may be due to surface dissolution leading to surface roughening increasing surface area and a structurally weak protective film which tends to fall off into solution (see Fig. A.19 and A.20).

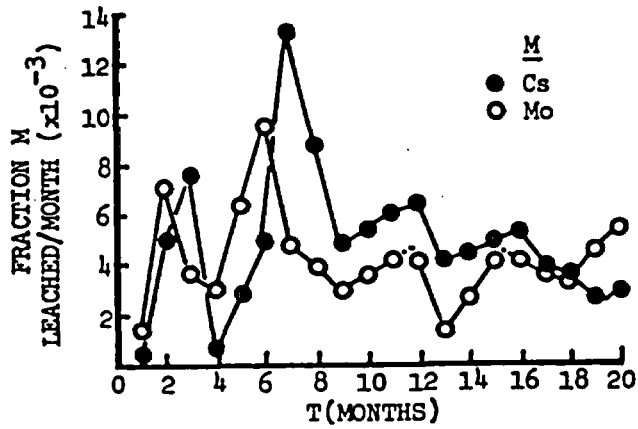


Figure A.19. Soxhlet leaching of Mo from glasses (SLA, BNW) and ceramic (STW) loaded with 25 w/o waste oxide simulant from Sandia Test. (16)

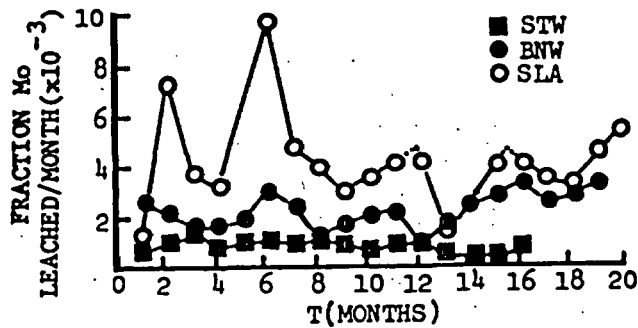


Figure A.20. Comparison of Soxhlet leaching of mobile (Cs) and immobile (Mo) elements from glass (SLA) loaded with 25 w/o waste oxide simulant from Sandia Test. (16)

Corning's investigations into glass corrosion led to testing five experimental glass candidates from the U.S., England, France, Germany, and India.⁽¹⁷⁾ A conventional soda-lime glass was included in the tests for the purpose of comparison (Table A.21). The composition of the simulated nuclear waste included in the waste glasses is given in Table A.22.

Table A.21
Glasses Tested by Corning⁽¹⁷⁾

Composition (Weight Percent) ^a	Glass A	Glass B	Glass C	Glass D	Glass E	Soda Lime
SiO ₂	43.	52.	35.	40.	27.	72.
B ₂ O ₃	22.	14.	9.	17.	11.	---
Na ₂ O ^b	12.5	11.0	21.9	9.1	6.8	14.
K ₂ O	0.4	0.4	0.5	0.3	4.6	0.2
CaO	---	---	1.9	3.0	1.5	11.5
BaO	0.6	0.6	0.7	---	1.5	---
SrO	0.4	0.4	0.5	---	1.5	---
Fe ₂ O ₃ ^b	1.9	1.9	2.3	13.1	2.0	---
ZnO	---	---	---	---	21.	---
Al ₂ O ₃	---	---	1.0	---	---	1.8
TiO ₂	---	---	2.9	---	---	---
Waste ^c	25.	25.8	30.5	20.2	26.2	None
Melting Temp. (°C)	1050	1150	1150	1050	1050	---
Time (hr)	6	6	6	5	5	---
Density (gm/cm ²)	2.69	2.66	2.93	2.78	3.27	2.47
Grain Surface Area (cm ²)	296	276	163	210	169	182

^aB₂O₃, Na₂O, K₂O, and Fe₂O₃ verified by AAS; others by spectrographic analysis.

^bIncludes Na₂O and Fe₂O₃ in waste.

^cNa₂O and Fe₂O₃ in waste included above; total will exceed 100%.

^dGas measurement slow to stabilize; possibly indicative of microcracks.
A-England; B-France; C-Germany; D-India; E-U.S.A.

The problem of determining a range of environmental events likely to occur was resolved by specifying a number of "most likely" conditions, presented in Table A.23. A subset of these conditions (Table A.24) was selected for the various tests. The test temperatures were selected as a matter of convenience and are probably lower than anticipated under actual repository conditions. The 30 cycles per minute oscillation is meant to provide stirring and dispersion of the reaction products away from the glass grains without introducing abrasion (which may disrupt film formation). The pH of the solution after the test was measured in order to determine change. The difference in pH levels is indicative of different corrosion mechanisms reflecting on the composition of the particular glass. Weight loss is a useful indicator of

Table A.22

Composition of Simulated Nuclear Waste Included in Waste Glass Tests
at Corning⁽¹⁷⁾

Oxide	Weight Percent	Oxide	Weight Percent
Na ₂ O	10.18	PdO	---
Fe ₂ O ₃	7.10	AgO	0.13
Cr ₂ O ₃	0.51	CdO	0.15
NiO	1.54	TeO ₂	1.07
P ₂ O ₅	9.34	Cs ₂ O	---
Gd ₂ O ₃	---	BaO	2.31
K ₂ O	1.68	La ₂ O	13.64
RbO	---	CeO ₂	15.49
SrO	1.57	Pr ₆ O ₁₁	3.13
Y ₂ O ₃	0.68	Nd ₂ O ₃	10.65
ZrO ₂	7.30	Pm ₂ O ₃	---
MoO ₃	9.39	Sm ₂ O ₃	1.72
Te ₂ O ₇	---	Eu ₂ O ₃	---
RuO ₂	---	Gd ₂ O ₃	1.25
Rh ₂ O ₃	---	Other REO	0.69
Co ₃ O ₄	0.45		

Table A.23

Natural Geochemical Environments⁽¹⁷⁾

Environment ^a	pH
Salt Mine	7.8
Sea Bed	7.8-8.0
Basalt Formation	3.0-7.0
Coal Mine	>3.0
Clay Formation	7.0-8.0
Limestone Formation	8.0-8.2
Acid Water ^b	<1.0
Alkali Lake Brine ^c	9.5
Range: "Normal"	3-8
"Sometimes"	1-10

^aAssumes water present.

^bContains approximately 1% H₂SO₄ - Devil's
Inkpot, Yellowstone Park.

^cSearles Lake, Mohave Desert.

Table A.24

Experimental Parameters of Corning Test(17)

Equipment for Testing:	
125 mL Erlenmeyer flasks, polypropylene	
Constant temperature water bath with oscillating flask holder	
Solutions (volume: 25 mL):	
0.1N acetic acid	pH 2.9
deionized water	pH 7
water saturated with CaCO ₃	pH 9.3
Agitation:	
30 cycles per minute	
1 1/2 inch path	
Temperature:	
25°C	
55°C	
Duration Time:	
1 day	
10 days	
Sample Form:	
grains approximately 0.5 mm (40-50 mesh)	
plates, 1/2 in. x 1/2 in. x 1 mm, polished	

total attack. Sodium (most readily leached or preferentially extracted element) and silica (least readily leached; indicative of network dissolution) were determined by flame spectroscopy. Film formation was determined through optical microscopy. The depth of reaction was extrapolated to 365 days and assumes a linear rate.

Corning's results for grain samples show pH, weight loss and sodium and silicon extracted into 25 ml of solution. The 'pH shift' (in Summary Table A.28) is the value obtained after 10 days at 55°C, indicating change in the nature of the reacting solution. The depth of reacted layer (assumes depth to which sodium has been leached and depth to which silicon has been removed) is given as an estimate. The estimated long-term reaction rate (item 8, Tables A.25 to A.27) is based on the limited data and a narrow range of minimum to maximum rates. The minimum long-term rate is assumed to relate to the rate of silica removal. The 10-day rate for silica removal has been used for the long-term estimates. A summary and record of performance for each glass type is given in Tables A.25 through A.27. The verticle bars in Figure A.21 (Estimated Corrosion Rates) represent the span between the estimated maximum and minimum corrosion rates. The solid square on each bar is the estimated "probable" rate (a "best guess"). Table A.29 presents the results of the plate tests for glasses A-E (55°C for 2 days).

The results of the comparative testing by Corning permits a certain ranking of glass durability based on its performance in leach tests. The leach tests cannot duplicate the effects of glass corrosion under burial/weathering conditions. Also, the extrapolation of results based on a 1- and 10- day test to estimate long-term leach rates is, as Corning points out, a "best guess" at best.

The comparative testing by Corning is useful in its evaluation of various glass compositions under similar conditions. Insights as to the performance of a glass based on composition could eliminate poor performers. The use of a standard, such as an NBS soda-lime glass as a reference material may provide a comparative base for the test design.

Table A.25

Corning Glass Grain Results - Acetic (pH 2.9)⁽¹⁷⁾

	Time	A		B		C		D		E		Soda Lime	
		25°C	55°C	25°C	55°C	25°C	55°C	25°C	55°C	25°C	55°C	25°C	55°C
1. pH	1 day	3.9	4.6	3.0	2.9	3.3	3.9	3.0	3.1	5.3	5.5	3.0	3.0
	10 days	4.4	6.2	3.1	3.4	4.0	---	3.2	3.7	6.1	5.8	3.1	3.1
2. Weight Loss (mg)	1 day	60	97	3.0	2.0	9.0	11.0	-4.0	56.	135.	105.	-2	4
	10 days	45	113	2.0	11.0	14.0	23.0	93.	6.	106.	103.	19	11
3. Na ⁺ (ppm)	1 day	480	1066	4.2	21.4	220.	412.	8.8	31.0	696.	650.	4.0	6.4
	10 days	834	2976	7.6	78.	448.	660.	34.	174.	776.	784.	5.4	22.0
4. Si ⁺ (ppm)	1 day	56	112	0.3	3.0	26.	90.	3.	18.	236.	140.	0.0	0.4
	10 days	78	52	0.4	34.0	74.	74.	14.	92.	92.	82.	0.0	0.0
5. Appearance (microscope)	1 day	slightly cracked	cracked	no change		slight film	Spall	no change	deposit	crack	crack	no change	no change
	10 days	cracked	cracked	no change		Spall	Spall	deposit	deposit	crack	crack	no change	no change
6. Relative Na ₂ O Extraction (Solution vs glass)	1 day	18	21	42	24	9	4	8	5	8	12	---	---
	10 days	23	123	56	46	9	9	7	5	21	24	---	---
7. Reacted Layer Depth (μm)	1 day	1.62	3.61	0.018	0.089	0.71	1.32	0.06	0.20	6.2	5.8	0.020	0.034
	10 days	2.82	10.1	0.032	0.033	1.44	2.13	0.22	1.10	6.9	7.0	0.030	0.118
Si ⁺	1 day	0.087	0.175	0.0004	0.004	0.083	0.28	0.01	0.04	0.84	0.49	0.000	0.001
	10 days	0.122	0.081	0.0006	0.047	0.236	0.24	0.03	0.21	0.32	0.29	0.000	0.000
8. Estimated long term rate at 25°C cm/yr	MAX.	0.06		0.0007		0.03		0.002		0.2		.001	
	MIN.	0.0004		0.000002		0.001		0.0001		0.001		0.00001	
	Probable	0.01		0.00001		0.005		0.0001		0.1		0.00001	

A-95

Table A.26

Corning Glass Grain Results: Deionized Water (pH 7)⁽¹⁷⁾

	Time	A		B		C		D		E		Soda Lime		
		25°C	55°C	25°C	55°C	25°C	55°C	25°C	55°C	25°C	55°C	25°C	55°C	
1. pH	1 day	8.8	8.8	5.9	8.8	8.5	10.7	8.3	8.8	7.1	8.0	6.7	9.0	
	10 days	9.0	9.3	5.8	8.8	10.5	11.7	7.8	8.9	6.7	7.0	7.8	9.6	
2. Weight Loss (mg)	1 day	5.	49.	7.	4.	12.	26.	10.	5.	37	15	11	0.4	
	10 days	21.	39.	19.	16.	10.	45.	-8.	-5.	19	27	4	11	
3. Na ⁺ (ppm)	1 day	52	346	3.0	26.6	62.	426.	5.0	36.	180	184	4.0	7.0	
	10 days	238	904	2.8	116.	406.	876.	23.4	62.	200	126	5.6	26.	
4. Si ⁺ (ppm)	1 day	28	102	0.3	31.	26.	126.	3.	29.	198	90	3.0	9.6	
	10 days	64	76	8.	58.	104.	228.	17.	46.	208	133	1.8	19.2	
5. Appearance (microscope)	1 days	slightly cracked	cracked	no change		slight film	Spall	no change	deposit	deposit	deposit	no change	no change	
	10 days	slightly cracked	cracked	no change		Spall	Spall	deposit	crazed	film	film	no change	no change	
6. Relative Na ₂ O Extraction (solution vs glass)	1 day	4.	8.	30.	2.5	3.	3.	4.	3.	3.	5.	4	3	
	10 days	8.	26.	1.0	5.9	4.	4.	4.	4.	3.	5.	10	4	
7. Reacted Layer Depth (μm)	Na ⁺		0.18	0.17	0.012	0.111	0.20	1.37	0.03	0.23	1.6	1.6	0.020	0.036
			0.81	3.06	0.012	0.93	1.30	2.82	0.15	0.39	1.8	1.1	0.030	0.138
	Si ⁺		0.044	0.159	0.0004	0.044	0.083	0.40	0.01	0.06	0.71	0.32	0.005	0.016
			0.100	0.119	0.0112	0.081	0.33	0.73	0.04	0.1	0.74	0.49	0.003	0.032
8. Estimated long term rate at 25°C cm/yr	MAX.	0.006		0.0004		0.007		0.001		0.06		0.001		
	MIN.	0.0004		0.00004		0.001		0.0001		0.002		0.0001		
	Probable	0.001		0.0001		0.001		0.0001		0.01		0.0001		

Table A.27

Corning Glass Grain Results - CaCO₃ (pH 9.3)⁽¹⁷⁾

	Time	A		B		C		D		E		Soda Lime		
		25°C	55°C	25°C	55°C	25°C	55°C	25°C	55°C	25°C	55°C	25°C	55°C	
1. pH	1 day	8.8	9.0	6.5	8.9	9.0	10.4	7.9	8.9	7.8	8.3	7.7	9.5	
	10 days	8.9	9.2	7.6	8.8	9.8	11.6	8.1	8.9	7.2	8.2	7.8	8.4	
2. Weight Loss (mg)	1 day	3.	7.	8.	3.	7.	31.	4.	2.	30.	50.	14	5	
	10 days	2.	2.5	2.	18.0	32.	39.	1.	9.	48.	28.	0.1	30	
3. Na ⁺ (ppm)	1 day	54	270	3.5	38.0	102.	256.	6.2	28.	174	120.	4.0	8.8	
	10 days	206	662	24	104.	454.	908.	23.4	58.	64	168	5.6	34.	
4. Si ⁺ (ppm)	1 day	28	98	2.6	42.	68.	66.	3.	26.	187	174	3.2	13.8	
	10 days	32	98	26.	60.	148.	206.	17.	36.	102.	152	3.4	42.6	
5. Appearance (microscope)	1 day	slightly cracked	slightly cracked	slight deposit	no change	slight Spalling	Spalling	no change	deposit	deposit	deposit	no change	no change	
	10 days	slightly cracked	cracked	slight deposit	no change	Spalling	Spalling	deposit	crazed	film	film	no change	no change	
6. Relative Na ₂ O Extraction (Solution vs Glass)	1 day	4	6	10	2.7	3	4	6	3	3.	2.	4	2	
	10 days	14	15	2.7	5	3	4	4	3	2.	3.	5	3	
7. Reacted Layer Depth (μm)	Na ⁺	1 day	0.18	0.91	0.014	0.158	0.52	0.82	0.04	0.18	1.6	1.1	0.020	0.048
		10 days	0.69	2.24	0.100	0.43	1.46	2.93	0.15	0.36	0.5	1.5	0.030	0.182
	Si ⁺	1 day	0.044	0.153	0.0036	0.058	0.22	0.21	0.01	0.06	0.67	0.62	0.006	0.023
		10 days	0.050	0.153	0.0032	0.084	0.47	0.66	0.04	0.08	0.36	0.54	0.006	0.071
8. Estimated Long Term Rate at 25°C cm/yr	MAX.	0.007		0.0005		0.02		0.002		0.06		0.001		
	MIN.	0.0002		0.00001		0.002		0.0005		0.001		0.0001		
	Probable	0.001		0.0001		0.002		0.0005		0.01		0.0001		

A-97

Table A.28

Summary of Interpreted Results for all Glasses of Corning Test(17)

		A	B	C	D	E	Soda-Lime	
pH Shift	Acetic	6.2	3.4	4.5	3.7	6.1	3.1	
	Water	9.3	8.8	11.7	8.9	7.0	9.6	
	CaCO ₃	9.2	8.8	11.6	8.9	8.2	9.4	
Temp. Ratio (55/25)	Acetic	3.	10.	2.	5.	1.	2.	
	Water	5.	20.	5.	5.	1.	3.	
	CaCO ₃	4.	10.	2.	4.	1.	4.	
Time Ratio (10/1)	Acetic	2.	4.	2.	5.	1.	2.	
	Water	5.	4.	4.	4.	1.	2.	
	CaCO ₃	4.	5.	3.	3.	1.	2.	
Relative Na ₂ O Extraction	Acetic	30.	20.	7.	7.	5.	---	
	Water	10.	5.	4.	4.	3.	4.	
	CaCO ₃	10.	5.	4.	4.	3.	4.	
Estimated Rate (cm/year)	Acetic	Max.	0.06	0.0007	0.03	0.002	0.2	0.001
		Min.	0.0004	0.00001	0.001	0.0001	0.001	0.00001
		Prob.	0.01	0.00001	0.005	0.001	0.1	0.00001
	Water	Max.	0.006	0.0004	0.007	0.001	0.06	0.001
		Min.	0.0004	0.00004	0.001	0.0001	0.002	0.0001
		Prob.	0.001	0.0001	0.001	0.0001	0.01	0.0001
	CaCO ₃	Max.	0.007	0.0005	0.02	0.002	0.06	0.001
		Min.	0.0002	0.00001	0.002	0.0005	0.0001	0.0001
		Prob.	0.001	0.0001	0.002	0.0005	0.01	0.0001
Appearance (1 day at 55°C)	Acetic	cracked	no change	spalled	deposit	cracked	no change	
	Water	cracked	no change	spalled	deposit	film	no change	
	CaCO ₃	slightly cracked	no change	spalled	deposit	film	no change	

A-98

66-V

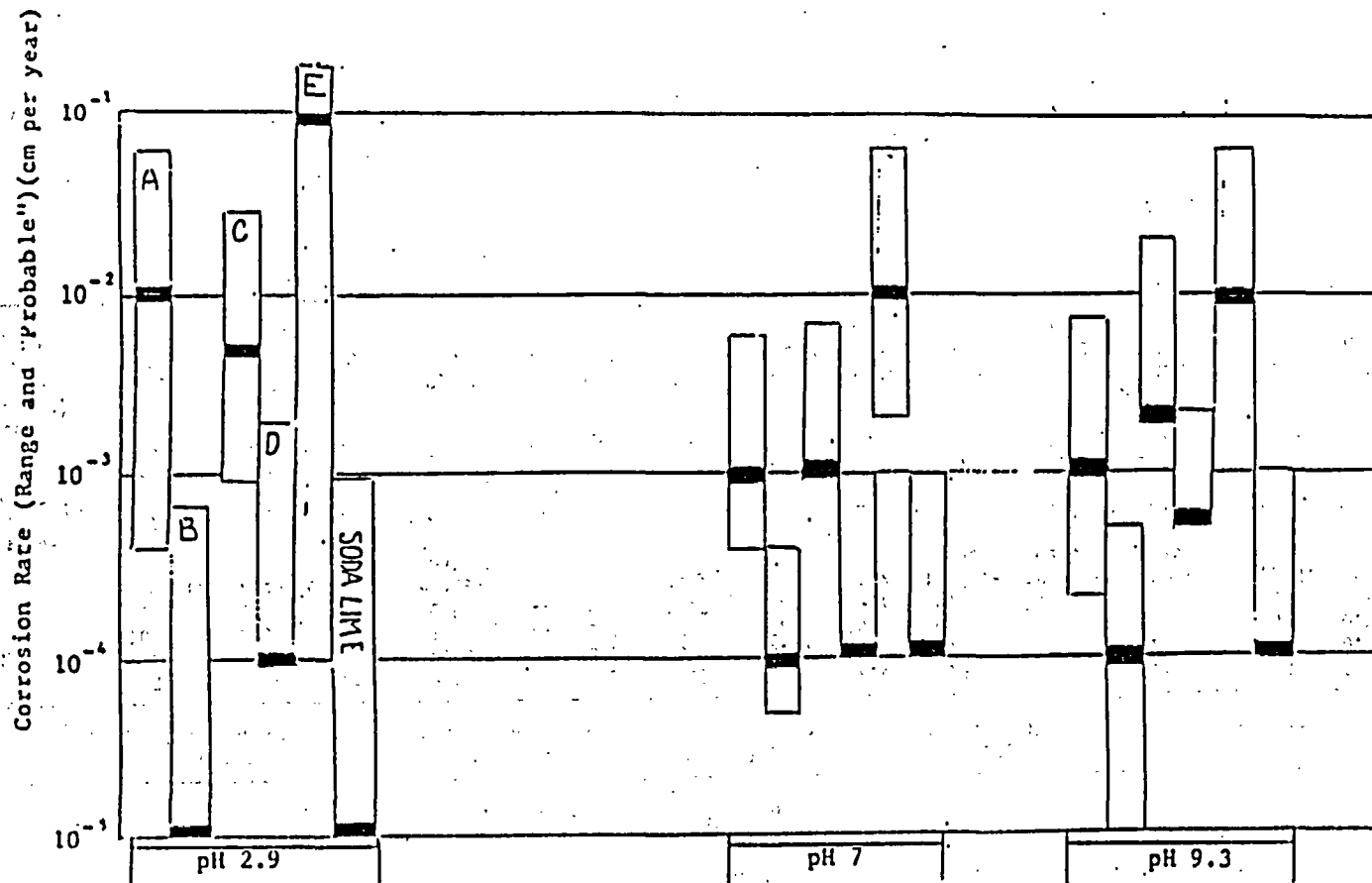


Figure A.21 Estimated corrosion rates (ranges and "probables") as a function of pH of Corning Test. (17)

Table A.29

Plate Test Results for Glasses A-E (55°C - 2 days)
 (Sample surface area: 3.6 cm²; solution volume: 25 mL)(17)

Variable	Glass A			Glass B			Glass C			Glass D			Glass E		
	Acetic	Water	CaCO	Acetic	Water	CaCO	Acetic	Water	CaCO	Acetic	Water	CaCO	Acetic	Water	CaCO
pH	3.2	8.0	8.4	2.9	--	6.5	3.1	8.7	8.4	2.9	5.4	6.3	4.1	5.8	6.3
Weight loss (mg/cm ²)	2.2	0.70	0.62	0.06	--	0.19	0.64	0.60	0.39	0.28	0.13	0.11	14.4	0.15	0.15
ppm Na ⁺	107.	22.	21.	1.2	--	3.4	33.	23.	15.	4.0	1.5	2.7	214.	0.8	0.4
ppm Si ⁺	31.	23.	24.	0.8	--	5.9	12.2	9.8	6.7	5.1	10.2	10.2	96.	5.2	5.6
Appearance	deposit	hazy	deposit	iridescent	--	hazy	hazy	OK	hazy	iridescent	iridescent	iridescent	deposit	OK	spotted
Relative Na ₂ O (solution vs glass)	7.	2.	2.	4.	--	2.	3.	2.	2.	2.	0.4	0.4	6.	0.4	0.2
Reacted layer depth um - Na ⁺	29.	6.	6.	0.4	--	1.1	5.	3.	2.	1.5	0.6	1.0	90.	0.3	0.2
- Si ⁺⁺	4.	3.	3.	0.1	--	0.6	2.	1.	1.	0.7	1.4	1.4	16.	0.9	0.9
Estimated long-term rate at 25°C (cm/yr)															
Maximum	0.16	0.03	0.03	0.002	--	0.006	0.03	0.02	0.01	0.008	0.003	0.005	0.5	0.002	0.001
Minimum	0.01	0.01	0.01	0.0002	--	0.001	0.004	0.003	0.002	0.002	0.003	0.003	0.04	0.002	0.002
Probable	0.05	0.02	0.02	0.0005	--	0.002	0.01	0.01	0.005	0.004	0.003	0.004	0.04	0.002	0.002

A.2 References

1. L. Holland, "Chapter 3. Surface Chemistry and Corrosion of Glass," in The Properties of Glass Surfaces, John Wiley, NY, (1964).
2. C. F. Cline, et al., "Durability of Beryllium Fluoride Glasses in Water," J. Non. Crystal. Solids 33, 147 (1979).
3. M. E. Nordberg, "Chemical Durability," Corning Glass Works, no date.
4. W. C. Taylor and R. D. Smith, J. Amer. Ceram. Soc. 19, 331 (1936).
5. G. W. Morey, The Properties of Glass, Chapter IV, Reinhold, NY, (1954).
6. R. H. Doremus, Glass Science, Wiley, NY, (1973).
7. E. Wichers, et al., "Comparative Tests of Chemical Glassware," NBS Research Paper, RP-1394, (1941).
8. L. Holland, "Surface Chemistry and Corrosion of Glass, Part I." The Glass Industry 44, 191 (1963).
9. A. Barkatt, et al., "Stability of Fixation Solids for High-Level Radioactive Wastes," in High-Level Radioactive Solid Waste Forms, Denver, NUREG/CP-0005, (1978).
10. J. H. Simmons, et al., "Chemical Durability of Nuclear Waste Glasses," Proceedings of Ceramics in Nuclear Waste Management, Cincinnati, CONF-790420, (1979), 263.
11. K. Scheffler, et al., "Long-Term Leaching of Silicate Systems: Testing Procedure, Actinides Behavior and Mechanism," Gesellschaft fur Kernforschung M.B.H., Karlsruhe KFK 2456/EUR5509e, (1977).
12. F. Lanza and E. Parnisari, "Evaluation of Long-Term Leaching of Borosilicate Glasses," Nuclear Science and Technology, EUR5947EN, (1978).
13. F. Lanza and E. Parnisari, "Evaluation of Long-Term Leaching of Borosilicate Glass in Pure Water," ibid. reference (10).
14. D. E. Clark, E. L. Yen-Bower, and L. L. Hench, "Corrosion Behavior of Zinc Borosilicate Simulated Nuclear Waste Glass," ibid. reference (10).
15. P. B. Adams, "Relative Leach Behavior of Waste Glasses and Naturally Occurring Glasses," ibid. reference (10).
16. B. T. Kenna, K. D. Murphy, and H. S. Levine, "Long-Term Elevated Temperature Leaching of Solid Waste Forms," in McCarthy, ed., Scientific Basis for Nuclear Waste Management, Vol. 1, (1979), 157.
17. D. B. Adams, J. D. Sundywis, and H. E. Rauscher, "Glasses for Nuclear Waste Fixation-Corrosion Research," Paper presented at the Amer. Ceramic Soc. Meeting, Cincinnati, Ohio, May 1-6, 1976; and personal communication.

APPENDIX B

Approximate Compositions of Glasses Mentioned in Text (weight percent)

	SiO ₂	B ₂ O ₃	Na ₂ O	Al ₂ O ₃	CaO	MgO	K ₂ O	Other components
"Pyrex" borosilicate								
7740	81	13	4	2				
NBS 717 borosilicate	70.0	17.0	1.0	3.0			8.0	LiF ₂ =1.0
Soda lime 0080	72.6	0.8	15.4	1.7	4.6	3.6		
NBS 710 soda-lime-silica	70.5	0.2	8.7	11.6			7.7	
Soda borosilicate								
7050	68	24	7	1				
1710	64	4.5	1.3	10.4	8.9	10.2	0.7	
Alkali lead 0010	77		9	1			5	PbO=8
Alkaline earth								
Aluminosilicate 1720	64	4.5	1.3	10.4	8.9	10.2	0.7	
Jena glass	64.58	10.03	7.38	6.28	0.08	0.12		ZnO=11.78; Fe ₂ O ₃ =0.10 LiF ₂ *33
33L glass	67			3				
FN glass	66	24	4	14.5	16.5	4.5	3	
E-glass	54.5	9.5	0.5	3		4		
7052	66	24	4	3				
G	77	19						
P	82						18	
Borosilicate crown I	69	11	10		0.2		7	
Borosilicate crown II	70	11	10		0.2		7	
S15	85		15					
P15	85						15	
U.K. borosilicate								
waste glass								
189 (M5)	41.5	21.9	7.7					LiF ₂ =3.7; waste=25.3
209 (M22)	50.9	11.1	8.3					LiF ₂ =4.0; waste=25.7
SRL borosilicate								
waste glass	40.4	7.2	16.2		4.5			LiF ₂ =2.9; TiO ₂ =7.2; waste=21.6
PNL borosilicate								
waste glass								
72-68	27.3	11.1	4.0		1.5		4.0	ZnO=21.3; waste=26.3
76-68	40.0	9.5	7.5		2.0			ZnO=5.0; TiO ₂ =3.0; waste=33.0
76-199	37.0	9.8	8.4	1.1	2.1		2.1	TiO ₂ =6.3; CuO=3.1; waste=30.0
77-107	38.0	13.0	2.0		2.0		4.0	ZnO=5.0; TiO ₂ =3.0; waste=33.0
77-260	36.0	9.0	8.0	2.0	1.0		2.0	TiO ₂ =6.9; CuO=3.0; waste=33.0
75-25	37.0	15.1	6.5		2.0	2.0	5.5	ZnO=28; waste=17.3
Strontium aluminoborosilicate glass	24.0	16.7		25.5				SrO ₂ =34.1
16th Century glass								
"crusted"	55.2-55.7		2.7-3.1		12.8-14.8	7.2-9.1	10.8-11.4	
"uncrusted"	57.5-59.9		2.5-3.3		8.3-13.0	7.3-8.7	9.0-11.3	

NRC FORM 335 (7-77)		U.S. NUCLEAR REGULATORY COMMISSION BIBLIOGRAPHIC DATA SHEET		1. REPORT NUMBER (Assigned by DDC) NUREG/CR-2482, Vol. 1 BNL-NUREG-51494	
4. TITLE AND SUBTITLE (Add Volume No., if appropriate) Review of DOE Waste Package Program Subtask 1.1 - National Waste Package Program		2. (Leave blank)		3. RECIPIENT'S ACCESSION NO.	
7. AUTHOR(S) M.S. Davis, D.G. Schweitzer		5. DATE REPORT COMPLETED MONTH YEAR November 1981		6. (Leave blank)	
9. PERFORMING ORGANIZATION NAME AND MAILING ADDRESS (Include Zip Code) Brookhaven National Laboratory Upton, NY 11973		DATE REPORT ISSUED MONTH YEAR February 1982		8. (Leave blank)	
12. SPONSORING ORGANIZATION NAME AND MAILING ADDRESS (Include Zip Code) Division of Waste Management Office of Nuclear Material Safety and Safeguards U.S. Nuclear Regulatory Commission Washington, DC 20555		10. PROJECT/TASK/WORK UNIT NO.		11. CONTRACT NO. NRC FIN A3164	
13. TYPE OF REPORT Final		PERIOD COVERED (Inclusive dates) May 1981 - September 1981			
15. SUPPLEMENTARY NOTES		14. (Leave blank)			
16. ABSTRACT (200 words or less) This report continues the assessment of the National Waste Package Program. Past reviews of waste forms, container materials and backfill materials are updated, with emphasis on the potential of these materials to meet NRC performance objectives. A start is made in describing information that NRC will need to review the waste package portion of a license application. DOE waste form programs will emphasize borosilicate glass and SYNROC. The data that NRC would need to make a positive finding for a waste package in which borosilicate glass is given full or partial credit for containment or controlled release does not exist at present. After 1000 year containment, the rate of release of radio-nuclides from a borosilicate glass waste form would depend on the rate at which long-lived actinides are leached from the waste form. Almost all the existing data deals with leaching of short-lived fission products. These will be essentially innocuous after 1000 years. Preliminary experiments on waste glass loaded with actinides indicate new and complex problems that have not been studied yet. For example, actinides exist in glass in various oxidation states which may have different leach properties. NRC's information needs to support 1000 year containment by TiCode-12 are summarized.					
17. KEY WORDS AND DOCUMENT ANALYSIS		17a. DESCRIPTORS			
17b. IDENTIFIERS/OPEN-ENDED TERMS					
18. AVAILABILITY STATEMENT Unlimited		19. SECURITY CLASS (This report) Unclassified		21. NO. OF PAGES	
		20. SECURITY CLASS (This page) Unclassified		22. PRICE S	

UNITED STATES
NUCLEAR REGULATORY COMMISSION
WASHINGTON, D.C. 20555

OFFICIAL BUSINESS
PENALTY FOR PRIVATE USE \$300

POSTAGE AND FEES PAID
U.S. NUCLEAR REGULATORY
COMMISSION

